Search for electroweak production of supersymmetric states in scenarios with compressed mass spectra at $\sqrt{s} = 13$ TeV with the ATLAS detector

M. Aaboud *et al.*[*]

(ATLAS Collaboration)

A search for electroweak production of supersymmetric particles in scenarios with compressed mass spectra in final states with two low-momentum leptons and missing transverse momentum is presented. This search uses proton-proton collision data recorded by the ATLAS detector at the Large Hadron Collider in 2015–2016, corresponding to 36.1 fb^{-1} of integrated luminosity at $\sqrt{s} = 13$ TeV. Events with same-flavor pairs of electrons or muons with opposite electric charge are selected. The data are found to be consistent with the Standard Model prediction. Results are interpreted using simplified models of R-parity-conserving supersymmetry in which there is a small mass difference between the masses of the produced supersymmetric particles and the lightest neutralino. Exclusion limits at 95% confidence level are set on next-to-lightest neutralino masses of up to 145 GeV for Higgsino production and 175 GeV for wino production, and slepton masses of up to 190 GeV for pair production of sleptons. In the compressed mass regime, the exclusion limits extend down to mass splittings of 2.5 GeV for Higgsino production, 2 GeV for wino production, and 1 GeV for slepton production. The results are also interpreted in the context of a radiatively-driven natural supersymmetry model with nonuniversal Higgs boson masses.

I. INTRODUCTION

Supersymmetry (SUSY) [1–6] predicts new states that differ by half a unit of spin from their partner Standard Model (SM) particles, and it offers elegant solutions to several problems in particle physics. In the minimal supersymmetric extension to the Standard Model [7,8], the SM is extended to contain two Higgs doublets, with supersymmetric partners of the Higgs bosons called Higgsinos. These Higgsinos mix with the partners of the electroweak gauge bosons, the so-called winos and the bino, to form neutralino $\tilde{\chi}^0_{1,2,3,4}$ and chargino $\tilde{\chi}^{\pm}_{1,2}$ mass eigenstates (subscripts indicate increasing mass). These states are collectively referred to as electroweakinos. In this work, the lightest neutralino $\tilde{\chi}^0_1$ is assumed to be the lightest SUSY particle (LSP) and to be stable due to R-parity conservation [9], which renders it a viable dark matter candidate [10,11].

Scenarios involving small mass differences between heavier SUSY particles and the LSP are referred to as compressed scenarios, or as having compressed mass spectra. This work considers three compressed scenarios, in which the heavier SUSY particles are produced via electroweak interactions. The first scenario is motivated by naturalness arguments [12,13], which suggest that the absolute value of the Higgsino mass parameter μ is near the weak scale [14,15], while the magnitude of the bino and wino mass parameters, M_1 and M_2, can be significantly larger (such as 1 TeV), i.e. $|\mu| \ll |M_1|, |M_2|$. This results in the three lightest electroweakino states, $\tilde{\chi}^0_1$, $\tilde{\chi}^{\pm}_1$, and $\tilde{\chi}^0_2$ being dominated by the Higgsino component. In this case the three lightest electroweakino masses are separated by hundreds of MeV to tens of GeV depending on the composition of these mass eigenstates, which is determined by the values of M_1 and M_2 [16]. The second scenario, motivated by dark matter coannihilation arguments [17,18], considers the absolute values of the M_1 and M_2 parameters to be near the weak scale and similar in magnitude, while the magnitude of μ is significantly larger, such that $|M_1| < |M_2| \ll |\mu|$. The $\tilde{\chi}^{\pm}_1$ and $\tilde{\chi}^0_2$ states are consequently wino-dominated, rendering them nearly mass degenerate [19], and have masses of order one to tens of GeV larger than a bino-dominated LSP. The third scenario is also favored by such dark matter arguments, but involves the pair production of the scalar partners of SM charged leptons (sleptons $\tilde{\ell}$). In this scenario, the sleptons have masses near the weak scale and just above the mass of a pure bino LSP.

Experimental constraints in these compressed scenarios are limited partly by small electroweak production cross sections, but also by the small momenta of the visible decay

products. The strongest limits from previous searches are from combinations of results from the Large Electron Positron collider (LEP) experiments [20–30]. The lower bounds on direct chargino production from these results correspond to $m(\tilde{\chi}_1^\pm) > 103.5$ GeV for $\Delta m(\tilde{\chi}_1^\pm, \tilde{\chi}_1^0) > 3$ GeV and $m(\tilde{\chi}_1^\pm) > 92.4$ GeV for smaller mass differences. For sleptons, conservative lower limits on the mass of the scalar partner of the right-handed muon, denoted $\tilde{\mu}_R$, are approximately $m(\tilde{\mu}_R) \gtrsim 94.6$ GeV for mass splittings down to $\Delta m(\tilde{\mu}_R, \tilde{\chi}_1^0) \gtrsim 2$ GeV. For the scalar partner of the right-handed electron, denoted $\tilde{e}_R$, a universal lower bound of $m(\tilde{e}_R) \gtrsim 73$ GeV independently of $\Delta m(\tilde{e}_R, \tilde{\chi}_1^0)$ exists. Recent phenomenological studies have proposed to probe compressed mass spectra in the electroweak SUSY sector by using leptons with small transverse momentum, p_T, referred to as soft leptons [16,31–37].

A search for electroweak production of supersymmetric particles in compressed mass spectra scenarios with final states containing two soft same-flavor opposite-charge leptons (electrons or muons) and a large magnitude (E_T^{miss}) of missing transverse momentum, $\mathbf{p}_T^{miss}$, is presented in this paper. The analysis uses proton-proton (pp) collision data collected by the ATLAS experiment from 2015 and 2016 at the Large Hadron Collider (LHC) [38], corresponding to 36.1 fb^{-1} of integrated luminosity at $\sqrt{s} = 13$ TeV. Figure 1 shows schematic diagrams representing the electro-weakino and slepton pair production, as well as decays targeted in this work. Same-flavor opposite-charge lepton pairs arise either from $\tilde{\chi}_2^0$ decays via an off-shell Z boson (denoted Z^*) or the slepton decays. The E_T^{miss} in the signal originates from the two LSPs recoiling against hadronic initial-state radiation. Electroweakino signal regions are constructed using the dilepton invariant mass $m_{\ell\ell}$ as a final discriminant, in which the signals have a kinematic endpoint given by the mass splitting of the $\tilde{\chi}_2^0$ and $\tilde{\chi}_1^0$, as illustrated in Fig. 2. Slepton signal regions exploit a similar feature in the stransverse mass m_{T2} [39,40]. This work complements the sensitivity of existing ATLAS searches at $\sqrt{s} = 8$ TeV

FIG. 2. Dilepton invariant mass ($m_{\ell\ell}$) for Higgsino and wino-bino simplified models. The endpoint of the $m_{\ell\ell}$ distribution is determined by the difference between the masses of the $\tilde{\chi}_2^0$ and $\tilde{\chi}_1^0$. The results from simulation (solid line) are compared with an analytic calculation of the expected line shape (dashed line) presented in Ref. [48], where the product of the signed mass eigenvalues ($m(\tilde{\chi}_2^0) \times m(\tilde{\chi}_1^0)$) is negative for Higgsino and positive for wino-bino scenarios.

[41–44], which set limits on the production of winos that decay via W or Z bosons for mass splittings of $\Delta m(\tilde{\chi}_1^\pm, \tilde{\chi}_1^0) \gtrsim 35$ GeV, and $\Delta m(\tilde{\ell}, \tilde{\chi}_1^0) \gtrsim 55$ GeV for slepton production. Similar searches have been reported by the CMS Collaboration at $\sqrt{s} = 8$ TeV [45,46] and at $\sqrt{s} = 13$ TeV [47], which probe winos decaying via W or Z bosons for mass splittings $\Delta m(\tilde{\chi}_1^\pm, \tilde{\chi}_1^0) \gtrsim 23$ GeV.

This paper has the following structure. After a brief description of the ATLAS detector in Sec. II, the data and Monte Carlo samples used are detailed in Sec. III. Sections IV and V present the event reconstruction and the signal region selections. The background estimation and the systematic uncertainties are discussed in Secs. VI and VII, respectively. Finally, the results and their interpretation are reported in Sec. VIII before Sec. IX summarizes the conclusions.

II. ATLAS DETECTOR

The ATLAS experiment [49] is a general-purpose particle detector that surrounds the interaction point with nearly 4π solid angle coverage.[1] It comprises an inner
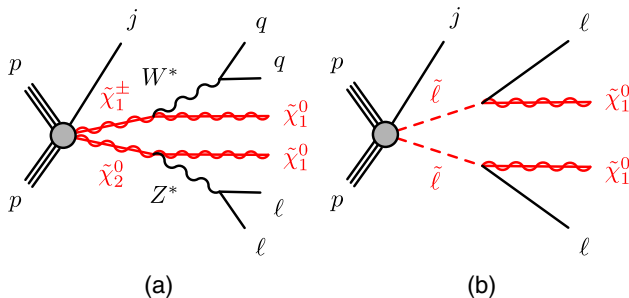

FIG. 1. Diagrams representing the two-lepton final state of (a) electroweakino $\tilde{\chi}_2^0 \tilde{\chi}_1^\pm$ and (b) slepton pair $\tilde{\ell}\tilde{\ell}$ production in association with a jet radiated from the initial state (labeled j). The Higgsino simplified model also considers $\tilde{\chi}_2^0 \tilde{\chi}_1^0$ and $\tilde{\chi}_1^+ \tilde{\chi}_1^-$ production.
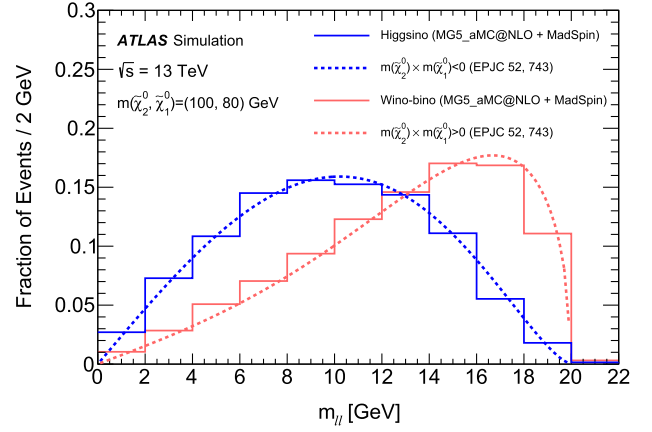
---

[1]ATLAS uses a right-handed coordinate system with its origin at the nominal interaction point (IP) in the center of the detector and the z axis along the beam pipe. The x axis points from the IP to the center of the LHC ring, and the y axis points upwards. Cylindrical coordinates (r, ϕ) are used in the transverse plane, ϕ being the azimuthal angle around the z axis. The pseudorapidity is defined in terms of the polar angle θ as $\eta = -\ln\tan(\theta/2)$. Angular distance is measured in units of $\Delta R \equiv \sqrt{(\Delta\eta)^2 + (\Delta\phi)^2}$. Rapidity is defined by $y = \frac{1}{2}\ln[(E + p_z)/(E - p_z)]$, where E is the energy and p_z is the longitudinal component of the momentum along the beam direction.

detector, calorimeter systems, and a muon spectrometer. The inner detector provides precision tracking of charged particles in the pseudorapidity region $|\eta| < 2.5$, consisting of pixel and microstrip silicon subsystems within a transition radiation tracker. The innermost pixel detector layer, the insertable B-layer [50], was added for $\sqrt{s} = 13$ TeV data-taking to improve tracking performance. The inner detector is immersed in a 2 T axial magnetic field provided by a superconducting solenoid. High-granularity lead/liquid-argon electromagnetic sampling calorimeters are used for $|\eta| < 3.2$. Hadronic energy deposits are measured in a steel/scintillator tile barrel calorimeter in the $|\eta| < 1.7$ region. Forward calorimeters cover the region $1.5 < |\eta| < 4.9$ for both the electromagnetic and hadronic measurements. The muon spectrometer comprises trigger and high-precision tracking chambers spanning $|\eta| < 2.4$ and $|\eta| < 2.7$, respectively, and by three large superconducting toroidal magnets. Events of interest are selected using a two-level trigger system [51], consisting of a first-level trigger implemented in hardware, which is followed by a software-based high-level trigger.

III. COLLISION DATA AND SIMULATED EVENT SAMPLES

Searches presented here use pp collision data at $\sqrt{s} = 13$ TeV from the LHC, collected by the ATLAS detector in 2015 and 2016. Events were selected using triggers requiring large E_T^{miss} with run-period-dependent thresholds of 70 to 110 GeV at the trigger level. These triggers are >95% efficient for events with an offline-reconstructed E_T^{miss} greater than 200 GeV. The data sample corresponds to an integrated luminosity of 36.1 fb^{-1} with an uncertainty of 2.1%, derived using methods similar to those described in Ref. [52]. The average number of pp interactions per bunch crossing was 13.5 in 2015 and 25 in 2016.

Samples of Monte Carlo (MC) simulated events are used to model both the signal and specific processes of the SM background. For the SUSY signals, two sets of simplified models [53–55] are used to guide the design of the analysis: one based on direct production of Higgsino states (referred to as the Higgsino model), and the other a model involving pair production of sleptons which decay to a pure bino LSP. For the interpretation of the results of the analysis, two additional scenarios are considered: a simplified model assuming the production of wino-dominated electroweakinos decaying to a bino LSP (referred to as the wino-bino model), and a full radiatively-driven SUSY model based on nonuniversal Higgs boson masses with two extra parameters (NUHM2) [56,57]. In all the models considered, the produced electroweakinos or sleptons are assumed to decay promptly.

The Higgsino simplified model includes the production of $\tilde{\chi}_2^0 \tilde{\chi}_1^\pm$, $\tilde{\chi}_2^0 \tilde{\chi}_1^0$ and $\tilde{\chi}_1^+ \tilde{\chi}_1^-$. The $\tilde{\chi}_1^0$ and $\tilde{\chi}_2^0$ masses were varied,

while the $\tilde{\chi}_1^\pm$ masses were set to $m(\tilde{\chi}_1^\pm) = \frac{1}{2}[m(\tilde{\chi}_1^0) + m(\tilde{\chi}_2^0)]$. The mass splittings of pure Higgsinos are generated by radiative corrections, and are of the order of hundreds of MeV [58], with larger mass splittings requiring some mixing with wino or bino states. However, in this simplified model, the calculated cross sections assume electroweakino mixing matrices corresponding to pure-Higgsino $\tilde{\chi}_1^0, \tilde{\chi}_1^\pm, \tilde{\chi}_2^0$ states for all mass combinations. The search for electroweakinos exploits a kinematic endpoint in the dilepton invariant mass distribution, where the lepton pair is produced in the decay chain $\tilde{\chi}_2^0 \to Z^* \tilde{\chi}_1^0, Z^* \to \ell^+ \ell^-$. Therefore, processes that include production of a $\tilde{\chi}_2^0$ neutralino are most relevant for this search, while $\tilde{\chi}_1^+ \tilde{\chi}_1^-$ production contributes little to the overall sensitivity. Example values of cross sections for $m(\tilde{\chi}_2^0) = 110$ GeV and $m(\tilde{\chi}_1^0) = 100$ GeV are 4.3 ± 0.1 pb for $\tilde{\chi}_2^0 \tilde{\chi}_1^\pm$ production and 2.73 ± 0.07 pb for $\tilde{\chi}_2^0 \tilde{\chi}_1^0$ production. The branching ratios for $\tilde{\chi}_2^0 \to Z^* \tilde{\chi}_1^0$ and $\tilde{\chi}_1^\pm \to W^* \tilde{\chi}_1^0$ were fixed to 100%. The $Z^* \to \ell^+ \ell^-$ branching ratios depend on the mass splittings and were computed using SUSY-HIT v1.5b [59], which accounts for finite b-quark and τ-lepton masses. At $\Delta m(\tilde{\chi}_2^0, \tilde{\chi}_1^0) = 60$ GeV the branching ratios for $Z^* \to e^+ e^-$ and $Z^* \to \mu^+ \mu^-$ are approximately 3.5%, while in the compressed scenario at $\Delta m(\tilde{\chi}_2^0, \tilde{\chi}_1^0) = 2$ GeV they increase to 5.1% and 4.9%, respectively, as the Z^* mass falls below the threshold needed to produce pairs of heavy quarks or τ leptons. The branching ratios for $W^* \to e\nu$ and $W^* \to \mu\nu$ also depend on the mass splitting, and increases from 11% for large $\Delta m(\tilde{\chi}_1^\pm, \tilde{\chi}_1^0)$ to 20% for $\Delta m(\tilde{\chi}_1^\pm, \tilde{\chi}_1^0) < 3$ GeV. Events were generated at leading order with MG5_aMC@NLO v2.4.2 [60] using the NNPDF23LO PDF set [61] with up to two extra partons in the matrix element (ME). The electroweakinos were decayed using MADSPIN [62], and were required to produce at least two leptons (e, μ) in the final state, including those from decays of τ-leptons. The resulting events were interfaced with PYTHIA v8.186 [63] using the A14 set of tuned parameters (tune) [64] to model the parton shower (PS), hadronization and underlying event. The ME-PS matching was performed using the CKKW-L scheme [65] with the merging scale set to 15 GeV.

The wino-bino simplified model considers $\tilde{\chi}_2^0 \tilde{\chi}_1^\pm$ production, where the mass of the $\tilde{\chi}_2^0$ is assumed to be equal to that of the $\tilde{\chi}_1^\pm$. The generator configuration as well as the decay branching ratios are consistent with those for the Higgsino samples. Pure wino production cross sections are used for this model. An example value of the $\tilde{\chi}_2^0 \tilde{\chi}_1^\pm$ production cross section for $m(\tilde{\chi}_2^0, \tilde{\chi}_1^\pm) = 110$ GeV is 16.0 ± 0.5 pb. The composition of the mass eigenstates differs between the wino-bino and Higgsino models. This results in different invariant mass spectra of the two leptons originating from the virtual Z^* boson in the $\tilde{\chi}_2^0$ to $\tilde{\chi}_1^0$ decay. The different spectra are illustrated in Fig. 2, where the leptonic decays modeled by MADSPIN are found to be in good agreement with theoretical predictions that depend on

the relative sign of the $\tilde{\chi}_1^0$ and $\tilde{\chi}_2^0$ mass parameters [48], which differs between the Higgsino and wino-bino models.

The slepton simplified model considers direct pair production of the selectron $\tilde{e}_{L,R}$ and smuon $\tilde{\mu}_{L,R}$, where the subscripts L, R denote the left- or right-handed chirality of the partner electron or muon. The four sleptons are assumed to be mass degenerate, i.e. $m(\tilde{e}_L) = m(\tilde{e}_R) = m(\tilde{\mu}_L) = m(\tilde{\mu}_R)$. An example value of the slepton production cross section for $m(\tilde{\ell}_{L,R}) = 110$ GeV is 0.55 ± 0.01 pb. The sleptons decay with a 100% branching ratio into the corresponding SM partner lepton and the $\tilde{\chi}_1^0$ neutralino. Events were generated at tree level using MG5_aMC@NLO v2.2.3 and the NNPDF23LO PDF set with up to two additional partons in the matrix element, and interfaced with PYTHIA v8.186 using the CKKW-L prescription for ME-PS matching. The merging scale was set to one quarter of the slepton mass.

Higgsino, wino-bino, and slepton samples are scaled to signal cross sections calculated at next-to-leading order (NLO) in the strong coupling, and at next-to-leading-logarithm (NLL) accuracy for soft-gluon resummation, using RESUMMINO v1.0.7 [66–68]. The nominal cross section and its uncertainty are taken from an envelope of cross section predictions using different parton distribution function (PDF) sets and factorization and renormalization scales, as described in Ref. [69].

In the NUHM2 model, the masses of the Higgs doublets that couple to the up-type and down-type quarks, m_{H_u} and m_{H_d} respectively, are allowed to differ from the universal scalar masses m_0 at the grand unification scale. The parameters of the model were fixed to the following values: $m_0 = 5$ TeV; the pseudoscalar Higgs boson mass $m_A = 1$ TeV; the trilinear SUSY breaking parameter $A_0 = -1.6$ m_0; the ratio of the Higgs field vacuum

expectation values $\tan\beta = 15$; and the Higgsino mass parameter $\mu = 150$ GeV. This choice of parameters is based on Ref. [70], which leads to a radiatively-driven natural SUSY model with low fine-tuning, featuring decoupled heavier Higgs bosons, a light Higgs boson with a mass of 125 GeV and couplings like those in the SM, colored SUSY particles with masses of the order of a few TeV, and Higgsino-like light electroweakinos with masses around the value of μ. The mass spectra and decay branching ratios were calculated using ISAJET v7.84 [71]. The universal gaugino mass $m_{1/2}$ is the free parameter in the model, and has values between 350 and 800 GeV in different event samples. This parameter primarily controls the $\tilde{\chi}_2^0$–$\tilde{\chi}_1^0$ mass splitting, for example $m(\tilde{\chi}_2^0, \tilde{\chi}_1^0) = (161, 123)$ GeV for $m_{1/2} = 400$ GeV and $m(\tilde{\chi}_2^0, \tilde{\chi}_1^0) = (159, 141)$ GeV for $m_{1/2} = 700$ GeV. The NUHM2 phenomenology relevant to this analysis is similar to that of the Higgsino simplified model described above, and samples of simulated $\tilde{\chi}_2^0\tilde{\chi}_1^0$ and $\tilde{\chi}_2^0\tilde{\chi}_1^\pm$ events were therefore generated with the same generator configuration as the Higgsino samples, but with mass spectra, cross sections, and branching ratios determined by the NUHM2 model parameters. The cross sections were calculated to NLO in the strong coupling constant using PROSPINO v2.1 [72]. They are in agreement with the NLO calculations matched to resummation at NLL accuracy within ∼2%. An example value of the $\tilde{\chi}_2^0\tilde{\chi}_1^\pm$ production cross section at $m_{1/2} = 700$ GeV, corresponding to a $\tilde{\chi}_2^0$ mass of 159 GeV and a $\tilde{\chi}_1^\pm$ mass of 155 GeV, is 1.07 ± 0.05 pb.

For the SM background processes, SHERPA versions 2.1.1, 2.2.1, and 2.2.2 [73] were used to generate $Z^{(*)}/\gamma^* +$ jets, diboson, and triboson events. Depending on the process, matrix elements were calculated for up to two partons at

TABLE I. Simulated samples of Standard Model background processes. The PDF set refers to that used for the matrix element.

Process	Matrix element	Parton shower	PDF set	Cross section
$Z^{(*)}/\gamma^* +$ jets	SHERPA 2.2.1		NNPDF 3.0 NNLO [86]	NNLO [87]
Diboson	SHERPA 2.1.1/2.2.1/2.2.2		NNPDF 3.0 NNLO	Generator NLO
Triboson	SHERPA 2.2.1		NNPDF 3.0 NNLO	Generator LO, NLO
$t\bar{t}$	POWHEG-BOX v2	PYTHIA 6.428	NLO CT10 [88]	NNLO + NNLL [89–92]
t (s-channel)	POWHEG-BOX v1	PYTHIA 6.428	NLO CT10	NNLO + NNLL [93]
t (t-channel)	POWHEG-BOX v1	PYTHIA 6.428	NLO CT10f4	NNLO + NNLL [94,95]
$t + W$	POWHEG-BOX v1	PYTHIA 6.428	NLO CT10	NNLO + NNLL [96]
$h(\to \ell\ell, WW)$	POWHEG-BOX v2	PYTHIA 8.186	NLO CTEQ6L1 [97]	NLO [98]
$h + W/Z$	MG5_aMC@NLO 2.2.2	PYTHIA 8.186	NNPDF 2.3 LO	NLO [98]
$t\bar{t} + W/Z/\gamma^*$	MG5_aMC@NLO 2.3.3	PYTHIA 8.186	NNPDF 3.0 LO	NLO [60]
$t\bar{t} + WW/t\bar{t}$	MG5_aMC@NLO 2.2.2	PYTHIA 8.186	NNPDF 2.3 LO	NLO [60]
$t + Z$	MG5_aMC@NLO 2.2.1	PYTHIA 6.428	NNPDF 2.3 LO	LO [60]
$t + WZ$	MG5_aMC@NLO 2.3.2	PYTHIA 8.186	NNPDF 2.3 LO	NLO [60]
$t + t\bar{t}$	MG5_aMC@NLO 2.2.2	PYTHIA 8.186	NNPDF 2.3 LO	LO [60]

NLO and up to four partons at LO using COMIX [74] and OPENLOOPS [75], and merged with the SHERPA parton shower [76] according to the ME+PS@NLO prescription [77]. The $Z^{(*)}/\gamma^*$ + jets and diboson samples provide coverage of dilepton invariant masses down to 0.5 GeV for $Z^{(*)}/\gamma^* \to e^+e^-/\mu^+\mu^-$, and 3.8 GeV for $Z^{(*)}/\gamma^* \to \tau^+\tau^-$. POWHEG-BOX v1 and v2 [78–80] interfaced to PYTHIA 6.428 with the PERUGIA2012 tune [81] were used to simulate $t\bar{t}$ and single-top production at NLO in the matrix element. POWHEG-BOX v2 was also used with PYTHIA 8.186 to simulate Higgs boson production. MG5_aMC@NLO v2.2.2 with PYTHIA versions 6.428 or 8.186 and the ATLAS A14 tune was used to simulate production of a Higgs boson in association with a W or Z boson, as well as events containing $t\bar{t}$ and one or more electroweak bosons. These processes were generated at NLO in the matrix element except for $t\bar{t} + WW/t\bar{t}$, $t + t\bar{t}$, and $t + Z$, which were generated at LO. Table I summarizes the generator configurations of the matrix element and parton shower programs, the PDF sets, and the cross section calculations used for normalization. Further details about the generator settings used for the above described processes can also be found in Refs. [82–85].

To simulate the effects of additional pp collisions, referred to as pileup, additional interactions were generated using the soft QCD processes of PYTHIA 8.186 with the A2 tune [99] and the MSTW2008LO PDF set [100], and were overlaid onto each simulated hard-scatter event. The MC samples were reweighted to match the pileup distribution observed in the data.

All MC samples underwent ATLAS detector simulation [101] based on GEANT4 [102]. The SUSY signal samples employed a fast simulation that parametrizes the response of the calorimeter [103]; the SM background samples used full GEANT4 simulation. EVTGEN v1.2.0 [104] was employed to model the decay of bottom and charm hadrons in all samples except those generated by SHERPA, which uses its internal modeling.

IV. EVENT RECONSTRUCTION

Candidate events are required to have at least one pp interaction vertex reconstructed with a minimum of two associated tracks with $p_T > 400$ MeV. The vertex with the highest $\sum p_T^2$ of the associated tracks is selected as the primary vertex of the event.

This analysis defines two categories of identified leptons and jets, referred to as *preselected* and *signal*, where signal leptons and jets are a subset of preselected leptons and jets, respectively.

Preselected electrons are reconstructed with $p_T > 4.5$ GeV and within the pseudorapidity range of $|\eta| < 2.47$. Furthermore, they are required to pass the likelihood-based *VeryLoose* identification, which is similar to the likelihood-based *Loose* identification defined

in Ref. [105] but has a higher electron identification efficiency. The likelihood-based electron identification criteria are based on calorimeter shower shape and inner detector track information. Preselected muons are identified using the *Medium* criterion defined in Ref. [106] and required to satisfy $p_T > 4$ GeV and $|\eta| < 2.5$. The longitudinal impact parameter z_0 relative to the primary vertex must satisfy $|z_0 \sin\theta| < 0.5$ mm for both the electrons and muons.

Preselected jets are reconstructed from calorimeter topological clusters [107] in the region $|\eta| < 4.5$ using the anti-k_t algorithm [108,109] with radius parameter $R = 0.4$. The jets are required to have $p_T > 20$ GeV after being calibrated in accord with Ref. [110] and having the expected energy contribution from pileup subtracted according to the jet area [111]. In order to suppress jets due to pileup, jets with $p_T < 60$ GeV and $|\eta| < 2.4$ are required to satisfy the *Medium* working point of the jet vertex tagger [111], which uses information from the tracks associated with the jet. To reject events with detector noise or noncollision backgrounds, events are rejected if they fail basic quality criteria [112].

Jets that contain a b-hadron, referred to as b-jets, are identified within $|\eta| < 2.5$ using the MV2C10 algorithm [113,114]. The working point is chosen so that b-jets from simulated $t\bar{t}$ events are identified with an 85% efficiency, with rejection factors of 3 for charm-quark jets and 34 for light-quark and gluon jets.

The following procedure is used to resolve ambiguities between the reconstructed leptons and jets. It employs the distance measure $\Delta R_y = \sqrt{(\Delta y)^2 + (\Delta \phi)^2}$, where y is the rapidity. Electrons that share an inner detector track with a muon candidate are discarded to remove bremsstrahlung from muons followed by a photon conversion into electron pairs. Non-b-tagged jets that are separated from the remaining electrons by $\Delta R_y < 0.2$ are removed. Jets that lie $\Delta R_y < 0.4$ from a muon candidate and contain fewer than three tracks with $p_T > 500$ MeV are removed to suppress muon bremsstrahlung. Electrons or muons that lie $\Delta R_y < 0.4$ from surviving jet candidates are removed to suppress bottom and charm hadron decays.

Additional requirements on leptons that survive preselection are optimized for signal efficiency and background rejection. Signal electrons must satisfy the *Tight* identification criterion [115], and be compatible with originating from the primary vertex, with the significance of the transverse impact parameter defined relative to the beam position satisfying $|d_0|/\sigma(d_0) < 5$. From the remaining preselected muons, signal muons must satisfy $|d_0|/\sigma(d_0) < 3$.

The *GradientLoose* and *FixedCutTightTrackOnly* isolation criteria, as detailed in Ref. [106], are imposed on signal electrons and muons, respectively, to reduce contributions from fake/nonprompt leptons arising from jets

misidentified as leptons, photon conversions, or semileptonic decays of heavy-flavor hadrons. These isolation requirements are either based on the presence of additional tracks or based on clusters of calorimeter energy depositions inside a small cone around the lepton candidate. Contributions from any other preselected leptons are excluded in order to preserve efficiencies for signals with small dilepton invariant mass.

After all lepton selection criteria are applied, the efficiency for reconstructing and identifying signal electrons within the detector acceptance in the Higgsino and slepton signal samples range from 15% for $p_T = 4.5$ GeV to over 70% for $p_T > 30$ GeV. The corresponding efficiency for signal muons ranges from approximately 50% at $p_T = 4$ GeV to over 85% for $p_T > 30$ GeV. Of the total predicted background, the fraction due to fake/nonprompt electrons in an event sample with opposite-sign, different-flavor leptons falls from approximately 80% at $p_T = 4.5$ GeV to less than 5% for $p_T > 30$ GeV, while the fraction of fake/nonprompt muons in the same sample falls from 80% at $p_T = 4$ GeV to less than 8% for $p_T > 30$ GeV.

From the sample of preselected jets, signal jets are selected if they satisfy $p_T > 30$ GeV and $|\eta| < 2.8$, except for b-tagged jets where the preselected jet requirement of $p_T > 20$ GeV is maintained to maximize the rejection of the $t\bar{t}$ background.

Small corrections are applied to reconstructed electrons, muons, and b-tagged jets in the simulated samples to match the reconstruction efficiencies in data. The corrections for b-tagged jets account for the differences in b-jet identification efficiencies as well as misidentification rates of c-, and light-flavor/gluon initiated jets between data and simulated samples. The corrections for low-momentum leptons are obtained from $J/\psi \to ee/\mu\mu$ events with the same tag-and-probe methods as used for higher-p_T electrons [105] and muons [106].

The missing transverse momentum $\mathbf{p}_T^{\text{miss}}$, with magnitude E_T^{miss}, is defined as the negative vector sum of the transverse momenta of all reconstructed objects (electrons, muons and jets) and an additional soft term. The soft term is constructed from all tracks that are not associated with any object, but that are associated with the primary vertex. In this way, E_T^{miss} is adjusted for the best calibration of the jets and the other identified physics objects above, while maintaining pileup independence in the soft term [116].

V. SIGNAL REGION SELECTION

Table II summarizes the event selection criteria for all signal regions (SRs). A candidate event is required to contain exactly two preselected same-flavor opposite-charge leptons (e^+e^- or $\mu^+\mu^-$), both of which must also be signal leptons. In the SUSY signals considered, the highest sensitivity from this selection arises from two

leptons produced either by the $\tilde{\chi}_2^0$ decay via an off-shell Z boson, or by the slepton decays. The lepton with the higher (lower) p_T of each pair is referred to as the leading (subleading) lepton and is denoted by ℓ_1 (ℓ_2). The leading lepton is required to have $p_T^{\ell_1} > 5$ GeV, which suppresses background due to fake/nonprompt leptons. The p_T threshold for the subleading lepton remains at 4.5 GeV for electrons and 4 GeV for muons to retain signal acceptance. Requiring the separation $\Delta R_{\ell\ell}$ between the two leptons to be greater than 0.05 suppresses nearly collinear lepton pairs originating from photon conversions or muons giving rise to spurious pairs of tracks with shared hits. The invariant mass $m_{\ell\ell}$ of the lepton pair is required to be greater than 1 GeV for the same reason. The dilepton invariant mass is further required to be outside of the [3.0, 3.2] GeV window to suppress contributions from J/ψ decays, and less than 60 GeV to suppress contributions from on-shell Z boson decays. No veto is implemented around other resonances such as Υ or ψ states, which are expected to contribute far less to the SRs.

The reconstructed E_T^{miss} is required to be greater than 200 GeV, where the efficiency of the triggers used in the analysis exceeds 95%. For signal events to pass this E_T^{miss} requirement, the two $\tilde{\chi}_1^0$ momenta must align by recoiling against hadronic initial-state radiation. This motivates the requirements on the leading jet (denoted by j_1) of $p_T^{j_1} > 100$ GeV and $\Delta\phi(j_1, \mathbf{p}_T^{\text{miss}}) > 2.0$, where $\Delta\phi(j_1, \mathbf{p}_T^{\text{miss}})$ is the azimuthal separation between j_1 and $\mathbf{p}_T^{\text{miss}}$. In addition, a minimum azimuthal separation requirement $\min(\Delta\phi(\text{any jet}, \mathbf{p}_T^{\text{miss}})) > 0.4$ between any signal jet in the event and $\mathbf{p}_T^{\text{miss}}$ reduces the effect of jet-energy mismeasurement on E_T^{miss}.

The leading sources of irreducible background are $t\bar{t}$, single-top, $WW/WZ +$ jets (hereafter referred to as WW/WZ), and $Z^{(*)}/\gamma^*(\to \tau\tau) +$ jets. The dominant source of reducible background arises from processes where one or more leptons are fake/nonprompt, such as in $W +$ jets production.

Events containing b-tagged jets are rejected to reduce the $t\bar{t}$ and single-top background. The $Z^{(*)}/\gamma^*(\to \tau\tau) +$ jets background is suppressed using the $m_{\tau\tau}$ variable [16,31,37], defined by $m_{\tau\tau} = \text{sign}(m_{\tau\tau}^2)\sqrt{|m_{\tau\tau}^2|}$, which is the signed square root of $m_{\tau\tau}^2 \equiv 2p_{\ell_1} \cdot p_{\ell_2}(1 + \xi_1)(1 + \xi_2)$, where p_{ℓ_1} and p_{ℓ_2} are the lepton four-momenta, while the parameters ξ_1 and ξ_2 are determined by solving $\mathbf{p}_T^{\text{miss}} = \xi_1 \mathbf{p}_T^{\ell_1} + \xi_2 \mathbf{p}_T^{\ell_2}$. The definition of $m_{\tau\tau}$ approximates the invariant mass of a leptonically decaying τ-lepton pair if both τ-leptons are sufficiently boosted so that the daughter neutrinos from each τ decay are collinear with the visible lepton momentum. The $m_{\tau\tau}$ variable can take negative values in events where one of the lepton momenta has a smaller magnitude than E_T^{miss} and points in the hemisphere

TABLE II. Summary of event selection criteria. The binning scheme used to define the final signal regions is shown in Table III. Signal leptons and signal jets are used when applying all requirements.

Variable	Common requirement	
Number of leptons	$=2$	
Lepton charge and flavor	e^+e^- or $\mu^+\mu^-$	
Leading lepton $p_T^{\ell_1}$	>5 (5) GeV for electron (muon)	
Subleading lepton $p_T^{\ell_2}$	>4.5 (4) GeV for electron (muon)	
$\Delta R_{\ell\ell}$	>0.05	
$m_{\ell\ell}$	$\in [1, 60]$ GeV excluding $[3.0, 3.2]$ GeV	
E_T^{miss}	>200 GeV	
Number of jets	≥ 1	
Leading jet p_T	>100 GeV	
$\Delta\phi(j_1, \mathbf{p}_T^{\mathrm{miss}})$	>2.0	
$\min(\Delta\phi(\text{any jet}, \mathbf{p}_T^{\mathrm{miss}}))$	>0.4	
Number of b-tagged jets	$= 0$	
$m_{\tau\tau}$	<0 or >160 GeV	
	Electroweakino SRs	Slepton SRs
$\Delta R_{\ell\ell}$	<2	$\cdots$
$m_T^{\ell_1}$	<70 GeV	$\cdots$
$E_T^{\mathrm{miss}}/H_T^{\mathrm{lep}}$	$> \max\left(5, 15 - 2\frac{m_{\ell\ell}}{1\,\mathrm{GeV}}\right)$	$> \max\left(3, 15 - 2\left(\frac{m_{\mathrm{T2}}^{100}}{1\,\mathrm{GeV}} - 100\right)\right)$
Binned in	$m_{\ell\ell}$	m_{T2}^{100}

opposite to the $\mathbf{p}_T^{\mathrm{miss}}$ vector. Events with $0 < m_{\tau\tau} < 160$ GeV are rejected. After the common and electroweakino SR selections in Table II are applied, this veto retains 75% of the Higgsino signal with $m(\tilde{\chi}_2^0) = 110$ GeV and $m(\tilde{\chi}_1^0) = 100$ GeV, while 87% of the $Z^{(*)}/\gamma^*(\to \tau\tau)+$ jets background is rejected.

After applying the common selection requirements above, two sets of SRs are constructed to separately target the production of electroweakinos and sleptons.

In electroweakino production, the two leptons originating from $Z^* \to \ell\ell$ are both soft, and their invariant mass is small. Because of the recoil of the SUSY particle system against a jet from initial-state radiation, the angular separation $\Delta R_{\ell\ell}$ between the two leptons is required to be smaller than 2.0. The transverse mass of the leading lepton and E_T^{miss}, defined as $m_T^{\ell_1} = \sqrt{2(E_T^{\ell_1}E_T^{\mathrm{miss}} - \mathbf{p}_T^{\ell_1} \cdot \mathbf{p}_T^{\mathrm{miss}})}$, is required to be smaller than 70 GeV to reduce the background from $t\bar{t}$, WW/WZ, and $W + $ jets. The dilepton invariant mass $m_{\ell\ell}$ is correlated with $\Delta m(\tilde{\chi}_2^0, \tilde{\chi}_1^0)$, illustrated in Fig. 2, and is used to define the binning of the electroweakino SRs as further described below.

In slepton pair production, the event topology can be used to infer the slepton mass given the LSP mass. The stransverse mass [39,40] is defined by

$$m_{\mathrm{T2}}^{m_\chi}(\mathbf{p}_T^{\ell_1}, \mathbf{p}_T^{\ell_2}, \mathbf{p}_T^{\mathrm{miss}})$$
$$= \min_{\mathbf{q}_T}[\max(m_T(\mathbf{p}_T^{\ell_1}, \mathbf{q}_T, m_\chi), m_T(\mathbf{p}_T^{\ell_2}, \mathbf{p}_T^{\mathrm{miss}} - \mathbf{q}_T, m_\chi))],$$

where m_χ is the hypothesized mass of the invisible particles, and the transverse vector $\mathbf{q}_T$ with magnitude q_T is chosen to minimize the larger of the two transverse masses, defined by

$$m_T(\mathbf{p}_T, \mathbf{q}_T, m_\chi)$$
$$= \sqrt{m_\ell^2 + m_\chi^2 + 2\left(\sqrt{p_T^2 + m_\ell^2}\sqrt{q_T^2 + m_\chi^2} - \mathbf{p}_T \cdot \mathbf{q}_T\right)}.$$

For events arising from signals with slepton mass $m(\tilde{\ell})$ and LSP mass $m(\tilde{\chi}_1^0)$, the values of $m_{\mathrm{T2}}^{m_\chi}$ are bounded from above by $m(\tilde{\ell})$ when m_χ is equal to $m(\tilde{\chi}_1^0)$, i.e. $m_{\mathrm{T2}}^{m_\chi} \leq m(\tilde{\ell})$ for $m_\chi = m(\tilde{\chi}_1^0)$. The stransverse mass with $m_\chi = 100$ GeV, denoted m_{T2}^{100}, is used to define the binning of the slepton SRs as further described below. The chosen value of 100 GeV is based on the expected LSP masses of the signals targeted by this analysis. The distribution of m_{T2}^{100} does not vary significantly for signals where $m(\tilde{\chi}_1^0) \neq 100$ GeV.

The scalar sum of the lepton transverse momenta $H_T^{\mathrm{lep}} = p_T^{\ell_1} + p_T^{\ell_2}$ is smaller in compressed-scenario SUSY signal events than in background events such as SM production of WW or WZ. The ratio $E_T^{\mathrm{miss}}/H_T^{\mathrm{lep}}$ provides signal-to-background discrimination which improves for smaller mass splittings in the signals and is therefore used as a sensitive variable in both the electroweakino and slepton SRs. The minimum value of the $E_T^{\mathrm{miss}}/H_T^{\mathrm{lep}}$ requirement is adjusted event by event
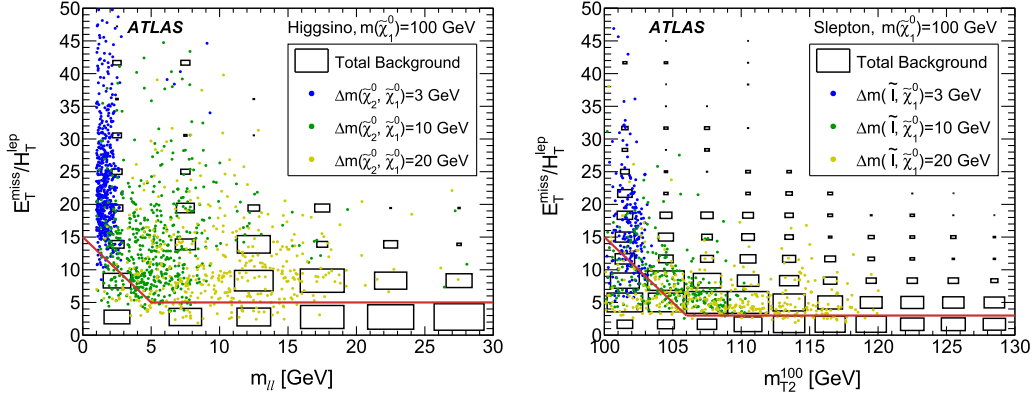
FIG. 3.   Distributions of E_T^{miss}/H_T^{lep} for the electroweakino (left) and slepton (right) SRs, after applying all signal region selection criteria except those on E_T^{miss}/H_T^{lep}, $m_{\ell\ell}$, and m_{T2}. The solid red line indicates the requirement applied in the signal region; events in the region below the red line are rejected. Representative benchmark signals for the Higgsino (left) and slepton (right) simplified models are shown as circles. Both signal and background are normalized to their expected yields in 36.1 fb^{-1}. The total background includes the MC prediction for all the processes listed in Table I and a data-driven estimate for fake/nonprompt leptons discussed further in Sec. VI.

according to the size of the mass splitting inferred from the event kinematics. For the electroweakino SRs, this is achieved with $m_{\ell\ell}$ as $E_T^{miss}/H_T^{lep} > \max[5, 15 - 2m_{\ell\ell}/(1 \text{ GeV})]$. For the slepton SRs, $m_{T2}^{100} - 100$ GeV is used as $E_T^{miss}/H_T^{lep} > \max[3, 15 - 2\{m_{T2}^{100}/(1 \text{ GeV}) - 100\}]$. Figure 3 illustrates the E_T^{miss}/H_T^{lep} requirement for electroweakino and slepton SRs.

Table III defines the binning of the SRs. The electroweakino SRs are divided into seven nonoverlapping ranges of $m_{\ell\ell}$, which are further divided by lepton flavor (ee, $\mu\mu$), and referred to as exclusive regions. Seven inclusive regions are also defined, characterized by overlapping ranges of $m_{\ell\ell}$. For the slepton SRs, m_{T2}^{100} is used to define 12 exclusive regions and 6 inclusive regions. When setting model-dependent limits on the electroweakino (slepton) signals, only the exclusive SRee-$m_{\ell\ell}$ and SR$\mu\mu$-$m_{\ell\ell}$ regions (SRee-m_{T2}^{100} and SR$\mu\mu$-m_{T2}^{100} regions) are statistically combined in a simultaneous fit. When setting model-independent upper limits on new physics signals,

only the inclusive SR$\ell\ell$-$m_{\ell\ell}$ and SR$\ell\ell$-m_{T2}^{100} regions are considered. The details of these statistical procedures are given in Sec. VIII.

After all selection criteria are applied, the Higgsino model with $m(\tilde{\chi}_2^0) = 110$ GeV and $m(\tilde{\chi}_1^0) = 100$ GeV has an acceptance times efficiency of 6.5×10^{-5} in SR$\ell\ell$-$m_{\ell\ell}$ [1, 60]. The acceptance times efficiency in SR$\ell\ell$-m_{T2}^{100} [100, ∞] for the slepton model, with $m(\tilde{\ell}) = 110$ GeV and $m(\tilde{\chi}_1^0) = 100$ GeV, is 3.3×10^{-3}.

VI. BACKGROUND ESTIMATON

A common strategy is used to determine the SM background in all SRs. The dominant sources of irreducible background events that contain two prompt leptons, missing transverse momentum and jets are $t\bar{t}$, tW, WW/WZ, and $Z^{(*)}/\gamma^*(\to \tau\tau) +$ jets, which are estimated using MC simulation. The main reducible backgrounds are from events containing fake/nonprompt leptons. These processes are estimated collectively with a data-driven method. While

TABLE III.   Signal region binning for the electroweakino and slepton SRs. Each SR is defined by the lepton flavor (ee, $\mu\mu$, or $\ell\ell$ for both) and a range of $m_{\ell\ell}$ (for electroweakino SRs) or m_{T2}^{100} (for slepton SRs) in GeV. The inclusive bins are used to set model-independent limits, while the exclusive bins are used to derive exclusion limits on signal models.

	Electroweakino SRs							
Exclusive	SRee-$m_{\ell\ell}$, SR$\mu\mu$-$m_{\ell\ell}$	[1, 3]	[3.2, 5]	[5, 10]	[10, 20]	[20, 30]	[30, 40]	[40, 60]
Inclusive	SR$\ell\ell$-$m_{\ell\ell}$	[1, 3]	[1, 5]	[1, 10]	[1, 20]	[1, 30]	[1, 40]	[1, 60]
	Slepton SRs							
Exclusive	SRee-m_{T2}^{100}, SR$\mu\mu$-m_{T2}^{100}		[100, 102]	[102, 105]	[105, 110]	[110, 120]	[120, 130]	[130, ∞]
Inclusive	SR$\ell\ell$-m_{T2}^{100}		[100, 102]	[100, 105]	[100, 110]	[100, 120]	[100, 130]	[100, ∞]

TABLE IV.   Definition of control and validation regions. The common selection criteria in Table II are implied unless otherwise specified.

Region	Leptons	E_T^{miss}/H_T^{lep}	Additional requirements
CR-top	$e^\pm e^\mp$, $\mu^\pm\mu^\mp$, $e^\pm\mu^\mp$, $\mu^\pm e^\mp$	>5	≥ 1 b-tagged jet(s)
CR-tau	$e^\pm e^\mp$, $\mu^\pm\mu^\mp$, $e^\pm\mu^\mp$, $\mu^\pm e^\mp$	$\in [4, 8]$	$m_{\tau\tau} \in [60, 120]$ GeV
VR-VV	$e^\pm e^\mp$, $\mu^\pm\mu^\mp$, $e^\pm\mu^\mp$, $\mu^\pm e^\mp$	<3	
VR-SS	$e^\pm e^\pm$, $\mu^\pm\mu^\pm$, $e^\pm\mu^\pm$, $\mu^\pm e^\pm$	>5	
VRDF-$m_{\ell\ell}$	$e^\pm\mu^\mp$, $\mu^\pm e^\mp$	$> \max\left(5, 15 - 2\frac{m_{\ell\ell}}{1\,\text{GeV}}\right)$	$\Delta R_{\ell\ell} < 2$, $m_T^{\ell_1} < 70$ GeV
VRDF-m_{T2}^{100}	$e^\pm\mu^\mp$, $\mu^\pm e^\mp$	$> \max\left(3, 15 - 2(\frac{m_{T2}^{100}}{1\,\text{GeV}} - 100)\right)$	

the fake/nonprompt lepton background tends to be dominant at low values of $m_{\ell\ell}$ and m_{T2}^{100}, the irreducible $t\bar{t}$, tW, WW/WZ processes are more important at the upper end of the distributions.

A. Irreducible background

The MC simulations of $t\bar{t}$, tW and $Z^{(*)}/\gamma^*(\to \tau\tau) + $ jets background processes are normalized in a simultaneous fit to the observed data counts in control regions (CRs) using statistical procedures detailed in Sec. VIII. The CRs are designed to be statistically disjoint from the SRs, to be enriched in a particular background process, to have minimal contamination from the signals considered, and to exhibit kinematic properties similar to the SRs. The event rates in the SRs are then predicted by extrapolating from the CRs using the simulated MC distributions. This extrapolation is validated using events in dedicated validation

regions (VRs), which are not used to constrain the fit and are orthogonal in selection to the CRs and SRs. The definitions of these regions are summarized in Table IV.

The $t\bar{t}$ and tW, diboson WW/WZ, and $Z^{(*)}/\gamma^*(\to \tau\tau) + $ jets processes containing two prompt leptons all yield same-flavor lepton pairs (ee and $\mu\mu$) at the same rate as for different-flavor pairs ($e\mu$ and μe, where the first lepton is the leading lepton). To enhance the statistical constraining power of the respective CRs, all possible flavor assignments (ee, $\mu\mu$, $e\mu$, and μe) are selected when defining the CRs.

Two single-bin CRs are considered, which have all the selections in Table II applied unless stated otherwise in Table IV. A sample enriched in top quarks with 71% purity, CR-top, is defined by selecting events with at least one b-tagged jet. This CR has 1100 observed events and is used to constrain the normalization of the $t\bar{t}$ and tW processes with dilepton final states. A sample enriched
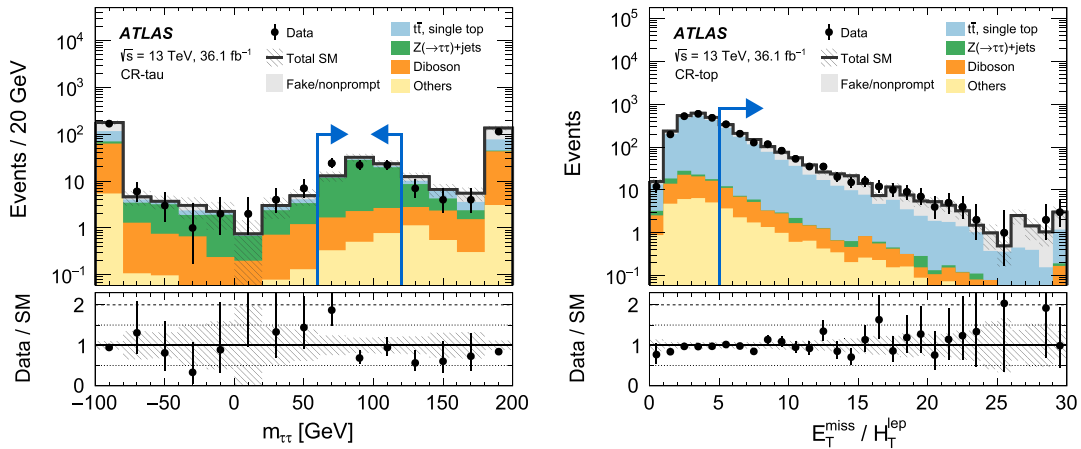
FIG. 4.   Examples of kinematic distributions after the background-only fit showing the data as well as the expected background in control regions CR-tau (left) and CR-top (right). The full event selection of the corresponding regions is applied, except for the requirement that is imposed on the variable being plotted. This requirement is indicated by blue arrows in the distributions. The first (last) bin includes underflow (overflow). Background processes containing fewer than two prompt leptons are categorized as "Fake/nonprompt." The category "Others" contains rare backgrounds from triboson, Higgs boson, and the remaining top-quark production processes listed in Table I. The uncertainty bands plotted include all statistical and systematic uncertainties.

in the $Z^{(*)}/\gamma^*(\to \tau\tau) +$ jets processes with 83% purity, CR-tau, is constructed by selecting events satisfying $60 < m_{\tau\tau} < 120\,\mathrm{GeV}$. This CR has 68 observed events and the variable $E_{\mathrm{T}}^{\mathrm{miss}}/H_{\mathrm{T}}^{\mathrm{lep}}$ is required to have a value between 4 and 8 to reduce potential contamination from signal events. Figure 4 shows the background composition of the CR-tau and CR-top regions. The signal contamination in both regions is typically below 3% and is at most 11%.

It is difficult to select a sample of diboson events pure enough to be used to constrain their contribution to the SRs. The diboson background is therefore estimated with MC simulation. A diboson VR, denoted by VR-VV, is constructed by requiring $E_{\mathrm{T}}^{\mathrm{miss}}/H_{\mathrm{T}}^{\mathrm{lep}} < 3.0$. This sample consists of approximately 40% diboson events, 20% fake/nonprompt lepton events, 25% $t\bar{t}$ and single-top events, and smaller contributions from $Z^{(*)}/\gamma^* \to \tau\tau$ and other processes. The signal contamination in VR-VV is at most 9%. This region is used to test the modeling of the diboson background and the associated systematic uncertainties.

Additional VRs are constructed from events with different-flavor ($e\mu$ and μe) leptons. These VRs, VRDF-$m_{\ell\ell}$ and VRDF-m_{T2}^{100}, are defined using the same selection criteria as the electroweakino and slepton SRs, respectively, and are used to validate the extrapolation of background in the fitting procedure within the same kinematic regime as the SRs. The electroweakino signal contamination in VRDF-$m_{\ell\ell}$ is always below 8%, while the slepton signal contamination in VRDF-m_{T2}^{100} is always negligible.

For each VR, the level of agreement between the kinematic distributions of data and predicted events is checked. The VRDF-$m_{\ell\ell}$ and VRDF-m_{T2}^{100} regions are also presented binned in $m_{\ell\ell}$ and m_{T2}^{100}, respectively, using the same intervals as the exclusive SRs in Table III to ensure that these VRs consist of events with the same kinematic selection as the SRs.

B. Reducible background

Two sources of reducible background are considered: processes where fake/nonprompt leptons are amongst the two selected signal leptons, and those where the reconstructed $E_{\mathrm{T}}^{\mathrm{miss}}$ values are instrumental in origin.

The fake/nonprompt lepton background arises from jets misidentified as leptons, photon conversions, or semileptonic decays of heavy-flavor hadrons. Studies based on simulated samples indicate that the last of these is the dominant component in the SRs. Since MC simulation is not expected to model these processes accurately, the data-driven fake factor method [117] is employed.

The fake factor procedure first defines a tight set of criteria, labeled ID, corresponding to the requirements applied to signal leptons used in the analysis. Second, a loose set of criteria, labeled anti-ID, has one or more of the identification, isolation, or $|d_0|/\sigma(d_0)$ requirements inverted relative to signal leptons to obtain an orthogonal sample enriched in fake/nonprompt leptons. The ratio of ID to anti-ID leptons defines the fake factor.

The fake factors are measured in events collected with prescaled single-lepton triggers. These single-lepton triggers have lepton identification requirements looser than those used in the anti-ID lepton selection, and have p_{T} thresholds ranging from 4 to 20 GeV. This sample, referred to as the measurement region, is dominated by multijet events with fake/nonprompt leptons. Both the electron and muon fake factors are measured in this region as a function of reconstructed lepton p_{T}. The muon fake factors are also found to have a dependence on the number of b-tagged jets in the event. The fake factors used in CR-top are therefore computed in events with >0 b-tagged jets, while all other regions use fake factors computed using events with zero b-tagged jets.

To obtain the fake/nonprompt lepton prediction in a particular region, these fake factors are applied to events satisfying the corresponding selection requirements, except with an anti-ID lepton replacing an ID lepton. MC studies indicate that the leptons in the anti-ID region arise from processes similar to those for fake/nonprompt leptons passing the signal selection requirements in the SR. The contributions from prompt leptons that pass the ID and anti-ID requirements in the measurement region, and that pass the anti-ID requirements in the region under study, are subtracted using MC simulation. The yields from this procedure are cross-checked in VRs, named VR-SS, which have similar kinematic selections as the SRs, but are enriched in fake/nonprompt leptons by requiring two leptons with the same electric charge. As the subleading lepton is found to be the fake/nonprompt lepton in most cases, the VR-SS are divided into $ee + \mu e$ and $\mu\mu + e\mu$, where the left (right) lepton of each pair denotes the leading (subleading) lepton. The fraction of events in which both leptons are fake/nonprompt is found to be small by considering the rate of anti-ID leptons in data. The electroweakino signal contamination in VR-SS is typically negligible, and always below 7%, while the slepton signal contamination in VR-SS is always negligible.

Background processes with no invisible particles can satisfy the $E_{\mathrm{T}}^{\mathrm{miss}} > 200\,\mathrm{GeV}$ requirement when the momenta of visible leptons or jets are mismeasured by the detector. Contributions of these events in the SRs arising from processes such as Drell–Yan dilepton production are studied with MC simulation and are found to be negligible. This estimate is cross-checked with a data-driven method using independent event samples defined by relaxed or inverted selection criteria. A lower $E_{\mathrm{T}}^{\mathrm{miss}}$ requirement is used to accept a higher rate of $Z^{(*)}/\gamma^* \to \ell^+\ell^-$
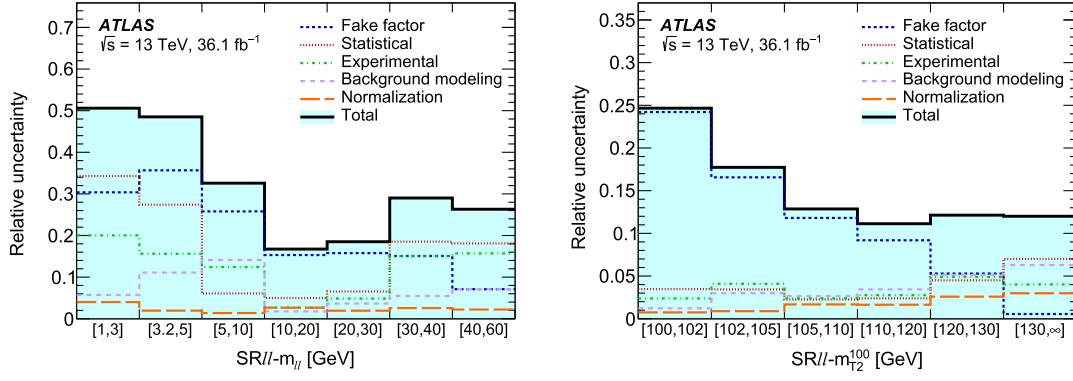
FIG. 5.   The relative systematic uncertainties in the background prediction in the exclusive electroweakino (left) and slepton (right) SRs. The individual uncertainties can be correlated and do not necessarily add up in quadrature to the total uncertainty.

events, while relaxed requirements on the kinematics of the leading jet, $m_{\tau\tau}$, E_T^{miss}/H_T^{lep}, and lepton isolation minimize the impact of any signal contamination. The results from the data-driven method are consistent with the estimates based on MC simulation.

VII. SYSTEMATIC UNCERTAINTIES

The sources of systematic uncertainty affecting the background and signal predictions consist of uncertainties due to experimental sources, which include those from the fake factor method, and uncertainties arising from the theoretical modeling in simulated samples.

The largest sources of experimental systematic uncertainty is the fake/nonprompt background prediction from the fake factor procedure. In this method, systematic uncertainties arise from the size of the samples used to measure the fake factors, which are uncorrelated between events with respect to the p_T and flavor of the anti-ID lepton, but otherwise correlated across the different CRs and SRs. Additional uncertainties are assigned to account for differences in the event and lepton kinematics between
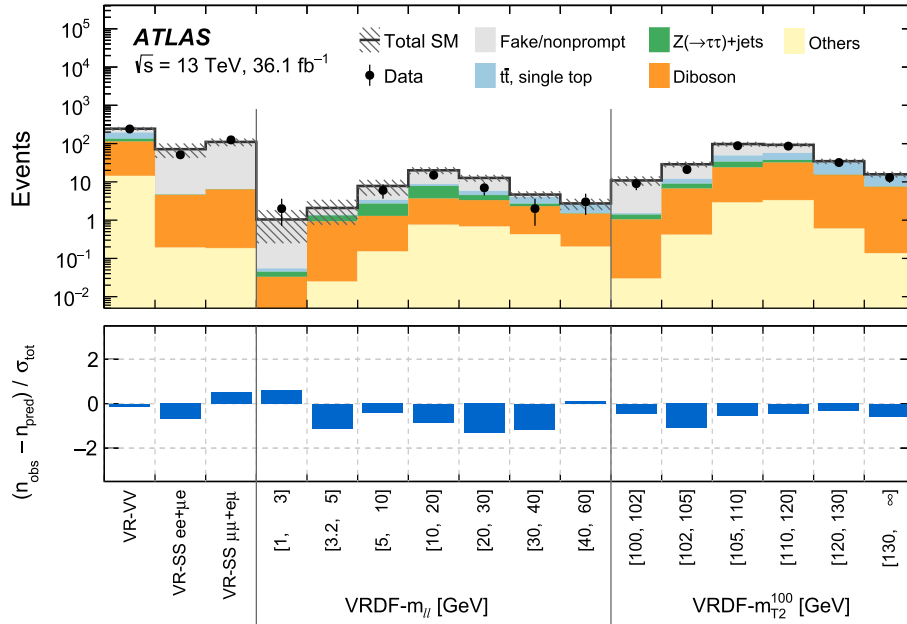
FIG. 6.   Comparison of observed and expected event yields in the validation regions after the background-only fit. Background processes containing fewer than two prompt leptons are categorized as "Fake/nonprompt." The category "Others" contains rare backgrounds from triboson, Higgs boson, and the remaining top-quark production processes listed in Table I. Uncertainties in the background estimates include both the statistical and systematic uncertainties, where σ_{tot} denotes the total uncertainty.

the measurement region and SRs. The differences between the fake factor prediction and observed data in the VR-SS regions are used to assign additional systematic uncertainties. These uncertainties are considered correlated across the different SRs, but uncorrelated as regards the flavor of the anti-ID lepton in the event. Uncertainties originating from the MC-based subtraction of prompt leptons in the fake factor measurement region are found to be negligible.

Further significant experimental systematic uncertainties are related to the jet energy scale and resolution, flavor-tagging, and the reweighting procedure applied to simulated events to match pileup conditions observed in data. Uncertainties in the lepton reconstruction and identification efficiencies, together with energy/momentum scale and resolution also contribute, but are found to be small. The systematic uncertainties for low-momentum leptons are

derived using the same procedure as for higher-p_T electrons [105] and muons [106].

In addition to the experimental uncertainties, several sources of theoretical modeling uncertainty affect the simulated samples of the dominant SM backgrounds, i.e. $t\bar{t}$, tW, $Z^{(*)}/\gamma^*(\to \tau\tau)$ + jets, and diboson processes. The effects of the QCD renormalization and factorization scale uncertainties are evaluated by independently varying the corresponding event generator parameters up and down by a factor of 2. The impact of the uncertainty of the strong coupling constant α_S on the acceptance is also considered. The effects of PDF uncertainties are evaluated by reweighting the simulated samples to the CT14 [118] and MMHT2014 [119] PDF sets and taking the envelope of the predicted yields. The theoretical modeling uncertainties are evaluated in each of the CRs and SRs and their effect is correlated for events across all regions. For the dileptonic
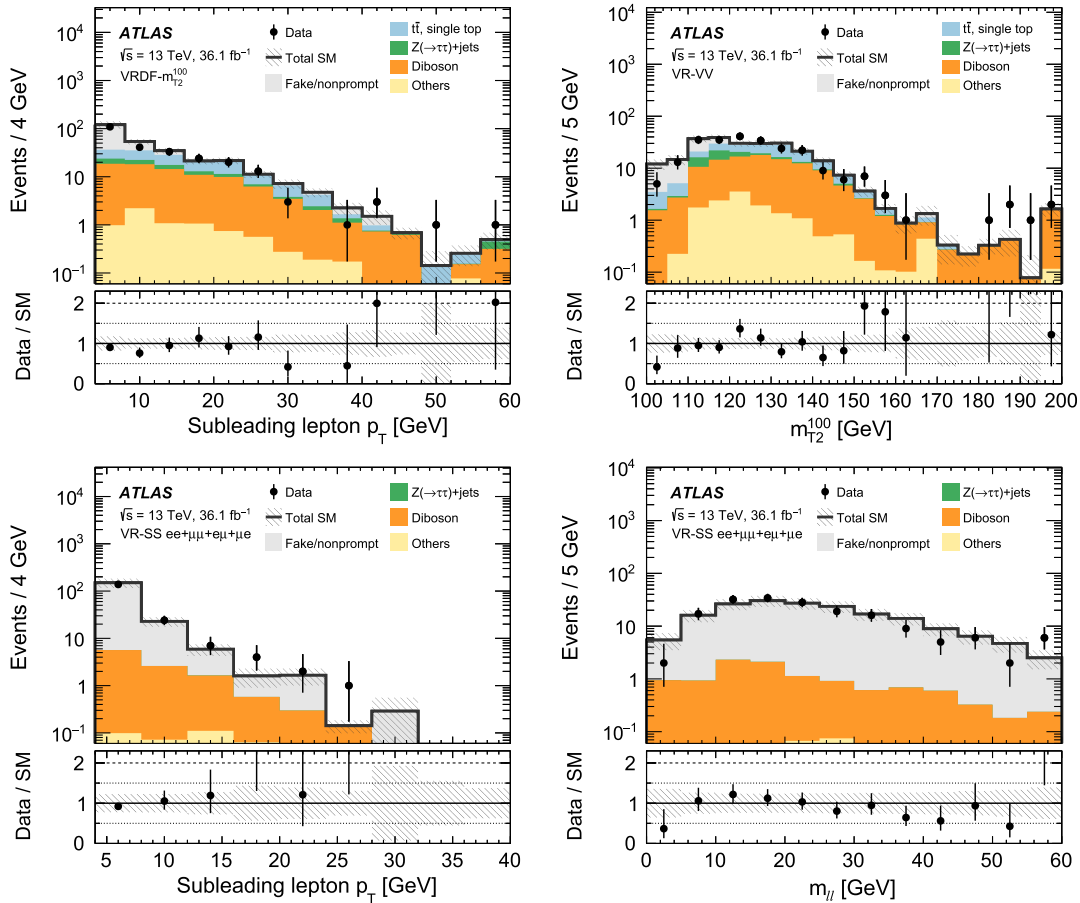
FIG. 7. Kinematic distributions after the background-only fit showing the data and the expected background in the different-flavor validation region VRDF-m_{T2}^{100} (top left), the diboson validation region VR-VV (top right), and the same-sign validation region VR-SS inclusive of lepton flavor (bottom). Similar levels of agreement are observed in other kinematic distributions for VR-SS and VR-VV. Background processes containing fewer than two prompt leptons are categorized as "Fake/nonprompt." The category "Others" contains rare backgrounds from triboson, Higgs boson, and the remaining top-quark production processes listed in Table I. The last bin includes overflow. The uncertainty bands plotted include all statistical and systematic uncertainties. Orange arrows in the data/SM panel indicate values that are beyond the y axis range.

diboson background, the uncertainties of the normalization and shape in the SRs are dominated by the QCD scale variations. The normalization uncertainties of the top quark and $Z^{(*)}/\gamma^*(\to \tau\tau)$ + jets contributions are constrained by the simultaneous fit, and only the shape uncertainties relating the CRs to the SRs affect the results.

Figure 5 shows the relative size of the various classes of uncertainty in the background predictions in the exclusive electroweakino and slepton SRs. The uncertainties related to the fake factor method are displayed separately from the remaining experimental uncertainties due to their relatively large contribution. The breakdown also includes the uncertainties in the normalization factors of the $Z^{(*)}/\gamma^*(\to \tau\tau)$ + jets and the combined $t\bar{t}$ and tW backgrounds as obtained from CR-tau and CR-top, respectively.

The theoretical modeling uncertainties in the expected yields for SUSY signal models are estimated by varying by a factor of 2 the MG5_aMC@NLO parameters corresponding to the renormalization, factorization and CKKW-L matching scales, as well as the PYTHIA8 shower tune parameters. The overall uncertainties in the signal acceptance range from about 20% to 40% and depend on the SUSY particle mass splitting and the production process. Uncertainties in the signal acceptance due to PDF uncertainties are evaluated following the PDF4LHC15 recommendations [120] and amount to 15% at most for large $\tilde{\chi}^0_2$ or $\tilde{\ell}$ masses. Uncertainties in the shape of the $m_{\ell\ell}$ or m^{100}_{T2} signal distributions due to the sources above are found to be small, and are neglected.
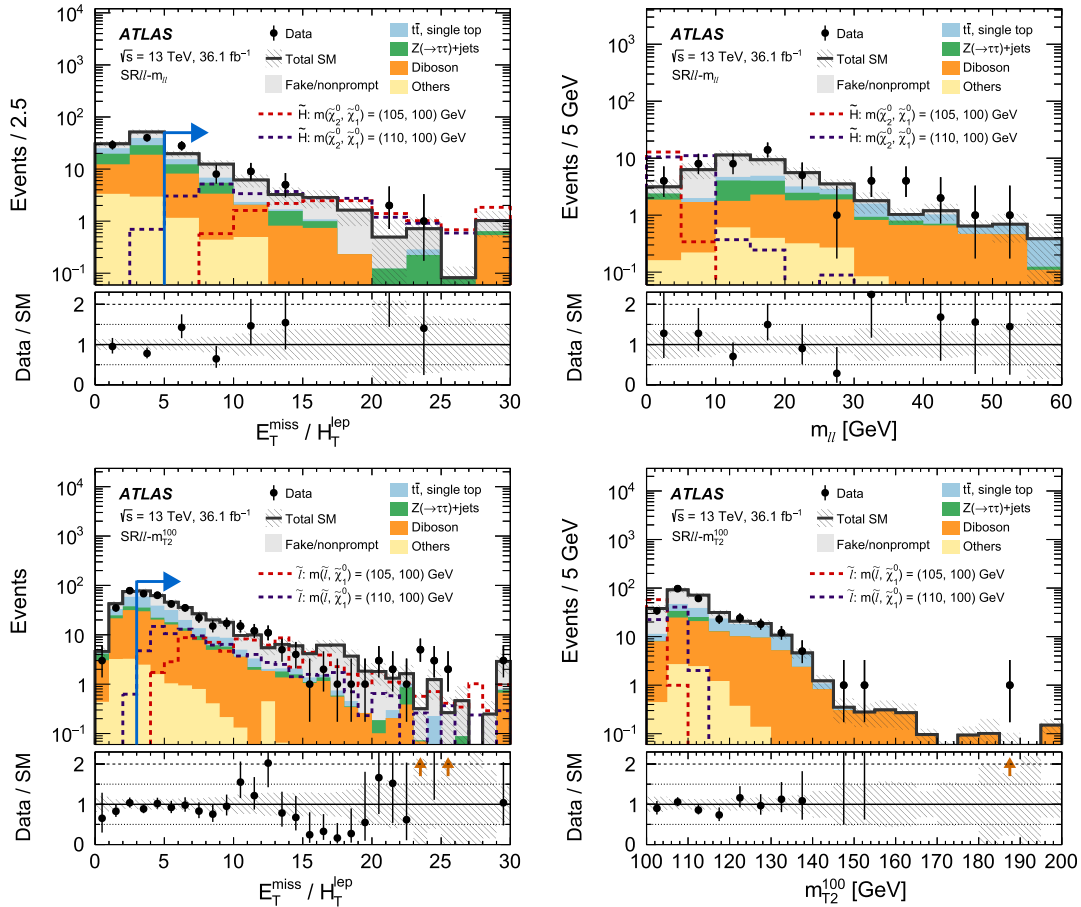
FIG. 8.   Kinematic distributions after the background-only fit showing the data as well as the expected background in the inclusive electroweakino SR$\ell\ell$-$m_{\ell\ell}$ [1, 60] (top) and slepton SR$\ell\ell$-m^{100}_{T2} [100, ∞] (bottom) signal regions. The arrow in the E^{miss}_T/H^{lep}_T variables indicates the minimum value of the requirement imposed in the final SR selection. The $m_{\ell\ell}$ and m_{T2} distributions (right) have all the SR requirements applied. Background processes containing fewer than two prompt leptons are categorized as "Fake/nonprompt." The category "Others" contains rare backgrounds from triboson, Higgs boson, and the remaining top-quark production processes listed in Table I. The uncertainty bands plotted include all statistical and systematic uncertainties. The last bin includes overflow. The dashed lines represent benchmark signal samples corresponding to the Higgsino $\tilde{H}$ and slepton $\tilde{\ell}$ simplified models. Orange arrows in the data/SM panel indicate values that are beyond the y axis range.

TABLE V. Left to right: The first two columns present observed (N_{obs}) and expected (N_{exp}) event yields in the inclusive signal regions. The latter are obtained by the background-only fit of the control regions, and the errors include both statistical and systematic uncertainties. The next two columns show the observed 95% C.L. upper limits on the visible cross section ($\langle \epsilon \sigma \rangle^{95}_{\mathrm{obs}}$) and on the number of signal events (S^{95}_{obs}). The fifth column (S^{95}_{exp}) shows what the 95% C.L. upper limit on the number of signal events would be, given an observed number of events equal to the expected number (and $\pm 1\sigma$ deviations from the expectation) of background events. The last column indicates the discovery p-value ($p(s=0)$), which is capped at 0.5.

Signal Region	N_{obs}	N_{exp}	$\langle \epsilon \sigma \rangle^{95}_{\mathrm{obs}}$ [fb]	S^{95}_{obs}	S^{95}_{exp}	$p(s=0)$
SR$\ell\ell$-$m_{\ell\ell}$ [1, 3]	1	1.7 ± 0.9	0.10	3.8	$4.3^{+1.7}_{-0.7}$	0.50
SR$\ell\ell$-$m_{\ell\ell}$ [1, 5]	4	3.1 ± 1.2	0.18	6.6	$5.6^{+2.3}_{-1.0}$	0.32
SR$\ell\ell$-$m_{\ell\ell}$ [1, 10]	12	8.9 ± 2.5	0.34	12.3	$9.6^{+3.2}_{-1.9}$	0.21
SR$\ell\ell$-$m_{\ell\ell}$ [1, 20]	34	29 ± 6	0.61	22	17^{+7}_{-6}	0.25
SR$\ell\ell$-$m_{\ell\ell}$ [1, 30]	40	38 ± 6	0.59	21	20^{+9}_{-5}	0.38
SR$\ell\ell$-$m_{\ell\ell}$ [1, 40]	48	41 ± 7	0.72	26	20^{+8}_{-5}	0.20
SR$\ell\ell$-$m_{\ell\ell}$ [1, 60]	52	43 ± 7	0.80	29	24^{+5}_{-10}	0.18
SR$\ell\ell$-m^{100}_{T2} [100, 102]	8	12.4 ± 3.1	0.18	7	9^{+4}_{-2}	0.50
SR$\ell\ell$-m^{100}_{T2} [100, 105]	34	38 ± 7	0.49	18	23^{+7}_{-7}	0.50
SR$\ell\ell$-m^{100}_{T2} [100, 110]	131	129 ± 18	1.3	48	47^{+13}_{-15}	0.37
SR$\ell\ell$-m^{100}_{T2} [100, 120]	215	232 ± 29	1.4	52	62^{+21}_{-15}	0.50
SR$\ell\ell$-m^{100}_{T2} [100, 130]	257	271 ± 32	1.7	61	69^{+22}_{-17}	0.50
SR$\ell\ell$-m^{100}_{T2} [100, ∞]	277	289 ± 33	1.8	66	72^{+24}_{-17}	0.50

VIII. RESULTS AND INTERPRETATION

The HISTFITTER package [121] is used to implement the statistical interpretation based on a profile likelihood method [122]. Systematic uncertainties are treated as nuisance parameters in the likelihood.

To determine the SM background predictions independent of the SRs, only the CRs are used to constrain the fit parameters by likelihood maximization assuming no signal events in the CRs; this is referred to as the background-only fit. The normalizations, $\mu_{Z^{(*)}/\gamma^* \to \tau\tau}$ and μ_{top}, respectively for the $Z^{(*)}/\gamma^*(\to \tau\tau) + \mathrm{jets}$ MC sample and the combined $t\bar{t}$ and tW MC samples are extracted in a simultaneous fit to the data events in CR-tau and CR-top, as defined in Sec. VI. The normalization parameters, as obtained from the background-only fit, are $\mu_{Z^{(*)}/\gamma^* \to \tau\tau} = 0.72 \pm 0.13$ and $\mu_{\mathrm{top}} = 1.02 \pm 0.09$, whose uncertainties include statistical and systematic contributions combined.

The accuracy of the background predictions is tested in the VRs discussed in Sec. VI. As illustrated in Fig. 6, the background predictions in the VRs are in good agreement with the observed data yields (deviations $< 1.5\sigma$). Figure 7 shows distributions of the data and the expected backgrounds for a selection of VRs and kinematic variables including the $m_{\ell\ell}$ distribution in VR-VV and the m^{100}_{T2}

distribution in VR-SS. Data and background predictions are compatible within uncertainties.

Figure 8 shows kinematic distributions of the data and the expected backgrounds for the inclusive SRs. No significant excesses of the data above the expected background are observed.

The observed and predicted event yields from the background-only fit are used to set model-independent upper limits on processes beyond the SM by including one inclusive SR at a time in a simultaneous fit with the CRs. Using the CL$_{\mathrm{s}}$ prescription [123], a hypothesis test is performed to set upper limits at the 95% confidence level (C.L.) on the observed (expected) number of signal events $S^{95}_{\mathrm{obs(exp)}}$ in each SR. Dividing S^{95}_{obs} by the integrated luminosity of 36.1 fb^{-1} defines the upper limits on the visible cross sections $\langle \epsilon \sigma \rangle^{95}_{\mathrm{obs}}$. These results are shown in Table V. To quantify the probability under the background-only hypothesis to produce event yields greater than or equal to the observed data the discovery p-values are given as well.

In the absence of any significant deviations from the SM expectation in the inclusive SRs, the results are interpreted as constraints on the SUSY models discussed in Sec. III using the exclusive electroweakino and slepton SRs. The background-only fit is extended to allow for a signal model

TABLE VI. Observed event yields and exclusion fit results with the signal strength parameter set to zero for the exclusive electroweakino and slepton signal regions. Background processes containing fewer than two prompt leptons are categorized as "Fake/nonprompt." The category "Others" contains rare backgrounds from triboson, Higgs boson, and the remaining top-quark production processes listed in Table I. Uncertainties in the fitted background estimates combine statistical and systematic uncertainties.

SRee-$m_{\ell\ell}$	[1, 3] GeV	[3.2, 5] GeV	[5, 10] GeV	[10, 20] GeV	[20, 30] GeV	[30, 40] GeV	[40, 60] GeV
Observed events	0	1	1	10	4	6	2
Fitted SM events	$0.01^{+0.11}_{-0.01}$	$0.6^{+0.7}_{-0.6}$	2.4 ± 1.0	8.3 ± 1.6	4.0 ± 1.0	2.4 ± 0.6	1.4 ± 0.5
Fake/nonprompt leptons	$0.00^{+0.08}_{-0.00}$	$0.02^{+0.12}_{-0.02}$	1.4 ± 0.9	4.0 ± 1.5	1.6 ± 0.9	0.7 ± 0.6	$0.02^{+0.11}_{-0.02}$
Diboson	$0.007^{+0.014}_{-0.007}$	$0.28^{+0.29}_{-0.28}$	0.51 ± 0.28	1.9 ± 0.6	1.36 ± 0.31	0.72 ± 0.22	0.80 ± 0.28
$Z(\to\tau\tau)+$jets	$0.000^{+0.007}_{-0.000}$	$0.3^{+0.8}_{-0.3}$	$0.3^{+0.5}_{-0.3}$	1.7 ± 0.7	$0.25^{+0.26}_{-0.25}$	0.20 ± 0.18	$0.04^{+0.28}_{-0.04}$
$t\bar{t}$, single top	$0.00^{+0.08}_{-0.00}$	$0.02^{+0.12}_{-0.02}$	$0.11^{+0.14}_{-0.11}$	0.44 ± 0.29	0.63 ± 0.35	0.7 ± 0.4	0.6 ± 0.4
Others	$0.002^{+0.015}_{-0.002}$	$0.012^{+0.013}_{-0.012}$	0.12 ± 0.11	0.25 ± 0.16	0.21 ± 0.12	$0.05^{+0.06}_{-0.05}$	$0.0018^{+0.0033}_{-0.0018}$

SR$\mu\mu$-$m_{\ell\ell}$	[1, 3] GeV	[3.2, 5] GeV	[5, 10] GeV	[10, 20] GeV	[20, 30] GeV	[30, 40] GeV	[40, 60] GeV
Observed events	1	2	7	12	2	2	2
Fitted SM events	1.1 ± 0.6	1.3 ± 0.6	4.9 ± 1.3	13.1 ± 2.2	4.2 ± 1.0	1.4 ± 0.6	1.6 ± 0.6
Fake/nonprompt leptons	$0.00^{+0.33}_{-0.00}$	$0.4^{+0.5}_{-0.4}$	3.0 ± 1.3	7.3 ± 2.1	$0.4^{+0.8}_{-0.4}$	$0.03^{+0.19}_{-0.03}$	$0.0^{+0.5}_{-0.0}$
Diboson	0.9 ± 0.5	0.7 ± 0.4	1.3 ± 0.6	1.4 ± 0.5	1.9 ± 0.4	0.9 ± 0.5	0.97 ± 0.28
$Z(\to\tau\tau)+$jets	$0.18^{+0.25}_{-0.18}$	0.13 ± 0.12	$0.3^{+0.5}_{-0.3}$	2.4 ± 0.8	0.7 ± 0.4	$0.001^{+0.011}_{-0.001}$	$0.05^{+0.06}_{-0.05}$
$t\bar{t}$, single top	$0.01^{+0.10}_{-0.01}$	$0.02^{+0.12}_{-0.02}$	0.19 ± 0.13	1.4 ± 0.6	0.8 ± 0.4	0.37 ± 0.21	0.51 ± 0.33
Others	0.047 ± 0.030	$0.07^{+0.09}_{-0.07}$	0.13 ± 0.12	0.7 ± 0.5	0.35 ± 0.20	0.09 ± 0.07	0.020 ± 0.020

SRee-m_{T2}^{100}	[100, 102] GeV	[102, 105] GeV	[105, 110] GeV	[110, 120] GeV	[120, 130] GeV	[130, ∞] GeV
Observed events	3	10	37	42	10	7
Fitted SM events	3.5 ± 1.2	11.0 ± 2.0	33 ± 4	42 ± 4	15.7 ± 2.0	7.5 ± 1.1
Fake/nonprompt leptons	2.9 ± 1.2	6.8 ± 2.0	13 ± 4	14 ± 4	1.9 ± 1.2	$0.01^{+0.10}_{-0.01}$
Diboson	0.33 ± 0.12	2.3 ± 0.6	8.5 ± 1.6	12.7 ± 2.4	7.4 ± 1.4	4.3 ± 0.9
$Z(\to\tau\tau)+$jets	$0.13^{+0.23}_{-0.13}$	0.6 ± 0.4	4.1 ± 1.8	2.9 ± 1.0	$0.00^{+0.08}_{-0.00}$	$0.00^{+0.20}_{-0.00}$
$t\bar{t}$, single top	0.08 ± 0.08	1.2 ± 0.5	6.5 ± 1.6	10.7 ± 2.4	6.3 ± 1.4	3.2 ± 0.9
Others	$0.011^{+0.012}_{-0.011}$	0.17 ± 0.11	0.8 ± 0.4	1.3 ± 0.7	0.14 ± 0.09	0.06 ± 0.04

SR$\mu\mu$-m_{T2}^{100}	[100, 102] GeV	[102, 105] GeV	[105, 110] GeV	[110, 120] GeV	[120, 130] GeV	[130, ∞] GeV
Observed events	5	16	60	42	32	13
Fitted SM events	6.8 ± 1.5	15.0 ± 2.1	57 ± 5	53 ± 4	24.9 ± 2.9	11.0 ± 1.4
Fake/nonprompt leptons	5.1 ± 1.5	8.2 ± 2.1	26 ± 5	18 ± 4	1.2 ± 0.8	$0.02^{+0.17}_{-0.02}$
Diboson	0.89 ± 0.22	4.1 ± 0.9	14.3 ± 2.2	18.0 ± 2.7	12.9 ± 2.2	5.9 ± 1.1
$Z(\to\tau\tau)+$jets	0.31 ± 0.23	$1.0^{+1.3}_{-1.0}$	6.6 ± 1.7	$1.6^{+1.8}_{-1.6}$	$0.03^{+0.25}_{-0.03}$	$0.02^{+0.24}_{-0.02}$
$t\bar{t}$, single top	0.43 ± 0.22	1.4 ± 0.5	8.3 ± 2.2	12.4 ± 2.9	10.5 ± 2.6	5.0 ± 1.3
Others	$0.020^{+0.024}_{-0.020}$	0.24 ± 0.15	1.8 ± 1.0	2.4 ± 1.3	0.35 ± 0.23	0.11 ± 0.07
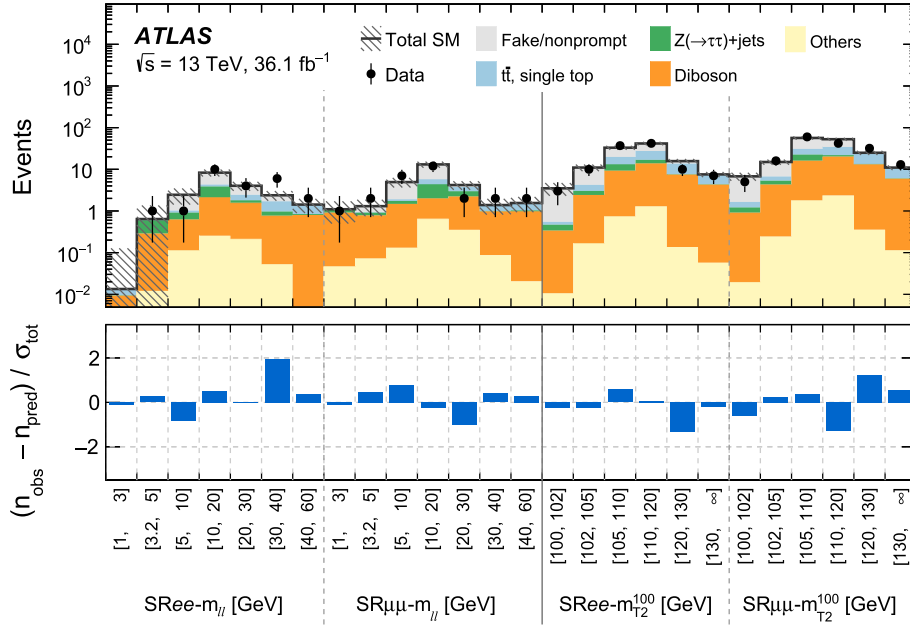
FIG. 9. Comparison of observed and expected event yields after the exclusion fit with the signal strength parameter set to zero in the exclusive signal regions. Background processes containing fewer than two prompt leptons are categorized as "Fake/nonprompt." The category "Others" contains rare backgrounds from triboson, Higgs boson, and the remaining top-quark production processes listed in Table I. Uncertainties in the background estimates include both the statistical and systematic uncertainties, where σ_{tot} denotes the total uncertainty.

with a corresponding signal strength parameter in a simultaneous fit of all CRs and relevant SRs; this is referred to as the exclusion fit. When an electroweakino signal is assumed, the 14 exclusive SRee-$m_{\ell\ell}$ and SR$\mu\mu$-$m_{\ell\ell}$ regions binned in $m_{\ell\ell}$ are considered. By statistically combining these SRs, the signal shape of the $m_{\ell\ell}$ spectrum can be exploited to improve the sensitivity. When a slepton signal is assumed, the 12 exclusive SRee-m_{T2}^{100} and SR$\mu\mu$-m_{T2}^{100} regions binned in m_{T2}^{100} are used for the fit.

Table VI summarizes the fitted and observed event yields in the exclusive electroweakino and slepton SRs using an exclusion fit configuration where the signal strength parameter is fixed to zero. The predicted yields differ slightly from those obtained in the background-only fit, as expected, because inclusion of the SRs to the fit further constrains the background contributions in the absence of signal. Figure 9 illustrates the compatibility of the fitted and observed event yields in these regions. No significant differences between the fitted background and the observed event yields are found in the exclusive SRs.

Hypothesis tests are then performed to set limits on simplified model scenarios using the CL$_s$ prescription. Figure 10 (top) shows the 95% C.L. limits on the Higgsino simplified model, based on an exclusion fit that

exploits the shape of the $m_{\ell\ell}$ spectrum using the exclusive electroweakino SRs. The exclusion limits are projected into the next-to-lightest neutralino mass $\Delta m(\tilde{\chi}_2^0, \tilde{\chi}_1^0)$ versus $m(\tilde{\chi}_2^0)$ plane, where $\tilde{\chi}_2^0$ are excluded up to masses of ~145 GeV for $\Delta m(\tilde{\chi}_2^0, \tilde{\chi}_1^0)$ between 5 and 10 GeV, and down to $\Delta m(\tilde{\chi}_2^0, \tilde{\chi}_1^0) \sim 2.5$ GeV for $m(\tilde{\chi}_2^0) \sim 100$ GeV. The 95% C.L. limits of the wino-bino simplified model are shown in Fig. 10 (bottom), where $\tilde{\chi}_2^0$ neutralino is excluded up to masses of ~175 GeV for $\Delta m(\tilde{\chi}_2^0, \tilde{\chi}_1^0) \sim$ 10 GeV, and down $\Delta m(\tilde{\chi}_2^0, \tilde{\chi}_1^0) \sim 2$ GeV for $m(\tilde{\chi}_2^0) \sim$ 100 GeV.

Figure 11 shows the 95% C.L. limits on the slepton simplified model, based on an exclusion fit that exploits the shape of the m_{T2}^{100} spectrum using the exclusive slepton SRs. Here, $\tilde{\ell}$ with masses of up to ~190 GeV are excluded for $\Delta m(\tilde{\ell}, \tilde{\chi}_1^0) \sim 5$ GeV, and down to mass splittings $\Delta m(\tilde{\ell}, \tilde{\chi}_1^0)$ of approximately 1 GeV for $m(\tilde{\ell}) \sim 70$ GeV. A fourfold degeneracy is assumed in selectron and smuon masses.

Finally, Fig. 12 shows the 95% C.L. exclusion bounds on the production cross sections for the NUHM2 scenario as a function of the universal gaugino mass $m_{1/2}$. The NUHM2 fit exploits the shape of the $m_{\ell\ell}$ spectrum using the exclusive electroweakino SRs. At $m_{1/2} = 350$ GeV, which

FIG. 11.   Expected 95% C.L. exclusion sensitivity (blue dashed line) with $\pm 1\sigma_{\mathrm{exp}}$ (yellow band) from experimental systematic uncertainties and observed limits (red solid line) with $\pm 1\sigma_{\mathrm{theory}}$ (dotted red line) from signal cross section uncertainties for simplified models of direct slepton production. A fit of slepton signals to the m_{T2}^{100} spectrum is used to derive the limit, which is projected into the $\Delta m(\tilde{\ell}, \tilde{\chi}_1^0)$ vs. $m(\tilde{\ell})$ plane. Slepton $\tilde{\ell}$ refers to the scalar partners of left- and right-handed electrons and muons, which are assumed to be fourfold mass degenerate $m(\tilde{e}_L) = m(\tilde{e}_R) = m(\tilde{\mu}_L) = m(\tilde{\mu}_R)$. The gray region is the $\tilde{e}_R$ limit from LEP [20,24], while the blue region is the fourfold mass degenerate slepton limit from ATLAS Run 1 [41].

FIG. 10.   Expected 95% C.L. exclusion sensitivity (blue dashed line) with $\pm 1\sigma_{\mathrm{exp}}$ (yellow band) from experimental systematic uncertainties and observed limits (red solid line) with $\pm 1\sigma_{\mathrm{theory}}$ (dotted red line) from signal cross section uncertainties for simplified models of direct Higgsino (top) and wino (bottom) production. A fit of signals to the $m_{\ell\ell}$ spectrum is used to derive the limit, which is projected into the $\Delta m(\tilde{\chi}_2^0, \tilde{\chi}_1^0)$ vs. $m(\tilde{\chi}_2^0)$ plane. For Higgsino production, the chargino $\tilde{\chi}_1^\pm$ mass is assumed to be halfway between the two lightest neutralino masses, while $m(\tilde{\chi}_2^0) = m(\tilde{\chi}_1^\pm)$ is assumed for the wino-bino model. The gray regions denote the lower chargino mass limit from LEP [20]. The blue region in the lower plot indicates the limit from the $2\ell + 3\ell$ combination of ATLAS Run 1 [41,42].

FIG. 12.   Observed and expected 95% C.L. cross section upper limits as a function of the universal gaugino mass $m_{1/2}$ for the NUHM2 model. The green and yellow bands around the expected limit indicate the $\pm 1\sigma$ and $\pm 2\sigma$ uncertainties, respectively. The expected signal production cross sections as well as the associated uncertainty are indicated with the blue solid and dashed lines. The lower x-axis indicates the difference between the $\tilde{\chi}_2^0$ and $\tilde{\chi}_1^0$ masses for different values of $m_{1/2}$. A fit of signals to the $m_{\ell\ell}$ spectrum is used to derive this limit.

corresponds to a mass splitting $\Delta m(\tilde{\chi}_2^0, \tilde{\chi}_1^0)$ of approximately 45 GeV, the signal cross section is constrained to be less than five times the predicted value in the NUHM2 scenario at 95% C.L. For $m_{1/2} = 800$ GeV, corresponding to a mass splitting of approximately 15 GeV, the 95% C.L. cross section upper limit is twice the NUHM2 prediction.

In these interpretations, sensitivity is lost when the mass splitting between the produced SUSY particle and the LSP becomes less than a few GeV due to the reduced acceptance and reconstruction efficiency of the soft leptons. Meanwhile, sensitivity decreases for larger mass splittings above approximately 20 to 30 GeV due to the $m_{\ell\ell}$ or m_{T2}^{100} shapes of the signal becoming increasingly similar to those of the SM backgrounds.

IX. CONCLUSION

A search for the electroweak production of supersymmetric states with low-momentum visible decay products is performed using LHC proton-proton collision data collected by the ATLAS detector at $\sqrt{s} = 13$ TeV, corresponding to an integrated luminosity of 36.1 fb^{-1}. Events with significant missing transverse momentum and same-flavor opposite-charge lepton pairs are selected, with the minimum p_T of the electrons (muons) being 4.5 (4) GeV. The dilepton invariant mass and stranverse mass are the main discriminating variables used to construct signal regions. No excess over the Standard Model expectation is observed.

The results are interpreted using simplified models of R-parity-conserving supersymmetry, where the produced states have small mass splittings with the lightest neutralino $\tilde{\chi}_1^0$. For the Higgsino simplified model, exclusion limits at 95% C.L. are set on the $\tilde{\chi}_2^0$ neutralino up to masses of ~ 145 GeV and down to mass splittings $\Delta m(\tilde{\chi}_2^0, \tilde{\chi}_1^0) \sim 2.5$ GeV. In the wino-bino model, these limits on the $\tilde{\chi}_2^0$ extend to masses of up to ~ 175 GeV and down to mass splittings of approximately 2 GeV. Direct pair production of sleptons, assuming the scalar partners of the left- and right-handed electrons and muons are mass degenerate, is excluded for slepton masses up to masses of ~ 190 GeV and down to mass splittings $\Delta m(\tilde{\ell}, \tilde{\chi}_1^0) \sim 1$ GeV. These results extend previous constraints from the LEP experiments. In addition, an interpretation of the results in the NUHM2 scenario is provided, where the cross section upper limit ranges between 11 and 3.5 pb for $m_{1/2}$ values of 350 to 800 GeV.

[1] Yu. A. Golfand and E. P. Likhtman, Extension of the Algebra of Poincare Group Generators and Violation of p Invariance, Pis'ma Zh. Eksp. Teor. Fiz. **13**, 452 (1971) [JETP Lett. **13**, 323 (1971)].

[2] D. V. Volkov and V. P. Akulov, Is the neutrino a Goldstone article?, Phys. Lett. B **46**, 109 (1973).

[3] J. Wess and B. Zumino, Supergauge transformations in four dimensions, Nucl. Phys. **B70**, 39 (1974).

[4] J. Wess and B. Zumino, Supergauge invariant extension of quantum electrodynamics, Nucl. Phys. **B78**, 1 (1974).

[5] S. Ferrara and B. Zumino, Supergauge invariant Yang-Mills theories, Nucl. Phys. **B79**, 413 (1974).

[6] A. Salam and J. A. Strathdee, Supersymmetry and non-Abelian Gauges, Phys. Lett. B **51**, 353 (1974).

[7] P. Fayet, Supersymmetry and weak, electromagnetic and strong interactions, Phys. Lett. B **64**, 159 (1976).

[8] P. Fayet, Spontaneously broken supersymmetric theories of weak, electromagnetic and strong interactions, Phys. Lett. B **69**, 489 (1977).

[9] G. R. Farrar and P. Fayet, Phenomenology of the production, decay, and detection of new hadronic states associated with supersymmetry, Phys. Lett. B **76,** 575 (1978).

[10] H. Goldberg, Constraint on the Photino Mass from Cosmology, Phys. Rev. Lett. **50,** 1419 (1983); Erratum, Phys. Rev. Lett. **103,** 099905(E) (2009).

[11] J. R. Ellis, J. S. Hagelin, D. V. Nanopoulos, K. A. Olive, and M. Srednicki, Supersymmetric relics from the big bang, Nucl. Phys. **B238,** 453 (1984).

[12] R. Barbieri and G. F. Giudice, Upper bounds on supersymmetric particle masses, Nucl. Phys. **B306,** 63 (1988).

[13] B. de Carlos and J. A. Casas, One loop analysis of the electroweak breaking in supersymmetric models and the fine tuning problem, Phys. Lett. B **309,** 320 (1993).

[14] R. Barbieri and D. Pappadopulo, S-particles at their naturalness limits, J. High Energy Phys. 10 (2009) 061.

[15] M. Papucci, J. T. Ruderman, and A. Weiler, Natural SUSY endures, J. High Energy Phys. 09 (2012) 035.

[16] Z. Han, G. D. Kribs, A. Martin, and A. Menon, Hunting quasidegenerate Higgsinos, Phys. Rev. D **89,** 075007 (2014).

[17] K. Griest and D. Seckel, Three exceptions in the calculation of relic abundances, Phys. Rev. D **43,** 3191 (1991).

[18] J. Edsjo and P. Gondolo, Neutralino relic density including coannihilations, Phys. Rev. D **56,** 1879 (1997).

[19] M. Ibe, S. Matsumoto, and R. Sato, Mass splitting between charged and neutral winos at two-loop level, Phys. Lett. B **721,** 252 (2013).

[20] ALEPH, DELPHI, L3, OPAL Experiments, Report No. LEPSUSYWG/02-04.1, 2002, http://lepsusy.web.cern .ch/lepsusy/www/inoslowdmsummer02/charginolowdm_ pub.html.

[21] ALEPH, DELPHI, L3, OPAL Experiments, Report No. LEPSUSYWG/04-01.1, 2004, http://lepsusy.web.cern .ch/lepsusy/www/sleptons_summer04/slep_final.html.

[22] ALEPH Collaboration, Search for scalar leptons in e^+e^- collisions at center-of-mass energies up to 209 GeV, Phys. Lett. B **526,** 206 (2002).

[23] ALEPH Collaboration, Search for charginos nearly mass degenerate with the lightest neutralino in e^+e^- collisions at center-of-mass energies up to 209 GeV, Phys. Lett. B **533,** 223 (2002).

[24] ALEPH Collaboration, Absolute lower limits on the masses of selectrons and sneutrinos in the MSSM, Phys. Lett. B **544,** 73 (2002).

[25] ALEPH Collaboration, Absolute mass lower limit for the lightest neutralino of the MSSM from e^+e^- data at $\sqrt{s}$ up to 209 GeV, Phys. Lett. B **583,** 247 (2004).

[26] DELPHI Collaboration, Searches for supersymmetric particles in e^+e^- collisions up to 208 GeV and interpretation of the results within the MSSM, Eur. Phys. J. C **31,** 421 (2003).

[27] L3 Collaboration, Search for charginos with a small mass difference with the lightest supersymmetric particle at $\sqrt{s} = 189$ GeV, Phys. Lett. B **482,** 31 (2000).

[28] L3 Collaboration, Search for scalar leptons and scalar quarks at LEP, Phys. Lett. B **580,** 37 (2004).

[29] OPAL Collaboration, Search for anomalous production of dilepton events with missing transverse momentum in e^+e^- collisions at $\sqrt{s} = 183$ GeV to 209 GeV, Eur. Phys. J. C **32,** 453 (2004).

[30] OPAL Collaboration, Search for nearly mass degenerate charginos and neutralinos at LEP, Eur. Phys. J. C **29,** 479 (2003).

[31] H. Baer, A. Mustafayev, and X. Tata, Monojet plus soft dilepton signal from light higgsino pair production at LHC14, Phys. Rev. D **90,** 115007 (2014).

[32] G. F. Giudice, T. Han, K. Wang, and L.-T. Wang, Nearly degenerate gauginos and dark matter at the LHC, Phys. Rev. D **81,** 115011 (2010).

[33] P. Schwaller and J. Zurita, Compressed electroweakino spectra at the LHC, J. High Energy Phys. 03 (2014) 060.

[34] S. Gori, S. Jung, and L.-T. Wang, Cornering electroweakinos at the LHC, J. High Energy Phys. 10 (2013) 191.

[35] B. Dutta, T. Ghosh, A. Gurrola, W. Johns, T. Kamon, P. Sheldon, K. Sinha, K. Wang, and S. Wu, Probing compressed sleptons at the LHC using vector boson fusion processes, Phys. Rev. D **91,** 055025 (2015).

[36] Z. Han and Y. Liu, MT2 to the Rescue—Searching for Sleptons in Compressed Spectra at the LHC, Phys. Rev. D **92,** 015010 (2015).

[37] A. Barr and J. Scoville, A boost for the EW SUSY hunt: monojet-like search for compressed sleptons at LHC14 with 100 fb^{-1}, J. High Energy Phys. 04 (2015) 147.

[38] L. Evans and P. Bryant, LHC Machine, J. Instrum. **3,** S08001 (2008).

[39] C. G. Lester and D. J. Summers, Measuring masses of semi-invisibly decaying particles pair produced at hadron colliders, Phys. Lett. B **463,** 99 (1999).

[40] A. Barr, C. Lester, and P. Stephens, A variable for measuring masses at hadron colliders when missing energy is expected; m_{T2}: the truth behind the glamour, J. Phys. G **29,** 2343 (2003).

[41] ATLAS Collaboration, Search for direct production of charginos, neutralinos and sleptons in final states with two leptons and missing transverse momentum in pp collisions at $\sqrt{s} = 8$ TeV with the ATLAS detector, J. High Energy Phys. 05 (2014) 071.

[42] ATLAS Collaboration, Search for direct production of charginos and neutralinos in events with three leptons and missing transverse momentum in $\sqrt{s} = 8$ TeV pp collisions with the ATLAS detector, J. High Energy Phys. 04 (2014) 169.

[43] ATLAS Collaboration, Search for the electroweak production of supersymmetric particles in $\sqrt{s} = 8$ TeV pp collisions with the ATLAS detector, Phys. Rev. D **93,** 052002 (2016).

[44] ATLAS Collaboration, Dark matter interpretations of ATLAS searches for the electroweak production of supersymmetric particles in $\sqrt{s} = 8$ TeV proton-proton collisions, J. High Energy Phys. 09 (2016) 175.

[45] CMS Collaboration, Searches for electroweak production of charginos, neutralinos, and sleptons decaying to leptons and W, Z, and Higgs bosons in pp collisions at 8 TeV, Eur. Phys. J. C **74,** 3036 (2014).

[46] CMS Collaboration, Search for supersymmetry in events with soft leptons, low jet multiplicity, and missing transverse energy in proton-proton collisions at $\sqrt{s} = 8$ TeV, Phys. Lett. B **759,** 9 (2016).

[47] CMS Collaboration, Search for electroweak production of charginos and neutralinos in multilepton final states in proton-proton collisions at $\sqrt{s} = 13$ TeV, arXiv:1709 .05406.

[48] U. De Sanctis, T. Lari, S. Montesano, and C. Troncon, Perspectives for the detection and measurement of supersymmetry in the focus point region of mSUGRA models with the ATLAS detector at LHC, Eur. Phys. J. C **52,** 743 (2007).

[49] ATLAS Collaboration, The ATLAS Experiment at the CERN Large Hadron Collider, J. Instrum. **3,** S08003 (2008).

[50] ATLAS Collaboration, ATLAS Insertable B-Layer Technical Design Report, Report No. ATLAS-TDR-19, 2010, https://cds.cern.ch/record/1291633, Report No. AT-LAS-TDR-19-ADD-1, 2012, https://cds.cern.ch/record/1451888.

[51] ATLAS Collaboration, Performance of the ATLAS trigger system in 2015, Eur. Phys. J. C **77,** 317 (2017).

[52] ATLAS Collaboration, Luminosity determination in pp collisions at $\sqrt{s} = 8$ TeV using the ATLAS detector at the LHC, Eur. Phys. J. C **76,** 653 (2016).

[53] J. Alwall, M.-P. Le, M. Lisanti, and J. G. Wacker, Searching for directly decaying gluinos at the Tevatron, Phys. Lett. B **666,** 34 (2008).

[54] J. Alwall, P. Schuster, and N. Toro, Simplified models for a first characterization of new physics at the LHC, Phys. Rev. D **79,** 075020 (2009).

[55] D. Alves *et al.*, Simplified models for LHC new physics searches, J. Phys. G **39,** 105005 (2012).

[56] J. R. Ellis, K. A. Olive, and Y. Santoso, The MSSM parameter space with nonuniversal Higgs masses, Phys. Lett. B **539,** 107 (2002).

[57] J. R. Ellis, T. Falk, K. A. Olive, and Y. Santoso, Exploration of the MSSM with nonuniversal Higgs masses, Nucl. Phys. **B652,** 259 (2003).

[58] S. D. Thomas and J. D. Wells, Phenomenology of Massive Vectorlike Doublet Leptons, Phys. Rev. Lett. **81,** 34 (1998).

[59] A. Djouadi, M. M. Muhlleitner, and M. Spira, Decays of supersymmetric particles: The Program SUSY-HIT (SUspect-SdecaY-Hdecay-InTerface), Acta Phys. Polon. B **38,** 635 (2007).

[60] J. Alwall, R. Frederix, S. Frixione, V. Hirschi, F. Maltoni, O. Mattelaer, H.-S. Shao, T. Stelzer, P. Torrielli, and M. Zaro, The automated computation of tree-level and next-to-leading order differential cross sections, and their matching to parton shower simulations, J. High Energy Phys. 07 (2014) 079.

[61] R. D. Ball *et al.*, Parton distributions with LHC data, Nucl. Phys. **B867,** 244 (2013).

[62] P. Artoisenet, R. Frederix, O. Mattelaer, and R. Rietkerk, Automatic spin-entangled decays of heavy resonances in Monte Carlo simulations, J. High Energy Phys. 03 (2013) 015.

[63] T. Sjöstrand, S. Mrenna, and P. Z. Skands, A brief introduction to PYTHIA 8.1, Comput. Phys. Commun. **178,** 852 (2008).

[64] ATLAS Collaboration, Report No. ATL-PHYS-PUB-2014-021, 2014, https://cds.cern.ch/record/1966419.

[65] L. Lönnblad and S. Prestel, Matching tree-level matrix elements with interleaved showers, J. High Energy Phys. 03 (2012) 019.

[66] B. Fuks, M. Klasen, D. R. Lamprea, and M. Rothering, Gaugino production in proton-proton collisions at a center-of-mass energy of 8 TeV, J. High Energy Phys. 10 (2012) 081.

[67] B. Fuks, M. Klasen, D. R. Lamprea, and M. Rothering, Precision predictions for electroweak superpartner production at hadron colliders with Resummino, Eur. Phys. J. C **73,** 2480 (2013).

[68] B. Fuks, M. Klasen, D. R. Lamprea, and M. Rothering, Revisiting slepton pair production at the Large Hadron Collider, J. High Energy Phys. 01 (2014) 168.

[69] C. Borschensky, M. Krämer, A. Kulesza, M. Mangano, S. Padhi, T. Plehn, and X. Portell, Squark and gluino production cross sections in pp collisions at $\sqrt{s} = 13$, 14, 33 and 100 TeV, Eur. Phys. J. C **74,** 3174 (2014).

[70] H. Baer, V. Barger, P. Huang, D. Mickelson, A. Mustafayev, W. Sreethawong, and X. Tata, Radiatively-driven natural supersymmetry at the LHC, J. High Energy Phys. 12 (2013) 013; Erratum, J. High Energy Phys. 06 (2015) 053(E).

[71] H. Baer, F. E. Paige, S. D. Protopopescu, and X. Tata, ISAJET 7.48: A Monte Carlo event generator for p p, anti-p, p, and e+ e- reactions, arXiv:hep-ph/0001086.

[72] W. Beenakker, M. Klasen, M. Krämer, T. Plehn, M. Spira, and P. M. Zerwas, Production of Charginos, Neutralinos, and Sleptons at Hadron Colliders, Phys. Rev. Lett. **83,** 3780 (1999); Erratum, Phys. Rev. Lett. **100,** 029901(E) (2008).

[73] T. Gleisberg, S. Höche, F. Krauss, M. Schönherr, S. Schumann, F. Siegert, and J. Winter, Event generation with SHERPA 1.1, J. High Energy Phys. 02 (2009) 007.

[74] T. Gleisberg and S. Höche, Comix, a new matrix element generator, J. High Energy Phys. 12 (2008) 039.

[75] F. Cascioli, P. Maierhofer, and S. Pozzorini, Scattering Amplitudes with Open Loops, Phys. Rev. Lett. **108,** 111601 (2012).

[76] S. Schumann and F. Krauss, A Parton shower algorithm based on Catani-Seymour dipole factorisation, J. High Energy Phys. 03 (2008) 038.

[77] S. Höche, F. Krauss, M. Schönherr, and F. Siegert, QCD matrix elements + parton showers: The NLO case, J. High Energy Phys. 04 (2013) 027.

[78] S. Alioli, P. Nason, C. Oleari, and E. Re, A general framework for implementing NLO calculations in shower Monte Carlo programs: the POWHEG BOX, J. High Energy Phys. 06 (2010) 043.

[79] S. Alioli, P. Nason, C. Oleari, and E. Re, NLO Higgs boson production via gluon fusion matched with shower in POWHEG, J. High Energy Phys. 04 (2009) 002.

[80] P. Nason and C. Oleari, NLO Higgs boson production via vector-boson fusion matched with shower in POWHEG, J. High Energy Phys. 02 (2010) 037.

[81] P. Z. Skands, Tuning Monte Carlo generators: The Perugia tunes, Phys. Rev. D **82,** 074018 (2010).

[82] ATLAS Collaboration, Report No. ATL-PHYS-PUB-2016-004, 2016, https://cds.cern.ch/record/2120417.

[83] ATLAS Collaboration, Report No. ATL-PHYS-PUB-2017-005, 2017, https://cds.cern.ch/record/2261933.

[84] ATLAS Collaboration, Report No. ATL-PHYS-PUB-2017-006, 2017, https://cds.cern.ch/record/2261937.

[85] ATLAS Collaboration, Report No. ATL-PHYS-PUB-2016-005, 2016, https://cds.cern.ch/record/2120826.

[86] R. D. Ball *et al.*, Parton distributions for the LHC Run II, J. High Energy Phys. 04 (2015) 040.

[87] S. Catani, L. Cieri, G. Ferrera, D. de Florian, and M. Grazzini, Vector Boson Production at Hadron Colliders: A Fully Exclusive QCD Calculation at NNLO, Phys. Rev. Lett. **103,** 082001 (2009).

[88] H.-L. Lai, M. Guzzi, J. Huston, Z. Li, P. M. Nadolsky, J. Pumplin, and C.-P. Yuan, New parton distributions for collider physics, Phys. Rev. D **82,** 074024 (2010).

[89] M. Cacciari, M. Czakon, M. Mangano, A. Mitov, and P. Nason, Top-pair production at hadron colliders with next-to-next-to-leading logarithmic soft-gluon resummation, Phys. Lett. B **710,** 612 (2012).

[90] M. Czakon and A. Mitov, NNLO corrections to top pair production at hadron colliders: the quark-gluon reaction, J. High Energy Phys. 01 (2013) 080.

[91] M. Czakon and A. Mitov, NNLO corrections to top-pair production at hadron colliders: The all-fermionic scattering channels, J. High Energy Phys. 12 (2012) 054.

[92] M. Czakon, P. Fiedler, and A. Mitov, Total Top-Quark Pair-Production Cross Section at Hadron Colliders Through $O(\alpha_S^4)$, Phys. Rev. Lett. **110,** 252004 (2013).

[93] N. Kidonakis, NNLL resummation for s-channel single top quark production, Phys. Rev. D **81,** 054028 (2010).

[94] N. Kidonakis, Next-to-next-to-leading-order collinear and soft gluon corrections for t-channel single top quark production, Phys. Rev. D **83,** 091503 (2011).

[95] R. Frederix, E. Re, and P. Torrielli, Single-top t-channel hadroproduction in the four-flavour scheme with POWHEG and aMC@NLO, J. High Energy Phys. 09 (2012) 130.

[96] N. Kidonakis, Two-loop soft anomalous dimensions for single top quark associated production with a W^- or H^-, Phys. Rev. D **82,** 054018 (2010).

[97] J. Pumplin, D. R. Stump, J. Huston, H.-L. Lai, P. Nadolsky, and W.-K. Tung, New generation of parton distributions with uncertainties from global QCD analysis, J. High Energy Phys. 07 (2002) 012.

[98] S. Dittmaier *et al.*, Report No. CERN-2012-002, 2012, arXiv:1201.3084.

[99] ATLAS Collaboration, Report No. ATL-PHYS-PUB-2012-003, 2012, https://cds.cern.ch/record/1474107.

[100] A. D. Martin, W. J. Stirling, R. S. Thorne, and G. Watt, Parton distributions for the LHC, Eur. Phys. J. C **63,** 189 (2009).

[101] ATLAS Collaboration, The ATLAS Simulation Infrastructure, Eur. Phys. J. C **70,** 823 (2010).

[102] S. Agostinelli *et al.*, GEANT4—a simulation toolkit, Nucl. Instrum. Methods Phys. Res., Sect. A **506,** 250 (2003).

[103] ATLAS Collaboration, Report No. ATL-PHYS-PUB-2010-013, 2010, https://cds.cern.ch/record/1300517.

[104] D. J. Lange, The EvtGen particle decay simulation package, Nucl. Instrum. Methods Phys. Res., Sect. A **462,** 152 (2001).

[105] ATLAS Collaboration, Electron efficiency measurements with the ATLAS detector using 2012 LHC proton-proton collision data, Eur. Phys. J. C **77,** 195 (2017).

[106] ATLAS Collaboration, Muon reconstruction performance of the ATLAS detector in proton-proton collision data at $\sqrt{s} = 13$ TeV, Eur. Phys. J. C **76,** 292 (2016).

[107] ATLAS Collaboration, Topological cell clustering in the ATLAS calorimeters and its performance in LHC Run 1, Eur. Phys. J. C **77,** 490 (2017).

[108] M. Cacciari, G. P. Salam, and G. Soyez, The anti-kt jet clustering algorithm, J. High Energy Phys. 04 (2008) 063.

[109] M. Cacciari, G. P. Salam, and G. Soyez, FastJet User Manual, Eur. Phys. J. C **72,** 1896 (2012).

[110] ATLAS Collaboration, Jet energy scale measurements and their systematic uncertainties in proton-proton collisions at $\sqrt{s} = 13$ TeV with the ATLAS detector, Phys. Rev. D **96,** 072002 (2017).

[111] ATLAS Collaboration, Performance of pile-up mitigation techniques for jets in pp collisions at $\sqrt{s} = 8$ TeV using the ATLAS detector, Eur. Phys. J. C **76,** 581 (2016).

[112] ATLAS Collaboration, Characterisation and mitigation of beam-induced backgrounds observed in the ATLAS detector during the 2011 proton-proton run, J. Instrum. **8,** P07004 (2013).

[113] ATLAS Collaboration, Performance of b-jet identification in the ATLAS experiment, J. Instrum. **11,** P04008 (2016).

[114] ATLAS Collaboration, Report No. ATL-PHYS-PUB-2016-012, 2016, https://cds.cern.ch/record/2160731.

[115] ATLAS Collaboration, Report No. ATL-PHYS-PUB-2016-015, 2016, https://cds.cern.ch/record/2203514.

[116] ATLAS Collaboration, Report No. ATL-PHYS-PUB-2015-027, 2015, https://cds.cern.ch/record/2037904.

[117] ATLAS Collaboration, Observation and measurement of Higgs boson decays to WW^* with the ATLAS detector, Phys. Rev. D **92,** 012006 (2015).

[118] S. Dulat, T.-J. Hou, J. Gao, M. Guzzi, J. Huston, P. Nadolsky, J. Pumplin, C. Schmidt, D. Stump, and C.-P. Yuan, New parton distribution functions from a global analysis of quantum chromodynamics, Phys. Rev. D **93,** 033006 (2016).

[119] L. A. Harland-Lang, A. D. Martin, P. Motylinski, and R. S. Thorne, Parton distributions in the LHC era: MMHT 2014 PDFs, Eur. Phys. J. C **75,** 204 (2015).

[120] J. Butterworth *et al.*, PDF4LHC recommendations for LHC Run II, J. Phys. G **43,** 023001 (2016).

[121] M. Baak, G. J. Besjes, D. Côté, A. Koutsman, J. Lorenz, and D. Short, HistFitter software framework for statistical data analysis, Eur. Phys. J. C **75,** 153 (2015).

[122] G. Cowan, K. Cranmer, E. Gross, and O. Vitells, Asymptotic formulae for likelihood-based tests of new physics, Eur. Phys. J. C **71,** 1554 (2011); Erratum, Eur. Phys. J. C **73,** 2501(E) (2013).

[123] A. L. Read, Presentation of search results: The CL_s technique, J. Phys. G **28,** 2693 (2002).

[124] ATLAS Collaboration, Report No. ATL-GEN-PUB-2016-002, https://cds.cern.ch/record/2202407.

M. Aaboud,[137d] G. Aad,[88] B. Abbott,[115] O. Abdinov,[12,a] B. Abeloos,[119] S. H. Abidi,[161] O. S. AbouZeid,[139] N. L. Abraham,[151] H. Abramowicz,[155] H. Abreu,[154] Y. Abulaiti,[6] B. S. Acharya,[167a,167b,b] S. Adachi,[157] L. Adamczyk,[41a] J. Adelman,[110] M. Adersberger,[102] T. Adye,[133] A. A. Affolder,[139] Y. Afik,[154] C. Agheorghiesei,[28c] J. A. Aguilar-Saavedra,[128a,128f] S. P. Ahlen,[24] F. Ahmadov,[68,c] G. Aielli,[135a,135b] S. Akatsuka,[71] T. P. A. Åkesson,[84] E. Akilli,[52] A. V. Akimov,[98] G. L. Alberghi,[22a,22b] J. Albert,[172] P. Albicocco,[50] M. J. Alconada Verzini,[74] S. C. Alderweireldt,[108] M. Aleksa,[32] I. N. Aleksandrov,[68] C. Alexa,[28b] G. Alexander,[155] T. Alexopoulos,[10] M. Alhroob,[115] B. Ali,[130] M. Aliev,[76a,76b] G. Alimonti,[94a] J. Alison,[33] S. P. Alkire,[38] C. Allaire,[119] B. M. M. Allbrooke,[151] B. W. Allen,[118] P. P. Allport,[19] A. Aloisio,[106a,106b] A. Alonso,[39] F. Alonso,[74] C. Alpigiani,[140] A. A. Alshehri,[56] M. I. Alstaty,[88] B. Alvarez Gonzalez,[32] D. Álvarez Piqueras,[170] M. G. Alviggi,[106a,106b] B. T. Amadio,[16] Y. Amaral Coutinho,[26a] L. Ambroz,[122] C. Amelung,[25] D. Amidei,[92] S. P. Amor Dos Santos,[128a,128c] S. Amoroso,[32] C. Anastopoulos,[141] L. S. Ancu,[52] N. Andari,[19] T. Andeen,[11] C. F. Anders,[60b] J. K. Anders,[18] K. J. Anderson,[33] A. Andreazza,[94a,94b] V. Andrei,[60a] S. Angelidakis,[37] I. Angelozzi,[109] A. Angerami,[38] A. V. Anisenkov,[111,d] A. Annovi,[126a] C. Antel,[60a] M. Antonelli,[50] A. Antonov,[100,a] D. J. Antrim,[166] F. Anulli,[134a] M. Aoki,[69] L. Aperio Bella,[32] G. Arabidze,[93] Y. Arai,[69] J. P. Araque,[128a] V. Araujo Ferraz,[26a] R. Araujo Pereira,[26a] A. T. H. Arce,[48] R. E. Ardell,[80] F. A. Arduh,[74] J-F. Arguin,[97] S. Argyropoulos,[66] A. J. Armbruster,[32] L. J. Armitage,[79] O. Arnaez,[161] H. Arnold,[109] M. Arratia,[30] O. Arslan,[23] A. Artamonov,[99,a] G. Artoni,[122] S. Artz,[86] S. Asai,[157] N. Asbah,[45] A. Ashkenazi,[155] L. Asquith,[151] K. Assamagan,[27] R. Astalos,[146a] R. J. Atkin,[147a] M. Atkinson,[169] N. B. Atlay,[143] K. Augsten,[130] G. Avolio,[32] R. Avramidou,[36a] B. Axen,[16] M. K. Ayoub,[35a] G. Azuelos,[97,e] A. E. Baas,[60a] M. J. Baca,[19] H. Bachacou,[138] K. Bachas,[76a,76b] M. Backes,[122] P. Bagnaia,[134a,134b] M. Bahmani,[42] H. Bahrasemani,[144] J. T. Baines,[133] M. Bajic,[39] O. K. Baker,[179] P. J. Bakker,[109] D. Bakshi Gupta,[82] E. M. Baldin,[111,d] P. Balek,[175] F. Balli,[138] W. K. Balunas,[124] E. Banas,[42] A. Bandyopadhyay,[23] Sw. Banerjee,[176,f] A. A. E. Bannoura,[178] L. Barak,[155] E. L. Barberio,[91] D. Barberis,[53a,53b] M. Barbero,[88] T. Barillari,[103] M-S Barisits,[65] J. T. Barkeloo,[118] T. Barklow,[145] N. Barlow,[30] S. L. Barnes,[36c] B. M. Barnett,[133] R. M. Barnett,[16] Z. Barnovska-Blenessy,[36a] A. Baroncelli,[136a] G. Barone,[25] A. J. Barr,[122] L. Barranco Navarro,[170] F. Barreiro,[85] J. Barreiro Guimarães da Costa,[35a] R. Bartoldus,[145] A. E. Barton,[75] P. Bartos,[146a] A. Basalaev,[125] A. Bassalat,[119,g] R. L. Bates,[56] S. J. Batista,[161] J. R. Batley,[30] M. Battaglia,[139] M. Bauce,[134a,134b] F. Bauer,[138] K. T. Bauer,[166] H. S. Bawa,[145,h] J. B. Beacham,[113] M. D. Beattie,[75] T. Beau,[83] P. H. Beauchemin,[165] P. Bechtle,[23] H. P. Beck,[18,i] H. C. Beck,[57] K. Becker,[122] M. Becker,[86] C. Becot,[112] A. J. Beddall,[20d] A. Beddall,[20b] V. A. Bednyakov,[68] M. Bedognetti,[109] C. P. Bee,[150] T. A. Beermann,[32] M. Begalli,[26a] M. Begel,[27] A. Behera,[150] J. K. Behr,[45] A. S. Bell,[81] G. Bella,[155] L. Bellagamba,[22a] A. Bellerive,[31] M. Bellomo,[154] K. Belotskiy,[100] N. L. Belyaev,[100] O. Benary,[155,a] D. Benchekroun,[137a] M. Bender,[102] N. Benekos,[10] Y. Benhammou,[155] E. Benhar Noccioli,[179] J. Benitez,[66] D. P. Benjamin,[48] M. Benoit,[52] J. R. Bensinger,[25] S. Bentvelsen,[109] L. Beresford,[122] M. Beretta,[50] D. Berge,[45] E. Bergeaas Kuutmann,[168] N. Berger,[5] L. J. Bergsten,[25] J. Beringer,[16] S. Berlendis,[58] N. R. Bernard,[89] G. Bernardi,[83] C. Bernius,[145] F. U. Bernlochner,[23] T. Berry,[80] P. Berta,[86] C. Bertella,[35a] G. Bertoli,[148a,148b] I. A. Bertram,[75] C. Bertsche,[45] G. J. Besjes,[39] O. Bessidskaia Bylund,[148a,148b] M. Bessner,[45] N. Besson,[138] A. Bethani,[87] S. Bethke,[103] A. Betti,[23] A. J. Bevan,[79] J. Beyer,[103] R. M. Bianchi,[127] O. Biebel,[102] D. Biedermann,[17] R. Bielski,[87] K. Bierwagen,[86] N. V. Biesuz,[126a,126b] M. Biglietti,[136a] T. R. V. Billoud,[97] M. Bindi,[57] A. Bingul,[20b] C. Bini,[134a,134b] S. Biondi,[22a,22b] T. Bisanz,[57] C. Bittrich,[47] D. M. Bjergaard,[48] J. E. Black,[145] K. M. Black,[24] R. E. Blair,[6] T. Blazek,[146a] I. Bloch,[45] C. Blocker,[25] A. Blue,[56] U. Blumenschein,[79] Dr. Blunier,[34a] G. J. Bobbink,[109] V. S. Bobrovnikov,[111,d] S. S. Bocchetta,[84] A. Bocci,[48] C. Bock,[102] D. Boerner,[178] D. Bogavac,[102] A. G. Bogdanchikov,[111] C. Bohm,[148a] V. Boisvert,[80] P. Bokan,[168,j] T. Bold,[41a] A. S. Boldyrev,[101] A. E. Bolz,[60b] M. Bomben,[83] M. Bona,[79] J. S. Bonilla,[118] M. Boonekamp,[138] A. Borisov,[132] G. Borissov,[75] J. Bortfeldt,[32] D. Bortoletto,[122] V. Bortolotto,[62a] D. Boscherini,[22a] M. Bosman,[13] J. D. Bossio Sola,[29] J. Boudreau,[127] E. V. Bouhova-Thacker,[75] D. Boumediene,[37] C. Bourdarios,[119] S. K. Boutle,[56] A. Boveia,[113] J. Boyd,[32] I. R. Boyko,[68] A. J. Bozson,[80] J. Bracinik,[19] A. Brandt,[8] G. Brandt,[178] O. Brandt,[60a] F. Braren,[45] U. Bratzler,[158] B. Brau,[89] J. E. Brau,[118] W. D. Breaden Madden,[56] K. Brendlinger,[45] A. J. Brennan,[91] L. Brenner,[45] R. Brenner,[168] S. Bressler,[175] D. L. Briglin,[19] T. M. Bristow,[49] D. Britton,[56] D. Britzger,[60b] F. M. Brochu,[30] I. Brock,[23] R. Brock,[93] G. Brooijmans,[38] T. Brooks,[80] W. K. Brooks,[34b] E. Brost,[110] J. H Broughton,[19] P. A. Bruckman de Renstrom,[42] D. Bruncko,[146b] A. Bruni,[22a] G. Bruni,[22a] L. S. Bruni,[109] S. Bruno,[135a,135b] BH Brunt,[30] M. Bruschi,[22a] N. Bruscino,[127] P. Bryant,[33] L. Bryngemark,[45] T. Buanes,[15] Q. Buat,[32] P. Buchholz,[143] A. G. Buckley,[56] I. A. Budagov,[68] F. Buehrer,[51] M. K. Bugge,[121] O. Bulekov,[100] D. Bullock,[8] T. J. Burch,[110] S. Burdin,[77] C. D. Burgard,[109] A. M. Burger,[5] B. Burghgrave,[110] K. Burka,[42] S. Burke,[133] I. Burmeister,[46] J. T. P. Burr,[122] D. Büscher,[51] V. Büscher,[86] E. Buschmann,[57] P. Bussey,[56] J. M. Butler,[24] C. M. Buttar,[56] J. M. Butterworth,[81] P. Butti,[32] W. Buttinger,[32] A. Buzatu,[153]

A. R. Buzykaev,[111,d] Changqiao C.-Q.,[36a] G. Cabras,[22a,22b] S. Cabrera Urbán,[170] D. Caforio,[130] H. Cai,[169] V. M. M. Cairo,[2] O. Cakir,[4a] N. Calace,[52] P. Calafiura,[16] A. Calandri,[88] G. Calderini,[83] P. Calfayan,[64] G. Callea,[40a,40b] L. P. Caloba,[26a] S. Calvente Lopez,[85] D. Calvet,[37] S. Calvet,[37] T. P. Calvet,[88] R. Camacho Toro,[33] S. Camarda,[32] P. Camarri,[135a,135b] D. Cameron,[121] R. Caminal Armadans,[89] C. Camincher,[58] S. Campana,[32] M. Campanelli,[81] A. Camplani,[94a,94b] A. Campoverde,[143] V. Canale,[106a,106b] M. Cano Bret,[36c] J. Cantero,[116] T. Cao,[155] M. D. M. Capeans Garrido,[32] I. Caprini,[28b] M. Caprini,[28b] M. Capua,[40a,40b] R. M. Carbone,[38] R. Cardarelli,[135a] F. Cardillo,[51] I. Carli,[131] T. Carli,[32] G. Carlino,[106a] B. T. Carlson,[127] L. Carminati,[94a,94b] R. M. D. Carney,[148a,148b] S. Caron,[108] E. Carquin,[34b] S. Carrá,[94a,94b] G. D. Carrillo-Montoya,[32] D. Casadei,[19] M. P. Casado,[13,k] A. F. Casha,[161] M. Casolino,[13] D. W. Casper,[166] R. Castelijn,[109] V. Castillo Gimenez,[170] N. F. Castro,[128a,l] A. Catinaccio,[32] J. R. Catmore,[121] A. Cattai,[32] J. Caudron,[23] V. Cavaliere,[27] E. Cavallaro,[13] M. Cavalli-Sforza,[13] V. Cavasinni,[126a,126b] E. Celebi,[20c] F. Ceradini,[136a,136b] L. Cerda Alberich,[170] A. S. Cerqueira,[26b] A. Cerri,[151] L. Cerrito,[135a,135b] F. Cerutti,[16] A. Cervelli,[22a,22b] S. A. Cetin,[20c] A. Chafaq,[137a] D. Chakraborty,[110] S. K. Chan,[59] W. S. Chan,[109] Y. L. Chan,[62a] P. Chang,[169] J. D. Chapman,[30] D. G. Charlton,[19] C. C. Chau,[31] C. A. Chavez Barajas,[151] S. Che,[113] A. Chegwidden,[93] S. Chekanov,[6] S. V. Chekulaev,[163a] G. A. Chelkov,[68,m] M. A. Chelstowska,[32] C. Chen,[36a] C. Chen,[67] H. Chen,[27] J. Chen,[36a] J. Chen,[38] S. Chen,[35b] S. Chen,[157] X. Chen,[35c,n] Y. Chen,[70] H. C. Cheng,[92] H. J. Cheng,[35a,35d] A. Cheplakov,[68] E. Cheremushkina,[132] R. Cherkaoui El Moursli,[137e] E. Cheu,[7] K. Cheung,[63] L. Chevalier,[138] V. Chiarella,[50] G. Chiarelli,[126a] G. Chiodini,[76a] A. S. Chisholm,[32] A. Chitan,[28b] I. Chiu,[157] Y. H. Chiu,[172] M. V. Chizhov,[68] K. Choi,[64] A. R. Chomont,[37] S. Chouridou,[156] Y. S. Chow,[109] V. Christodoulou,[81] M. C. Chu,[62a] J. Chudoba,[129] A. J. Chuinard,[90] J. J. Chwastowski,[42] L. Chytka,[117] D. Cinca,[46] V. Cindro,[78] I. A. Cioară,[23] A. Ciocio,[16] F. Cirotto,[106a,106b] Z. H. Citron,[175] M. Citterio,[94a] A. Clark,[52] M. R. Clark,[38] P. J. Clark,[49] R. N. Clarke,[16] C. Clement,[148a,148b] Y. Coadou,[88] M. Cobal,[167a,167c] A. Coccaro,[53a,53b] J. Cochran,[67] L. Colasurdo,[108] B. Cole,[38] A. P. Colijn,[109] J. Collot,[58] P. Conde Muiño,[128a,128b] E. Coniavitis,[51] S. H. Connell,[147b] I. A. Connelly,[87] S. Constantinescu,[28b] G. Conti,[32] F. Conventi,[106a,o] A. M. Cooper-Sarkar,[122] K. J. R. Cormier,[171] M. Corradi,[134a,134b] E. E. Corrigan,[84] F. Corriveau,[90,p] A. Cortes-Gonzalez,[32] M. J. Costa,[170] D. Costanzo,[141] G. Cottin,[30] G. Cowan,[80] B. E. Cox,[87] K. Cranmer,[112] S. J. Crawley,[56] R. A. Creager,[124] G. Cree,[31] S. Crépé-Renaudin,[58] F. Crescioli,[83] M. Cristinziani,[23] V. Croft,[112] G. Crosetti,[40a,40b] A. Cueto,[85] T. Cuhadar Donszelmann,[141] A. R. Cukierman,[145] J. Cummings,[179] M. Curatolo,[50] J. Cúth,[86] S. Czekierda,[42] P. Czodrowski,[32] G. D'amen,[22a,22b] S. D'Auria,[56] L. D'eramo,[83] M. D'Onofrio,[77] M. J. Da Cunha Sargedas De Sousa,[128a,128b] C. Da Via,[87] W. Dabrowski,[41a] T. Dado,[146a] S. Dahbi,[137e] T. Dai,[92] O. Dale,[15] F. Dallaire,[97] C. Dallapiccola,[89] M. Dam,[39] J. R. Dandoy,[124] M. F. Daneri,[29] N. P. Dang,[176,f] N. S. Dann,[87] M. Danninger,[171] M. Dano Hoffmann,[138] V. Dao,[32] G. Darbo,[53a] S. Darmora,[8] A. Dattagupta,[118] T. Daubney,[45] W. Davey,[23] C. David,[45] T. Davidek,[131] D. R. Davis,[48] P. Davison,[81] E. Dawe,[91] I. Dawson,[141] K. De,[8] R. de Asmundis,[106a] A. De Benedetti,[115] S. De Castro,[22a,22b] S. De Cecco,[83] N. De Groot,[108] P. de Jong,[109] H. De la Torre,[93] F. De Lorenzi,[67] A. De Maria,[57] D. De Pedis,[134a] A. De Salvo,[134a] U. De Sanctis,[135a,135b] A. De Santo,[151] K. De Vasconcelos Corga,[88] J. B. De Vivie De Regie,[119] C. Debenedetti,[139] D. V. Dedovich,[68] N. Dehghanian,[3] I. Deigaard,[109] M. Del Gaudio,[40a,40b] J. Del Peso,[85] D. Delgove,[119] F. Deliot,[138] C. M. Delitzsch,[7] A. Dell'Acqua,[32] L. Dell'Asta,[24] M. Della Pietra,[106a,106b] D. della Volpe,[52] M. Delmastro,[5] C. Delporte,[119] P. A. Delsart,[58] D. A. DeMarco,[161] S. Demers,[179] M. Demichev,[68] S. P. Denisov,[132] D. Denysiuk,[109] D. Derendarz,[42] J. E. Derkaoui,[137d] F. Derue,[83] P. Dervan,[77] K. Desch,[23] C. Deterre,[45] K. Dette,[161] M. R. Devesa,[29] P. O. Deviveiros,[32] A. Dewhurst,[133] S. Dhaliwal,[25] F. A. Di Bello,[52] A. Di Ciaccio,[135a,135b] L. Di Ciaccio,[5] W. K. Di Clemente,[124] C. Di Donato,[106a,106b] A. Di Girolamo,[32] B. Di Micco,[136a,136b] R. Di Nardo,[32] K. F. Di Petrillo,[59] A. Di Simone,[51] R. Di Sipio,[161] D. Di Valentino,[31] C. Diaconu,[88] M. Diamond,[161] F. A. Dias,[39] M. A. Diaz,[34a] J. Dickinson,[16] E. B. Diehl,[92] J. Dietrich,[17] S. Díez Cornell,[45] A. Dimitrievska,[16] J. Dingfelder,[23] P. Dita,[28b] S. Dita,[28b] F. Dittus,[32] F. Djama,[88] T. Djobava,[54b] J. I. Djuvsland,[60a] M. A. B. do Vale,[26c] M. Dobre,[28b] D. Dodsworth,[25] C. Doglioni,[84] J. Dolejsi,[131] Z. Dolezal,[131] M. Donadelli,[26d] J. Donini,[37] J. Dopke,[133] A. Doria,[106a] M. T. Dova,[74] A. T. Doyle,[56] E. Drechsler,[57] E. Dreyer,[144] M. Dris,[10] Y. Du,[36b] J. Duarte-Campderros,[155] F. Dubinin,[98] A. Dubreuil,[52] E. Duchovni,[175] G. Duckeck,[102] A. Ducourthial,[83] O. A. Ducu,[97,q] D. Duda,[109] A. Dudarev,[32] A. Chr. Dudder,[86] E. M. Duffield,[16] L. Duflot,[119] M. Dührssen,[32] C. Dulsen,[178] M. Dumancic,[175] A. E. Dumitriu,[28b,r] A. K. Duncan,[56] M. Dunford,[60a] A. Duperrin,[88] H. Duran Yildiz,[4a] M. Düren,[55] A. Durglishvili,[54b] D. Duschinger,[47] B. Dutta,[45] D. Duvnjak,[1] M. Dyndal,[45] B. S. Dziedzic,[42] C. Eckardt,[45] K. M. Ecker,[103] R. C. Edgar,[92] T. Eifert,[32] G. Eigen,[15] K. Einsweiler,[16] T. Ekelof,[168] M. El Kacimi,[137c] R. El Kosseifi,[88] V. Ellajosyula,[88] M. Ellert,[168] F. Ellinghaus,[178] A. A. Elliot,[172] N. Ellis,[32] J. Elmsheuser,[27] M. Elsing,[32] D. Emeliyanov,[133] Y. Enari,[157] J. S. Ennis,[173] M. B. Epland,[48] J. Erdmann,[46] A. Ereditato,[18]

S. Errede,[169] M. Escalier,[119] C. Escobar,[170] B. Esposito,[50] O. Estrada Pastor,[170] A. I. Etienvre,[138] E. Etzion,[155] H. Evans,[64] A. Ezhilov,[125] M. Ezzi,[137e] F. Fabbri,[22a,22b] L. Fabbri,[22a,22b] V. Fabiani,[108] G. Facini,[81] R. M. Fakhrutdinov,[132] S. Falciano,[134a] J. Faltova,[131] Y. Fang,[35a] M. Fanti,[94a,94b] A. Farbin,[8] A. Farilla,[136a] E. M. Farina,[123a,123b] T. Farooque,[93] S. Farrell,[16] S. M. Farrington,[173] P. Farthouat,[32] F. Fassi,[137e] P. Fassnacht,[32] D. Fassouliotis,[9] M. Faucci Giannelli,[49] A. Favareto,[53a,53b] W. J. Fawcett,[52] L. Fayard,[119] O. L. Fedin,[125,s] W. Fedorko,[171] M. Feickert,[43] S. Feigl,[121] L. Feligioni,[88] C. Feng,[36b] E. J. Feng,[32] M. Feng,[48] M. J. Fenton,[56] A. B. Fenyuk,[132] L. Feremenga,[8] P. Fernandez Martinez,[170] J. Ferrando,[45] A. Ferrari,[168] P. Ferrari,[109] R. Ferrari,[123a] D. E. Ferreira de Lima,[60b] A. Ferrer,[170] D. Ferrere,[52] C. Ferretti,[92] F. Fiedler,[86] A. Filipčič,[78] F. Filthaut,[108] M. Fincke-Keeler,[172] K. D. Finelli,[24] M. C. N. Fiolhais,[128a,128c,t] L. Fiorini,[170] C. Fischer,[13] J. Fischer,[178] W. C. Fisher,[93] N. Flaschel,[45] I. Fleck,[143] P. Fleischmann,[92] R. R. M. Fletcher,[124] T. Flick,[178] B. M. Flierl,[102] L. R. Flores Castillo,[62a] N. Fomin,[15] G. T. Forcolin,[87] A. Formica,[138] F. A. Förster,[13] A. Forti,[87] A. G. Foster,[19] D. Fournier,[119] H. Fox,[75] S. Fracchia,[141] P. Francavilla,[126a,126b] M. Franchini,[22a,22b] S. Franchino,[60a] D. Francis,[32] L. Franconi,[121] M. Franklin,[59] M. Frate,[166] M. Fraternali,[123a,123b] D. Freeborn,[81] S. M. Fressard-Batraneanu,[32] B. Freund,[97] W. S. Freund,[26a] D. Froidevaux,[32] J. A. Frost,[122] C. Fukunaga,[158] T. Fusayasu,[104] J. Fuster,[170] O. Gabizon,[154] A. Gabrielli,[22a,22b] A. Gabrielli,[16] G. P. Gach,[41a] S. Gadatsch,[52] S. Gadomski,[80] G. Gagliardi,[53a,53b] L. G. Gagnon,[97] C. Galea,[108] B. Galhardo,[128a,128c] E. J. Gallas,[122] B. J. Gallop,[133] P. Gallus,[130] G. Galster,[39] K. K. Gan,[113] S. Ganguly,[175] Y. Gao,[77] Y. S. Gao,[145,h] F. M. Garay Walls,[34a] C. García,[170] J. E. García Navarro,[170] J. A. García Pascual,[35a] M. Garcia-Sciveres,[16] R. W. Gardner,[33] N. Garelli,[145] V. Garonne,[121] K. Gasnikova,[45] A. Gaudiello,[53a,53b] G. Gaudio,[123a] I. L. Gavrilenko,[98] C. Gay,[171] G. Gaycken,[23] E. N. Gazis,[10] C. N. P. Gee,[133] J. Geisen,[57] M. Geisen,[86] M. P. Geisler,[60a] K. Gellerstedt,[148a,148b] C. Gemme,[53a] M. H. Genest,[58] C. Geng,[92] S. Gentile,[134a,134b] C. Gentsos,[156] S. George,[80] D. Gerbaudo,[13] G. Geßner,[46] S. Ghasemi,[143] M. Ghneimat,[23] B. Giacobbe,[22a] S. Giagu,[134a,134b] N. Giangiacomi,[22a,22b] P. Giannetti,[126a] S. M. Gibson,[80] M. Gignac,[139] M. Gilchriese,[16] D. Gillberg,[31] G. Gilles,[178] D. M. Gingrich,[3,e] M. P. Giordani,[167a,167c] F. M. Giorgi,[22a] P. F. Giraud,[138] P. Giromini,[59] G. Giugliarelli,[167a,167c] D. Giugni,[94a] F. Giuli,[122] M. Giulini,[60b] S. Gkaitatzis,[156] I. Gkialas,[9,u] E. L. Gkougkousis,[13] P. Gkountoumis,[10] L. K. Gladilin,[101] C. Glasman,[85] J. Glatzer,[13] P. C. F. Glaysher,[45] A. Glazov,[45] M. Goblirsch-Kolb,[25] J. Godlewski,[42] S. Goldfarb,[91] T. Golling,[52] D. Golubkov,[132] A. Gomes,[128a,128b,128d] R. Gonçalo,[128a] R. Goncalves Gama,[26b] G. Gonella,[51] L. Gonella,[19] A. Gongadze,[68] F. Gonnella,[19] J. L. Gonski,[59] S. González de la Hoz,[170] S. Gonzalez-Sevilla,[52] L. Goossens,[32] P. A. Gorbounov,[99] H. A. Gordon,[27] B. Gorini,[32] E. Gorini,[76a,76b] A. Gorišek,[78] A. T. Goshaw,[48] C. Gössling,[46] M. I. Gostkin,[68] C. A. Gottardo,[23] C. R. Goudet,[119] D. Goujdami,[137c] A. G. Goussiou,[140] N. Govender,[147b,v] C. Goy,[5] E. Gozani,[154] I. Grabowska-Bold,[41a] P. O. J. Gradin,[168] E. C. Graham,[77] J. Gramling,[166] E. Gramstad,[121] S. Grancagnolo,[17] V. Gratchev,[125] P. M. Gravila,[28f] C. Gray,[56] H. M. Gray,[16] Z. D. Greenwood,[82,w] C. Grefe,[23] K. Gregersen,[81] I. M. Gregor,[45] P. Grenier,[145] K. Grevtsov,[45] J. Griffiths,[8] A. A. Grillo,[139] K. Grimm,[145] S. Grinstein,[13,x] Ph. Gris,[37] J.-F. Grivaz,[119] S. Groh,[86] E. Gross,[175] J. Grosse-Knetter,[57] G. C. Grossi,[82] Z. J. Grout,[81] A. Grummer,[107] L. Guan,[92] W. Guan,[176] J. Guenther,[32] A. Guerguichon,[119] F. Guescini,[163a] D. Guest,[166] O. Gueta,[155] R. Gugel,[51] B. Gui,[113] T. Guillemin,[5] S. Guindon,[32] U. Gul,[56] C. Gumpert,[32] J. Guo,[36c] W. Guo,[92] Y. Guo,[36a,y] R. Gupta,[43] S. Gurbuz,[20a] G. Gustavino,[115] B. J. Gutelman,[154] P. Gutierrez,[115] N. G. Gutierrez Ortiz,[81] C. Gutschow,[81] C. Guyot,[138] M. P. Guzik,[41a] C. Gwenlan,[122] C. B. Gwilliam,[77] A. Haas,[112] C. Haber,[16] H. K. Hadavand,[8] N. Haddad,[137e] A. Hadef,[88] S. Hageböck,[23] M. Hagihara,[164] H. Hakobyan,[180,a] M. Haleem,[177] J. Haley,[116] G. Halladjian,[93] G. D. Hallewell,[88] K. Hamacher,[178] P. Hamal,[117] K. Hamano,[172] A. Hamilton,[147a] G. N. Hamity,[141] K. Han,[36a,z] L. Han,[36a] S. Han,[35a,35d] K. Hanagaki,[69,aa] M. Hance,[139] D. M. Handl,[102] B. Haney,[124] R. Hankache,[83] P. Hanke,[60a] E. Hansen,[84] J. B. Hansen,[39] J. D. Hansen,[39] M. C. Hansen,[23] P. H. Hansen,[39] K. Hara,[164] A. S. Hard,[176] T. Harenberg,[178] S. Harkusha,[95] P. F. Harrison,[173] N. M. Hartmann,[102] Y. Hasegawa,[142] A. Hasib,[49] S. Hassani,[138] S. Haug,[18] R. Hauser,[93] L. Hauswald,[47] L. B. Havener,[38] M. Havranek,[130] C. M. Hawkes,[19] R. J. Hawkings,[32] D. Hayden,[93] C. P. Hays,[122] J. M. Hays,[79] H. S. Hayward,[77] S. J. Haywood,[133] T. Heck,[86] V. Hedberg,[84] L. Heelan,[8] S. Heer,[23] K. K. Heidegger,[51] S. Heim,[45] T. Heim,[16] B. Heinemann,[45,bb] J. J. Heinrich,[102] L. Heinrich,[112] C. Heinz,[55] J. Hejbal,[129] L. Helary,[32] A. Held,[171] S. Hellesund,[121] S. Hellman,[148a,148b] C. Helsens,[32] R. C. W. Henderson,[75] Y. Heng,[176] S. Henkelmann,[171] A. M. Henriques Correia,[32] G. H. Herbert,[17] H. Herde,[25] V. Herget,[177] Y. Hernández Jiménez,[147c] H. Herr,[86] G. Herten,[51] R. Hertenberger,[102] L. Hervas,[32] T. C. Herwig,[124] G. G. Hesketh,[81] N. P. Hessey,[163a] J. W. Hetherly,[43] S. Higashino,[69] E. Higón-Rodriguez,[170] K. Hildebrand,[33] E. Hill,[172] J. C. Hill,[30] K. H. Hiller,[45] S. J. Hillier,[19] M. Hils,[47] I. Hinchliffe,[16] M. Hirose,[51] D. Hirschbuehl,[178] B. Hiti,[78] O. Hladik,[129] D. R. Hlaluku,[147c] X. Hoad,[49] J. Hobbs,[150] N. Hod,[163a] M. C. Hodgkinson,[141] A. Hoecker,[32] M. R. Hoeferkamp,[107] F. Hoenig,[102] D. Hohn,[23] D. Hohov,[119]

T. R. Holmes,[33] M. Holzbock,[102] M. Homann,[46] S. Honda,[164] T. Honda,[69] T. M. Hong,[127] B. H. Hooberman,[169] W. H. Hopkins,[118] Y. Horii,[105] A. J. Horton,[144] L. A. Horyn,[33] J-Y. Hostachy,[58] A. Hostiuc,[140] S. Hou,[153] A. Hoummada,[137a] J. Howarth,[87] J. Hoya,[74] M. Hrabovsky,[117] J. Hrdinka,[32] I. Hristova,[17] J. Hrivnac,[119] T. Hryn'ova,[5] A. Hrynevich,[96] P. J. Hsu,[63] S.-C. Hsu,[140] Q. Hu,[27] S. Hu,[36c] Y. Huang,[35a] Z. Hubacek,[130] F. Hubaut,[88] F. Huegging,[23] T. B. Huffman,[122] E. W. Hughes,[38] M. Huhtinen,[32] R. F. H. Hunter,[31] P. Huo,[150] A. M. Hupe,[31] N. Huseynov,[68,c] J. Huston,[93] J. Huth,[59] R. Hyneman,[92] G. Iacobucci,[52] G. Iakovidis,[27] I. Ibragimov,[143] L. Iconomidou-Fayard,[119] Z. Idrissi,[137e] P. Iengo,[32] O. Igonkina,[109,cc] T. Iizawa,[174] Y. Ikegami,[69] M. Ikeno,[69] D. Iliadis,[156] N. Ilic,[145] F. Iltzsche,[47] G. Introzzi,[123a,123b] M. Iodice,[136a] K. Iordanidou,[38] V. Ippolito,[134a,134b] M. F. Isacson,[168] N. Ishijima,[120] M. Ishino,[157] M. Ishitsuka,[159] C. Issever,[122] S. Istin,[20a] F. Ito,[164] J. M. Iturbe Ponce,[62a] R. Iuppa,[162a,162b] H. Iwasaki,[69] J. M. Izen,[44] V. Izzo,[106a] S. Jabbar,[3] P. Jacka,[129] P. Jackson,[1] R. M. Jacobs,[23] V. Jain,[2] G. Jäkel,[178] K. B. Jakobi,[86] K. Jakobs,[51] S. Jakobsen,[65] T. Jakoubek,[129] D. O. Jamin,[116] D. K. Jana,[82] R. Jansky,[52] J. Janssen,[23] M. Janus,[57] P. A. Janus,[41a] G. Jarlskog,[84] N. Javadov,[68,c] T. Javůrek,[51] M. Javurkova,[51] F. Jeanneau,[138] L. Jeanty,[16] J. Jejelava,[54a,dd] A. Jelinskas,[173] P. Jenni,[51,ee] C. Jeske,[173] S. Jézéquel,[5] H. Ji,[176] J. Jia,[150] H. Jiang,[67] Y. Jiang,[36a] Z. Jiang,[145] S. Jiggins,[81] J. Jimenez Pena,[170] S. Jin,[35b] A. Jinaru,[28b] O. Jinnouchi,[159] H. Jivan,[147c] P. Johansson,[141] K. A. Johns,[7] C. A. Johnson,[64] W. J. Johnson,[140] K. Jon-And,[148a,148b] R. W. L. Jones,[75] S. D. Jones,[151] S. Jones,[7] T. J. Jones,[77] J. Jongmanns,[60a] P. M. Jorge,[128a,128b] J. Jovicevic,[163a] X. Ju,[176] A. Juste Rozas,[13,x] A. Kaczmarska,[42] M. Kado,[119] H. Kagan,[113] M. Kagan,[145] S. J. Kahn,[88] T. Kaji,[174] E. Kajomovitz,[154] C. W. Kalderon,[84] A. Kaluza,[86] S. Kama,[43] A. Kamenshchikov,[132] L. Kanjir,[78] Y. Kano,[157] V. A. Kantserov,[100] J. Kanzaki,[69] B. Kaplan,[112] L. S. Kaplan,[176] D. Kar,[147c] K. Karakostas,[10] N. Karastathis,[10] M. J. Kareem,[163b] E. Karentzos,[10] S. N. Karpov,[68] Z. M. Karpova,[68] V. Kartvelishvili,[75] A. N. Karyukhin,[132] K. Kasahara,[164] L. Kashif,[176] R. D. Kass,[113] A. Kastanas,[149] Y. Kataoka,[157] C. Kato,[157] A. Katre,[52] J. Katzy,[45] K. Kawade,[70] K. Kawagoe,[73] T. Kawamoto,[157] G. Kawamura,[57] E. F. Kay,[77] V. F. Kazanin,[111,d] R. Keeler,[172] R. Kehoe,[43] J. S. Keller,[31] E. Kellermann,[84] J. J. Kempster,[19] J Kendrick,[19] H. Keoshkerian,[161] O. Kepka,[129] B. P. Kerševan,[78] S. Kersten,[178] R. A. Keyes,[90] M. Khader,[169] F. Khalil-zada,[12] A. Khanov,[116] A. G. Kharlamov,[111,d] T. Kharlamova,[111,d] A. Khodinov,[160] T. J. Khoo,[52] V. Khovanskiy,[99,a] E. Khramov,[68] J. Khubua,[54b,ff] S. Kido,[70] M. Kiehn,[52] C. R. Kilby,[80] H. Y. Kim,[8] S. H. Kim,[164] Y. K. Kim,[33] N. Kimura,[167a,167c] O. M. Kind,[17] B. T. King,[77] D. Kirchmeier,[47] J. Kirk,[133] A. E. Kiryunin,[103] T. Kishimoto,[157] D. Kisielewska,[41a] V. Kitali,[45] O. Kivernyk,[5] E. Kladiva,[146b] T. Klapdor-Kleingrothaus,[51] M. H. Klein,[92] M. Klein,[77] U. Klein,[77] K. Kleinknecht,[86] P. Klimek,[110] A. Klimentov,[27] R. Klingenberg,[46,a] T. Klingl,[23] T. Klioutchnikova,[32] F. F. Klitzner,[102] E.-E. Kluge,[60a] P. Kluit,[109] S. Kluth,[103] E. Kneringer,[65] E. B. F. G. Knoops,[88] A. Knue,[51] A. Kobayashi,[157] D. Kobayashi,[73] T. Kobayashi,[157] M. Kobel,[47] M. Kocian,[145] P. Kodys,[131] T. Koffas,[31] E. Koffeman,[109] N. M. Köhler,[103] T. Koi,[145] M. Kolb,[60b] I. Koletsou,[5] T. Kondo,[69] N. Kondrashova,[36c] K. Köneke,[51] A. C. König,[108] T. Kono,[69,gg] R. Konoplich,[112,hh] N. Konstantinidis,[81] B. Konya,[84] R. Kopeliansky,[64] S. Koperny,[41a] K. Korcyl,[42] K. Kordas,[156] A. Korn,[81] I. Korolkov,[13] E. V. Korolkova,[141] O. Kortner,[103] S. Kortner,[103] T. Kosek,[131] V. V. Kostyukhin,[23] A. Kotwal,[48] A. Koulouris,[10] A. Kourkoumeli-Charalampidi,[123a,123b] C. Kourkoumelis,[9] E. Kourlitis,[141] V. Kouskoura,[27] A. B. Kowalewska,[42] R. Kowalewski,[172] T. Z. Kowalski,[41a] C. Kozakai,[157] W. Kozanecki,[138] A. S. Kozhin,[132] V. A. Kramarenko,[101] G. Kramberger,[78] D. Krasnopevtsev,[100] M. W. Krasny,[83] A. Krasznahorkay,[32] D. Krauss,[103] J. A. Kremer,[41a] J. Kretzschmar,[77] K. Kreutzfeldt,[55] P. Krieger,[161] K. Krizka,[16] K. Kroeninger,[46] H. Kroha,[103] J. Kroll,[129] J. Kroll,[124] J. Kroseberg,[23] J. Krstic,[14] U. Kruchonak,[68] H. Krüger,[23] N. Krumnack,[67] M. C. Kruse,[48] T. Kubota,[91] S. Kuday,[4b] J. T. Kuechler,[178] S. Kuehn,[32] A. Kugel,[60a] F. Kuger,[177] T. Kuhl,[45] V. Kukhtin,[68] R. Kukla,[88] Y. Kulchitsky,[95] S. Kuleshov,[34b] Y. P. Kulinich,[169] M. Kuna,[58] T. Kunigo,[71] A. Kupco,[129] T. Kupfer,[46] O. Kuprash,[155] H. Kurashige,[70] L. L. Kurchaninov,[163a] Y. A. Kurochkin,[95] M. G. Kurth,[35a,35d] E. S. Kuwertz,[172] M. Kuze,[159] J. Kvita,[117] T. Kwan,[172] A. La Rosa,[103] J. L. La Rosa Navarro,[26d] L. La Rotonda,[40a,40b] F. La Ruffa,[40a,40b] C. Lacasta,[170] F. Lacava,[134a,134b] J. Lacey,[45] D. P. J. Lack,[87] H. Lacker,[17] D. Lacour,[83] E. Ladygin,[68] R. Lafaye,[5] B. Laforge,[83] S. Lai,[57] S. Lammers,[64] W. Lampl,[7] E. Lançon,[27] U. Landgraf,[51] M. P. J. Landon,[79] M. C. Lanfermann,[52] V. S. Lang,[45] J. C. Lange,[13] R. J. Langenberg,[32] A. J. Lankford,[166] F. Lanni,[27] K. Lantzsch,[23] A. Lanza,[123a] A. Lapertosa,[53a,53b] S. Laplace,[83] J. F. Laporte,[138] T. Lari,[94a] F. Lasagni Manghi,[22a,22b] M. Lassnig,[32] T. S. Lau,[62a] A. Laudrain,[119] A. T. Law,[139] P. Laycock,[77] M. Lazzaroni,[94a,94b] B. Le,[91] O. Le Dortz,[83] E. Le Guirriec,[88] E. P. Le Quilleuc,[138] M. LeBlanc,[7] T. LeCompte,[6] F. Ledroit-Guillon,[58] C. A. Lee,[27] G. R. Lee,[34a] S. C. Lee,[153] L. Lee,[59] B. Lefebvre,[90] M. Lefebvre,[172] F. Legger,[102] C. Leggett,[16] G. Lehmann Miotto,[32] W. A. Leight,[45] A. Leisos,[156,ii] M. A. L. Leite,[26d] R. Leitner,[131] D. Lellouch,[175] B. Lemmer,[57] K. J. C. Leney,[81] T. Lenz,[23] B. Lenzi,[32] R. Leone,[7] S. Leone,[126a] C. Leonidopoulos,[49] G. Lerner,[151] C. Leroy,[97] R. Les,[161] A. A. J. Lesage,[138]

C. G. Lester,[30] M. Levchenko,[125] J. Levêque,[5] D. Levin,[92] L. J. Levinson,[175] M. Levy,[19] D. Lewis,[79] B. Li,[36a,y] H. Li,[36b] L. Li,[36c] Q. Li,[35a,35d] Q. Li,[36a] S. Li,[36d] X. Li,[36c] Y. Li,[143] Z. Liang,[35a] B. Liberti,[135a] A. Liblong,[161] K. Lie,[62c] A. Limosani,[152] C. Y. Lin,[30] K. Lin,[93] S. C. Lin,[182] T. H. Lin,[86] R. A. Linck,[64] B. E. Lindquist,[150] A. E. Lionti,[52] E. Lipeles,[124] A. Lipniacka,[15] M. Lisovyi,[60b] T. M. Liss,[169,jj] A. Lister,[171] A. M. Litke,[139] B. Liu,[67] H. Liu,[92] H. Liu,[27] J. K. K. Liu,[122] J. B. Liu,[36a] K. Liu,[83] M. Liu,[36a] P. Liu,[16] Y. L. Liu,[36a] Y. Liu,[36a] M. Livan,[123a,123b] A. Lleres,[58] J. Llorente Merino,[35a] S. L. Lloyd,[79] C. Y. Lo,[62b] F. Lo Sterzo,[43] E. M. Lobodzinska,[45] P. Loch,[7] F. K. Loebinger,[87] A. Loesle,[51] K. M. Loew,[25] T. Lohse,[17] K. Lohwasser,[141] M. Lokajicek,[129] B. A. Long,[24] J. D. Long,[169] R. E. Long,[75] L. Longo,[76a,76b] K. A. Looper,[113] J. A. Lopez,[34b] I. Lopez Paz,[13] A. Lopez Solis,[83] J. Lorenz,[102] N. Lorenzo Martinez,[5] M. Losada,[21] P. J. Lösel,[102] X. Lou,[35a] A. Lounis,[119] J. Love,[6] P. A. Love,[75] H. Lu,[62a] N. Lu,[92] Y. J. Lu,[63] H. J. Lubatti,[140] C. Luci,[134a,134b] A. Lucotte,[58] C. Luedtke,[51] F. Luehring,[64] I. Luise,[83] W. Lukas,[65] L. Luminari,[134a] B. Lund-Jensen,[149] M. S. Lutz,[89] P. M. Luzi,[83] D. Lynn,[27] R. Lysak,[129] E. Lytken,[84] F. Lyu,[35a] V. Lyubushkin,[68] H. Ma,[27] L. L. Ma,[36b] Y. Ma,[36b] G. Maccarrone,[50] A. Macchiolo,[103] C. M. Macdonald,[141] B. Maček,[78] J. Machado Miguens,[124,128b] D. Madaffari,[170] R. Madar,[37] W. F. Mader,[47] A. Madsen,[45] N. Madysa,[47] J. Maeda,[70] S. Maeland,[15] T. Maeno,[27] A. S. Maevskiy,[101] V. Magerl,[51] C. Maidantchik,[26a] T. Maier,[102] A. Maio,[128a,128b,128d] O. Majersky,[146a] S. Majewski,[118] Y. Makida,[69] N. Makovec,[119] B. Malaescu,[83] Pa. Malecki,[42] V. P. Maleev,[125] F. Malek,[58] U. Mallik,[66] D. Malon,[6] C. Malone,[30] S. Maltezos,[10] S. Malyukov,[32] J. Mamuzic,[170] G. Mancini,[50] I. Mandić,[78] J. Maneira,[128a,128b] L. Manhaes de Andrade Filho,[26b] J. Manjarres Ramos,[47] K. H. Mankinen,[84] A. Mann,[102] A. Manousos,[32] B. Mansoulie,[138] J. D. Mansour,[35a] R. Mantifel,[90] M. Mantoani,[57] S. Manzoni,[94a,94b] G. Marceca,[29] L. March,[52] L. Marchese,[122] G. Marchiori,[83] M. Marcisovsky,[129] C. A. Marin Tobon,[32] M. Marjanovic,[37] D. E. Marley,[92] F. Marroquim,[26a] Z. Marshall,[16] M. U. F Martensson,[168] S. Marti-Garcia,[170] C. B. Martin,[113] T. A. Martin,[173] V. J. Martin,[49] B. Martin dit Latour,[15] M. Martinez,[13,x] V. I. Martinez Outschoorn,[89] S. Martin-Haugh,[133] V. S. Martoiu,[28b] A. C. Martyniuk,[81] A. Marzin,[32] L. Masetti,[86] T. Mashimo,[157] R. Mashinistov,[98] J. Masik,[87] A. L. Maslennikov,[111,d] L. H. Mason,[91] L. Massa,[135a,135b] P. Mastrandrea,[5] A. Mastroberardino,[40a,40b] T. Masubuchi,[157] P. Mättig,[178] J. Maurer,[28b] S. J. Maxfield,[77] D. A. Maximov,[111,d] R. Mazini,[153] I. Maznas,[156] S. M. Mazza,[139] N. C. Mc Fadden,[107] G. Mc Goldrick,[161] S. P. Mc Kee,[92] A. McCarn,[92] T. G. McCarthy,[103] L. I. McClymont,[81] E. F. McDonald,[91] J. A. Mcfayden,[32] G. Mchedlidze,[57] M. A. McKay,[43] S. J. McMahon,[133] P. C. McNamara,[91] C. J. McNicol,[173] R. A. McPherson,[172,p] Z. A. Meadows,[89] S. Meehan,[140] T. J. Megy,[51] S. Mehlhase,[102] A. Mehta,[77] T. Meideck,[58] K. Meier,[60a] B. Meirose,[44] D. Melini,[170,kk] B. R. Mellado Garcia,[147c] J. D. Mellenthin,[57] M. Melo,[146a] F. Meloni,[18] A. Melzer,[23] S. B. Menary,[87] L. Meng,[77] X. T. Meng,[92] A. Mengarelli,[22a,22b] S. Menke,[103] E. Meoni,[40a,40b] S. Mergelmeyer,[17] C. Merlassino,[18] P. Mermod,[52] L. Merola,[106a,106b] C. Meroni,[94a] F. S. Merritt,[33] A. Messina,[134a,134b] J. Metcalfe,[6] A. S. Mete,[166] C. Meyer,[124] J-P. Meyer,[138] J. Meyer,[109] H. Meyer Zu Theenhausen,[60a] F. Miano,[151] R. P. Middleton,[133] S. Miglioranzi,[53a,53b] L. Mijović,[49] G. Mikenberg,[175] M. Mikestikova,[129] M. Mikuž,[78] M. Milesi,[91] A. Milic,[161] D. A. Millar,[79] D. W. Miller,[33] A. Milov,[175] D. A. Milstead,[148a,148b] A. A. Minaenko,[132] I. A. Minashvili,[54b] A. I. Mincer,[112] B. Mindur,[41a] M. Mineev,[68] Y. Minegishi,[157] Y. Ming,[176] L. M. Mir,[13] A. Mirto,[76a,76b] K. P. Mistry,[124] T. Mitani,[174] J. Mitrevski,[102] V. A. Mitsou,[170] A. Miucci,[18] P. S. Miyagawa,[141] A. Mizukami,[69] J. U. Mjörnmark,[84] T. Mkrtchyan,[180] M. Mlynarikova,[131] T. Moa,[148a,148b] K. Mochizuki,[97] P. Mogg,[51] S. Mohapatra,[38] S. Molander,[148a,148b] R. Moles-Valls,[23] M. C. Mondragon,[93] K. Mönig,[45] J. Monk,[39] E. Monnier,[88] A. Montalbano,[150] J. Montejo Berlingen,[32] F. Monticelli,[74] S. Monzani,[94a] R. W. Moore,[3] N. Morange,[119] D. Moreno,[21] M. Moreno Llácer,[32] P. Morettini,[53a] M. Morgenstern,[109] S. Morgenstern,[32] D. Mori,[144] T. Mori,[157] M. Morii,[59] M. Morinaga,[174] V. Morisbak,[121] A. K. Morley,[32] G. Mornacchi,[32] J. D. Morris,[79] L. Morvaj,[150] P. Moschovakos,[10] M. Mosidze,[54b] H. J. Moss,[141] J. Moss,[145,ll] K. Motohashi,[159] R. Mount,[145] E. Mountricha,[27] E. J. W. Moyse,[89] S. Muanza,[88] F. Mueller,[103] J. Mueller,[127] R. S. P. Mueller,[102] D. Muenstermann,[75] P. Mullen,[56] G. A. Mullier,[18] F. J. Munoz Sanchez,[87] P. Murin,[146b] W. J. Murray,[173,133] A. Murrone,[94a,94b] M. Muškinja,[78] C. Mwewa,[147a] A. G. Myagkov,[132,mm] J. Myers,[118] M. Myska,[130] B. P. Nachman,[16] O. Nackenhorst,[46] K. Nagai,[122] R. Nagai,[69,gg] K. Nagano,[69] Y. Nagasaka,[61] K. Nagata,[164] M. Nagel,[51] E. Nagy,[88] A. M. Nairz,[32] Y. Nakahama,[105] K. Nakamura,[69] T. Nakamura,[157] I. Nakano,[114] R. F. Naranjo Garcia,[45] R. Narayan,[11] D. I. Narrias Villar,[60a] I. Naryshkin,[125] T. Naumann,[45] G. Navarro,[21] R. Nayyar,[7] H. A. Neal,[92] P. Yu. Nechaeva,[98] T. J. Neep,[138] A. Negri,[123a,123b] M. Negrini,[22a] S. Nektarijevic,[108] C. Nellist,[57] M. E. Nelson,[122] S. Nemecek,[129] P. Nemethy,[112] M. Nessi,[32,nn] M. S. Neubauer,[169] M. Neumann,[178] P. R. Newman,[19] T. Y. Ng,[62c] Y. S. Ng,[17] H. D. N. Nguyen,[88] T. Nguyen Manh,[97] R. B. Nickerson,[122] R. Nicolaidou,[138] J. Nielsen,[139] N. Nikiforou,[11] V. Nikolaenko,[132,mm] I. Nikolic-Audit,[83] K. Nikolopoulos,[19] P. Nilsson,[27] Y. Ninomiya,[69] A. Nisati,[134a] N. Nishu,[36c] R. Nisius,[103] I. Nitsche,[46] T. Nitta,[174] T. Nobe,[157] Y. Noguchi,[71] M. Nomachi,[120] I. Nomidis,[31]

M. A. Nomura,[27] T. Nooney,[79] M. Nordberg,[32] N. Norjoharuddeen,[122] T. Novak,[78] O. Novgorodova,[47] R. Novotny,[130] M. Nozaki,[69] L. Nozka,[117] K. Ntekas,[166] E. Nurse,[81] F. Nuti,[91] K. O'connor,[25] D. C. O'Neil,[144] A. A. O'Rourke,[45] V. O'Shea,[56] F. G. Oakham,[31,e] H. Oberlack,[103] T. Obermann,[23] J. Ocariz,[83] A. Ochi,[70] I. Ochoa,[38] J. P. Ochoa-Ricoux,[34a] S. Oda,[73] S. Odaka,[69] A. Oh,[87] S. H. Oh,[48] C. C. Ohm,[149] H. Ohman,[168] H. Oide,[53a,53b] H. Okawa,[164] Y. Okumura,[157] T. Okuyama,[69] A. Olariu,[28b] L. F. Oleiro Seabra,[128a] S. A. Olivares Pino,[34a] D. Oliveira Damazio,[27] J. L. Oliver,[1] M. J. R. Olsson,[33] A. Olszewski,[42] J. Olszowska,[42] A. Onofre,[128a,128e] K. Onogi,[105] P. U. E. Onyisi,[11,oo] H. Oppen,[121] M. J. Oreglia,[33] Y. Oren,[155] D. Orestano,[136a,136b] E. C. Orgill,[87] N. Orlando,[62b] R. S. Orr,[161] B. Osculati,[53a,53b,a] R. Ospanov,[36a] G. Otero y Garzon,[29] H. Otono,[73] M. Ouchrif,[137d] F. Ould-Saada,[121] A. Ouraou,[138] K. P. Oussoren,[109] Q. Ouyang,[35a] M. Owen,[56] R. E. Owen,[19] V. E. Ozcan,[20a] N. Ozturk,[8] K. Pachal,[144] A. Pacheco Pages,[13] L. Pacheco Rodriguez,[138] C. Padilla Aranda,[13] S. Pagan Griso,[16] M. Paganini,[179] F. Paige,[27] G. Palacino,[64] S. Palazzo,[40a,40b] S. Palestini,[32] M. Palka,[41b] D. Pallin,[37] E. St. Panagiotopoulou,[10] I. Panagoulias,[10] C. E. Pandini,[52] J. G. Panduro Vazquez,[80] P. Pani,[32] D. Pantea,[28b] L. Paolozzi,[52] Th. D. Papadopoulou,[10] K. Papageorgiou,[9,u] A. Paramonov,[6] D. Paredes Hernandez,[62b] B. Parida,[36c] A. J. Parker,[75] M. A. Parker,[30] K. A. Parker,[45] F. Parodi,[53a,53b] J. A. Parsons,[38] U. Parzefall,[51] V. R. Pascuzzi,[161] J. M. Pasner,[139] E. Pasqualucci,[134a] S. Passaggio,[53a] Fr. Pastore,[80] S. Pataraia,[86] J. R. Pater,[87] T. Pauly,[32] B. Pearson,[103] S. Pedraza Lopez,[170] R. Pedro,[128a,128b] S. V. Peleganchuk,[111,d] O. Penc,[129] C. Peng,[35a,35d] H. Peng,[36a] J. Penwell,[64] B. S. Peralva,[26b] M. M. Perego,[138] D. V. Perepelitsa,[27] F. Peri,[17] L. Perini,[94a,94b] H. Pernegger,[32] S. Perrella,[106a,106b] V. D. Peshekhonov,[68,a] K. Peters,[45] R. F. Y. Peters,[87] B. A. Petersen,[32] T. C. Petersen,[39] E. Petit,[58] A. Petridis,[1] C. Petridou,[156] P. Petroff,[119] E. Petrolo,[134a] M. Petrov,[122] F. Petrucci,[136a,136b] N. E. Pettersson,[89] A. Peyaud,[138] R. Pezoa,[34b] T. Pham,[91] F. H. Phillips,[93] P. W. Phillips,[133] G. Piacquadio,[150] E. Pianori,[173] A. Picazio,[89] M. A. Pickering,[122] R. Piegaia,[29] J. E. Pilcher,[33] A. D. Pilkington,[87] M. Pinamonti,[135a,135b] J. L. Pinfold,[3] M. Pitt,[175] M.-A. Pleier,[27] V. Pleskot,[131] E. Plotnikova,[68] D. Pluth,[67] P. Podberezko,[111] R. Poettgen,[84] R. Poggi,[123a,123b] L. Poggioli,[119] I. Pogrebnyak,[93] D. Pohl,[23] I. Pokharel,[57] G. Polesello,[123a] A. Poley,[45] A. Policicchio,[40a,40b] R. Polifka,[32] A. Polini,[22a] C. S. Pollard,[45] V. Polychronakos,[27] D. Ponomarenko,[100] L. Pontecorvo,[134a] G. A. Popeneciu,[28d] D. M. Portillo Quintero,[83] S. Pospisil,[130] K. Potamianos,[45] I. N. Potrap,[68] C. J. Potter,[30] H. Potti,[11] T. Poulsen,[84] J. Poveda,[32] M. E. Pozo Astigarraga,[32] P. Pralavorio,[88] S. Prell,[67] D. Price,[87] M. Primavera,[76a] S. Prince,[90] N. Proklova,[100] K. Prokofiev,[62c] F. Prokoshin,[34b] S. Protopopescu,[27] J. Proudfoot,[6] M. Przybycien,[41a] A. Puri,[169] P. Puzo,[119] J. Qian,[92] Y. Qin,[87] A. Quadt,[57] M. Queitsch-Maitland,[45] A. Qureshi,[1] V. Radeka,[27] S. K. Radhakrishnan,[150] P. Rados,[91] F. Ragusa,[94a,94b] G. Rahal,[181] J. A. Raine,[87] S. Rajagopalan,[27] T. Rashid,[119] S. Raspopov,[5] M. G. Ratti,[94a,94b] D. M. Rauch,[45] F. Rauscher,[102] S. Rave,[86] I. Ravinovich,[175] J. H. Rawling,[87] M. Raymond,[32] A. L. Read,[121] N. P. Readioff,[58] M. Reale,[76a,76b] D. M. Rebuzzi,[123a,123b] A. Redelbach,[177] G. Redlinger,[27] R. Richter,[103] S. Richter,[81] E. Richter-Was,[41b] O. Ricken,[23] M. Ridel,[83] P. Rieck,[103] C. J. Riegel,[178] O. Rifki,[45] M. Rijssenbeek,[150] A. Rimoldi,[123a,123b] M. Rimoldi,[18] L. Rinaldi,[22a] G. Ripellino,[149] B. Ristić,[32] E. Ritsch,[32] I. Riu,[13] J. C. Rivera Vergara,[34a] F. Rizatdinova,[116] E. Rizvi,[79] C. Rizzi,[13] R. T. Roberts,[87] S. H. Robertson,[90,p] A. Robichaud-Veronneau,[90] D. Robinson,[30] J. E. M. Robinson,[45] A. Robson,[56] E. Rocco,[86] C. Roda,[126a,126b] Y. Rodina,[88,pp] S. Rodriguez Bosca,[170] A. Rodriguez Perez,[13] D. Rodriguez Rodriguez,[170] A. M. Rodríguez Vera,[163b] S. Roe,[32] C. S. Rogan,[59] O. Røhne,[121] R. Röhrig,[103] J. Roloff,[59] A. Romaniouk,[100] M. Romano,[22a,22b] S. M. Romano Saez,[37] E. Romero Adam,[170] N. Rompotis,[77] M. Ronzani,[51] L. Roos,[83] S. Rosati,[134a] K. Rosbach,[51] P. Rose,[139] N.-A. Rosien,[57] E. Rossi,[106a,106b] L. P. Rossi,[53a] L. Rossini,[94a,94b] J. H. N. Rosten,[30] R. Rosten,[140] M. Rotaru,[28b] J. Rothberg,[140] D. Rousseau,[119] D. Roy,[147c] A. Rozanov,[88] Y. Rozen,[154] X. Ruan,[147c] F. Rubbo,[145] F. Rühr,[51] A. Ruiz-Martinez,[31] Z. Rurikova,[51] N. A. Rusakovich,[68] H. L. Russell,[90] J. P. Rutherfoord,[7] N. Ruthmann,[32] E. M. Rüttinger,[45] Y. F. Ryabov,[125] M. Rybar,[169] G. Rybkin,[119] S. Ryu,[6] A. Ryzhov,[132] G. F. Rzehorz,[57] A. F. Saavedra,[152] G. Sabato,[109] S. Sacerdoti,[119] H. F-W. Sadrozinski,[139] R. Sadykov,[68] F. Safai Tehrani,[134a] P. Saha,[110] M. Sahinsoy,[60a] M. Saimpert,[45] M. Saito,[157] T. Saito,[157] H. Sakamoto,[157] G. Salamanna,[136a,136b] J. E. Salazar Loyola,[34b] D. Salek,[109] P. H. Sales De Bruin,[168] D. Salihagic,[103] A. Salnikov,[145] J. Salt,[170] D. Salvatore,[40a,40b] F. Salvatore,[151] A. Salvucci,[62a,62b,62c] A. Salzburger,[32] D. Sammel,[51] D. Sampsonidis,[156] D. Sampsonidou,[156] J. Sánchez,[170] A. Sanchez Pineda,[167a,167c] H. Sandaker,[121] C. O. Sander,[45] M. Sandhoff,[178] C. Sandoval,[21] D. P. C. Sankey,[133] M. Sannino,[53a,53b] Y. Sano,[105] A. Sansoni,[50] C. Santoni,[37] H. Santos,[128a] I. Santoyo Castillo,[151] A. Sapronov,[68] J. G. Saraiva,[128a,128d] O. Sasaki,[69] K. Sato,[164] E. Sauvan,[5] P. Savard,[161,e] N. Savic,[103] R. Sawada,[157] C. Sawyer,[133] L. Sawyer,[82,w] C. Sbarra,[22a] A. Sbrizzi,[22a,22b] T. Scanlon,[81] D. A. Scannicchio,[166]

J. Schaarschmidt,[140] P. Schacht,[103] B. M. Schachtner,[102] D. Schaefer,[33] L. Schaefer,[124] J. Schaeffer,[86] S. Schaepe,[32] U. Schäfer,[86] A. C. Schaffer,[119] D. Schaile,[102] R. D. Schamberger,[150] V. A. Schegelsky,[125] D. Scheirich,[131] F. Schenck,[17] M. Schernau,[166] C. Schiavi,[53a,53b] S. Schier,[139] L. K. Schildgen,[23] Z. M. Schillaci,[25] C. Schillo,[51] E. J. Schioppa,[32] M. Schioppa,[40a,40b] K. E. Schleicher,[51] S. Schlenker,[32] K. R. Schmidt-Sommerfeld,[103] K. Schmieden,[32] C. Schmitt,[86] S. Schmitt,[45] S. Schmitz,[86] U. Schnoor,[51] L. Schoeffel,[138] A. Schoening,[60b] E. Schopf,[23] M. Schott,[86] J. F. P. Schouwenberg,[108] J. Schovancova,[32] S. Schramm,[52] N. Schuh,[86] A. Schulte,[86] H.-C. Schultz-Coulon,[60a] M. Schumacher,[51] B. A. Schumm,[139] Ph. Schune,[138] A. Schwartzman,[145] T. A. Schwarz,[92] H. Schweiger,[87] Ph. Schwemling,[138] R. Schwienhorst,[93] J. Schwindling,[138] A. Sciandra,[23] G. Sciolla,[25] M. Scornajenghi,[40a,40b] F. Scuri,[126a] F. Scutti,[91] L. M. Scyboz,[103] J. Searcy,[92] P. Seema,[23] S. C. Seidel,[107] A. Seiden,[139] J. M. Seixas,[26a] G. Sekhniaidze,[106a] K. Sekhon,[92] S. J. Sekula,[43] N. Semprini-Cesari,[22a,22b] S. Senkin,[37] C. Serfon,[121] L. Serin,[119] L. Serkin,[167a,167b] M. Sessa,[136a,136b] H. Severini,[115] T. Šfiligoj,[78] F. Sforza,[165] A. Sfyrla,[52] E. Shabalina,[57] J. D. Shahinian,[139] N. W. Shaikh,[148a,148b] L. Y. Shan,[35a] R. Shang,[169] J. T. Shank,[24] M. Shapiro,[16] A. S. Sharma,[1] P. B. Shatalov,[99] K. Shaw,[167a,167b] S. M. Shaw,[87] A. Shcherbakova,[148a,148b] C. Y. Shehu,[151] Y. Shen,[115] N. Sherafati,[31] A. D. Sherman,[24] P. Sherwood,[81] L. Shi,[153,qq] S. Shimizu,[70] C. O. Shimmin,[179] M. Shimojima,[104] I. P. J. Shipsey,[122] S. Shirabe,[73] M. Shiyakova,[68,rr] J. Shlomi,[175] A. Shmeleva,[98] D. Shoaleh Saadi,[97] M. J. Shochet,[33] S. Shojaii,[91] D. R. Shope,[115] S. Shrestha,[113] E. Shulga,[100] P. Sicho,[129] A. M. Sickles,[169] P. E. Sidebo,[149] E. Sideras Haddad,[147c] O. Sidiropoulou,[177] A. Sidoti,[22a,22b] F. Siegert,[47] Dj. Sijacki,[14] J. Silva,[128a,128d] M. Silva Jr.,[176] S. B. Silverstein,[148a] L. Simic,[68] S. Simion,[119] E. Simioni,[86] B. Simmons,[81] M. Simon,[86] P. Sinervo,[161] N. B. Sinev,[118] M. Sioli,[22a,22b] G. Siragusa,[177] I. Siral,[92] S. Yu. Sivoklokov,[101] J. Sjölin,[148a,148b] M. B. Skinner,[75] P. Skubic,[115] M. Slater,[19] T. Slavicek,[130] M. Slawinska,[42] K. Sliwa,[165] R. Slovak,[131] V. Smakhtin,[175] B. H. Smart,[5] J. Smiesko,[146a] N. Smirnov,[100] S. Yu. Smirnov,[100] Y. Smirnov,[100] L. N. Smirnova,[101,ss] O. Smirnova,[84] J. W. Smith,[57] M. N. K. Smith,[38] R. W. Smith,[38] M. Smizanska,[75] K. Smolek,[130] A. A. Snesarev,[98] I. M. Snyder,[118] S. Snyder,[27] R. Sobie,[172,p] F. Socher,[47] A. M. Soffa,[166] A. Soffer,[155] A. Søgaard,[49] D. A. Soh,[153] G. Sokhrannyi,[78] C. A. Solans Sanchez,[32] M. Solar,[130] E. Yu. Soldatov,[100] U. Soldevila,[170] A. A. Solodkov,[132] A. Soloshenko,[68] O. V. Solovyanov,[132] V. Solovyev,[125] P. Sommer,[141] H. Son,[165] W. Song,[133] A. Sopczak,[130] F. Sopkova,[146b] D. Sosa,[60b] C. L. Sotiropoulou,[126a,126b] S. Sottocornola,[123a,123b] R. Soualah,[167a,167c] A. M. Soukharev,[111,d] D. South,[45] B. C. Sowden,[80] S. Spagnolo,[76a,76b] M. Spalla,[103] M. Spangenberg,[173] F. Spanò,[80] D. Sperlich,[17] F. Spettel,[103] T. M. Spieker,[60a] R. Spighi,[22a] G. Spigo,[32] L. A. Spiller,[91] M. Spousta,[131] R. D. St. Denis,[56,a] A. Stabile,[94a,94b] R. Stamen,[60a] S. Stamm,[17] E. Stanecka,[42] R. W. Stanek,[6] C. Stanescu,[136a] M. M. Stanitzki,[45] B. S. Stapf,[109] S. Stapnes,[121] E. A. Starchenko,[132] G. H. Stark,[33] J. Stark,[58] S. H Stark,[39] P. Staroba,[129] P. Starovoitov,[60a] S. Stärz,[32] R. Staszewski,[42] M. Stegler,[45] P. Steinberg,[27] B. Stelzer,[144] H. J. Stelzer,[32] O. Stelzer-Chilton,[163a] H. Stenzel,[55] T. J. Stevenson,[79] G. A. Stewart,[32] M. C. Stockton,[118] G. Stoicea,[28b] P. Stolte,[57] S. Stonjek,[103] A. Straessner,[47] M. E. Stramaglia,[18] J. Strandberg,[149] S. Strandberg,[148a,148b] M. Strauss,[115] P. Strizenec,[146b] R. Ströhmer,[177] D. M. Strom,[118] R. Stroynowski,[43] A. Strubig,[49] S. A. Stucci,[27] B. Stugu,[15] N. A. Styles,[45] D. Su,[145] J. Su,[127] S. Suchek,[60a] Y. Sugaya,[120] M. Suk,[130] V. V. Sulin,[98] DMS Sultan,[52] S. Sultansoy,[4c] T. Sumida,[71] S. Sun,[92] X. Sun,[3] K. Suruliz,[151] C. J. E. Suster,[152] M. R. Sutton,[151] S. Suzuki,[69] M. Svatos,[129] M. Swiatlowski,[33] S. P. Swift,[2] A. Sydorenko,[86] I. Sykora,[146a] T. Sykora,[131] D. Ta,[86] K. Tackmann,[45] J. Taenzer,[155] A. Taffard,[166] R. Tafirout,[163a] E. Tahirovic,[79] N. Taiblum,[155] H. Takai,[27] R. Takashima,[72] E. H. Takasugi,[103] K. Takeda,[70] T. Takeshita,[142] Y. Takubo,[69] M. Talby,[88] A. A. Talyshev,[111,d] J. Tanaka,[157] M. Tanaka,[159] R. Tanaka,[119] R. Tanioka,[70] B. B. Tannenwald,[113] S. Tapia Araya,[34b] S. Tapprogge,[86] A. T. Tarek Abouelfadl Mohamed,[83] S. Tarem,[154] G. Tarna,[28b,r] G. F. Tartarelli,[94a] P. Tas,[131] M. Tasevsky,[129] T. Tashiro,[71] E. Tassi,[40a,40b] A. Tavares Delgado,[128a,128b] Y. Tayalati,[137e] A. C. Taylor,[107] A. J. Taylor,[49] G. N. Taylor,[91] P. T. E. Taylor,[91] W. Taylor,[163b] P. Teixeira-Dias,[80] D. Temple,[144] H. Ten Kate,[32] P. K. Teng,[153] J. J. Teoh,[120] F. Tepel,[178] S. Terada,[69] K. Terashi,[157] J. Terron,[85] S. Terzo,[13] M. Testa,[50] R. J. Teuscher,[161,p] S. J. Thais,[179] T. Theveneaux-Pelzer,[45] F. Thiele,[39] J. P. Thomas,[19] P. D. Thompson,[19] A. S. Thompson,[56] L. A. Thomsen,[179] E. Thomson,[124] Y. Tian,[38] R. E. Ticse Torres,[57] V. O. Tikhomirov,[98,tt] Yu. A. Tikhonov,[111,d] S. Timoshenko,[100] P. Tipton,[179] S. Tisserant,[88] K. Todome,[159] S. Todorova-Nova,[5] S. Todt,[47] J. Tojo,[73] S. Tokár,[146a] K. Tokushuku,[69] E. Tolley,[113] M. Tomoto,[105] L. Tompkins,[145,uu] K. Toms,[107] B. Tong,[59] P. Tornambe,[51] E. Torrence,[118] H. Torres,[47] E. Torró Pastor,[140] J. Toth,[88,vv] F. Touchard,[88] D. R. Tovey,[141] C. J. Treado,[112] T. Trefzger,[177] F. Tresoldi,[151] A. Tricoli,[27] I. M. Trigger,[163a] S. Trincaz-Duvoid,[83] M. F. Tripiana,[13] W. Trischuk,[161] B. Trocmé,[58] A. Trofymov,[45] C. Troncon,[94a] M. Trovatelli,[172] L. Truong,[147b] M. Trzebinski,[42] A. Trzupek,[42] K. W. Tsang,[62a] J. C-L. Tseng,[122] P. V. Tsiareshka,[95] N. Tsirintanis,[9] S. Tsiskaridze,[13]

V. Tsiskaridze,[150] E. G. Tskhadadze,[54a] I. I. Tsukerman,[99] V. Tsulaia,[16] S. Tsuno,[69] D. Tsybychev,[150] Y. Tu,[62b] A. Tudorache,[28b] V. Tudorache,[28b] T. T. Tulbure,[28a] A. N. Tuna,[59] S. Turchikhin,[68] D. Turgeman,[175] I. Turk Cakir,[4b,ww] R. Turra,[94a] P. M. Tuts,[38] G. Ucchielli,[22a,22b] I. Ueda,[69] M. Ughetto,[148a,148b] F. Ukegawa,[164] G. Unal,[32] A. Undrus,[27] G. Unel,[166] F. C. Ungaro,[91] Y. Unno,[69] K. Uno,[157] J. Urban,[146b] P. Urquijo,[91] P. Urrejola,[86] G. Usai,[8] J. Usui,[69] L. Vacavant,[88] V. Vacek,[130] B. Vachon,[90] K. O. H. Vadla,[121] A. Vaidya,[81] C. Valderanis,[102] E. Valdes Santurio,[148a,148b] M. Valente,[52] S. Valentinetti,[22a,22b] A. Valero,[170] L. Valéry,[45] A. Vallier,[5] J. A. Valls Ferrer,[170] W. Van Den Wollenberg,[109] H. van der Graaf,[109] P. van Gemmeren,[6] J. Van Nieuwkoop,[144] I. van Vulpen,[109] M. C. van Woerden,[109] M. Vanadia,[135a,135b] W. Vandelli,[32] A. Vaniachine,[160] P. Vankov,[109] R. Vari,[134a] E. W. Varnes,[7] C. Varni,[53a,53b] T. Varol,[43] D. Varouchas,[119] A. Vartapetian,[8] K. E. Varvell,[152] J. G. Vasquez,[179] G. A. Vasquez,[34b] F. Vazeille,[37] D. Vazquez Furelos,[13] T. Vazquez Schroeder,[90] J. Veatch,[57] L. M. Veloce,[161] F. Veloso,[128a,128c] S. Veneziano,[134a] A. Ventura,[76a,76b] M. Venturi,[172] N. Venturi,[32] V. Vercesi,[123a] M. Verducci,[136a,136b] W. Verkerke,[109] A. T. Vermeulen,[109] J. C. Vermeulen,[109] M. C. Vetterli,[144,e] N. Viaux Maira,[34b] O. Viazlo,[84] I. Vichou,[169,a] T. Vickey,[141] O. E. Vickey Boeriu,[141] G. H. A. Viehhauser,[122] S. Viel,[16] L. Vigani,[122] M. Villa,[22a,22b] M. Villaplana Perez,[94a,94b] E. Vilucchi,[50] M. G. Vincter,[31] V. B. Vinogradov,[68] A. Vishwakarma,[45] C. Vittori,[22a,22b] I. Vivarelli,[151] S. Vlachos,[10] M. Vogel,[178] P. Vokac,[130] G. Volpi,[13] S. E. von Buddenbrock,[147c] E. von Toerne,[23] V. Vorobel,[131] K. Vorobev,[100] M. Vos,[170] J. H. Vossebeld,[77] N. Vranjes,[14] M. Vranjes Milosavljevic,[14] V. Vrba,[130] M. Vreeswijk,[109] R. Vuillermet,[32] I. Vukotic,[33] P. Wagner,[23] W. Wagner,[178] J. Wagner-Kuhr,[102] H. Wahlberg,[74] S. Wahrmund,[47] K. Wakamiya,[70] J. Walder,[75] R. Walker,[102] W. Walkowiak,[143] V. Wallangen,[148a,148b] A. M. Wang,[59] C. Wang,[36b,r] F. Wang,[176] H. Wang,[16] H. Wang,[3] J. Wang,[60b] J. Wang,[152] Q. Wang,[115] R.-J. Wang,[83] R. Wang,[6] S. M. Wang,[153] T. Wang,[38] W. Wang,[35b] W. Wang,[36a,xx] Z. Wang,[36c] C. Wanotayaroj,[45] A. Warburton,[90] C. P. Ward,[30] D. R. Wardrope,[81] A. Washbrook,[49] P. M. Watkins,[19] A. T. Watson,[19] M. F. Watson,[19] G. Watts,[140] S. Watts,[87] B. M. Waugh,[81] A. F. Webb,[11] S. Webb,[86] M. S. Weber,[18] S. M. Weber,[60a] S. A. Weber,[31] J. S. Webster,[6] A. R. Weidberg,[122] B. Weinert,[64] J. Weingarten,[57] M. Weirich,[86] C. Weiser,[51] P. S. Wells,[32] T. Wenaus,[27] T. Wengler,[32] S. Wenig,[32] N. Wermes,[23] M. D. Werner,[67] P. Werner,[32] M. Wessels,[60a] T. D. Weston,[18] K. Whalen,[118] N. L. Whallon,[140] A. M. Wharton,[75] A. S. White,[92] A. White,[8] M. J. White,[1] R. White,[34b] D. Whiteson,[166] B. W. Whitmore,[75] F. J. Wickens,[133] W. Wiedenmann,[176] M. Wielers,[133] C. Wiglesworth,[39] L. A. M. Wiik-Fuchs,[51] A. Wildauer,[103] F. Wilk,[87] H. G. Wilkens,[32] H. H. Williams,[124] S. Williams,[30] C. Willis,[93] S. Willocq,[89] J. A. Wilson,[19] I. Wingerter-Seez,[5] E. Winkels,[151] F. Winklmeier,[118] O. J. Winston,[151] B. T. Winter,[23] M. Wittgen,[145] M. Wobisch,[82,w] A. Wolf,[86] T. M. H. Wolf,[109] R. Wolff,[88] M. W. Wolter,[42] H. Wolters,[128a,128c] V. W. S. Wong,[171] N. L. Woods,[139] S. D. Worm,[19] B. K. Wosiek,[42] K. W. Wozniak,[42] M. Wu,[33] S. L. Wu,[176] X. Wu,[52] Y. Wu,[36a] T. R. Wyatt,[87] B. M. Wynne,[49] S. Xella,[39] Z. Xi,[92] L. Xia,[35c] D. Xu,[35a] L. Xu,[27] T. Xu,[138] W. Xu,[92] B. Yabsley,[152] S. Yacoob,[147a] K. Yajima,[120] D. P. Yallup,[81] D. Yamaguchi,[159] Y. Yamaguchi,[159] A. Yamamoto,[69] T. Yamanaka,[157] F. Yamane,[70] M. Yamatani,[157] T. Yamazaki,[157] Y. Yamazaki,[70] Z. Yan,[24] H. Yang,[36c] H. Yang,[16] S. Yang,[66] Y. Yang,[153] Z. Yang,[15] W-M. Yao,[16] Y. C. Yap,[45] Y. Yasu,[69] E. Yatsenko,[5] K. H. Yau Wong,[23] J. Ye,[43] S. Ye,[27] I. Yeletskikh,[68] E. Yigitbasi,[24] E. Yildirim,[86] K. Yorita,[174] K. Yoshihara,[124] C. Young,[145] C. J. S. Young,[32] J. Yu,[8] J. Yu,[67] S. P. Y. Yuen,[23] I. Yusuff,[30,yy] B. Zabinski,[42] G. Zacharis,[10] R. Zaidan,[13] A. M. Zaitsev,[132,mm] N. Zakharchuk,[45] J. Zalieckas,[15] S. Zambito,[59] D. Zanzi,[32] C. Zeitnitz,[178] G. Zemaityte,[122] J. C. Zeng,[169] Q. Zeng,[145] O. Zenin,[132] T. Ženiš,[146a] D. Zerwas,[119] D. Zhang,[36b] D. Zhang,[92] F. Zhang,[176] G. Zhang,[36a,xx] H. Zhang,[119] J. Zhang,[6] L. Zhang,[51] L. Zhang,[36a] M. Zhang,[169] P. Zhang,[35b] R. Zhang,[23] R. Zhang,[36a,r] X. Zhang,[36b] Y. Zhang,[35a,35d] Z. Zhang,[119] X. Zhao,[43] Y. Zhao,[36b,z] Z. Zhao,[36a] A. Zhemchugov,[68] B. Zhou,[92] C. Zhou,[176] L. Zhou,[43] M. Zhou,[35a,35d] M. Zhou,[150] N. Zhou,[36c] Y. Zhou,[7] C. G. Zhu,[36b] H. Zhu,[35a] J. Zhu,[92] Y. Zhu,[36a] X. Zhuang,[35a] K. Zhukov,[98] V. Zhulanov,[111] A. Zibell,[177] D. Zieminska,[64] N. I. Zimine,[68] S. Zimmermann,[51] Z. Zinonos,[103] M. Zinser,[86] M. Ziolkowski,[143] L. Živković,[14] G. Zobernig,[176] A. Zoccoli,[22a,22b] T. G. Zorbas,[141] R. Zou,[33] M. zur Nedden,[17] and L. Zwalinski[32]

(ATLAS Collaboration)

[1]*Department of Physics, University of Adelaide, Adelaide, Australia*
[2]*Physics Department, SUNY Albany, Albany, New York, USA*
[3]*Department of Physics, University of Alberta, Edmonton, Alberta, Canada*
[4a]*Department of Physics, Ankara University, Ankara, Turkey*
[4b]*Istanbul Aydin University, Istanbul, Turkey*
[4c]*Division of Physics, TOBB University of Economics and Technology, Ankara, Turkey*

[5]*LAPP, CNRS/IN2P3 and Université Savoie Mont Blanc, Annecy-le-Vieux, France*
[6]*High Energy Physics Division, Argonne National Laboratory, Argonne, Illinois, USA*
[7]*Department of Physics, University of Arizona, Tucson, Arizona, USA*
[8]*Department of Physics, The University of Texas at Arlington, Arlington, Texas, USA*
[9]*Physics Department, National and Kapodistrian University of Athens, Athens, Greece*
[10]*Physics Department, National Technical University of Athens, Zografou, Greece*
[11]*Department of Physics, The University of Texas at Austin, Austin, Texas, USA*
[12]*Institute of Physics, Azerbaijan Academy of Sciences, Baku, Azerbaijan*
[13]*Institut de Física d'Altes Energies (IFAE), The Barcelona Institute of Science and Technology,
Barcelona, Spain*
[14]*Institute of Physics, University of Belgrade, Belgrade, Serbia*
[15]*Department for Physics and Technology, University of Bergen, Bergen, Norway*
[16]*Physics Division, Lawrence Berkeley National Laboratory and University of California, Berkeley,
California, USA*
[17]*Department of Physics, Humboldt University, Berlin, Germany*
[18]*Albert Einstein Center for Fundamental Physics and Laboratory for High Energy Physics,
University of Bern, Bern, Switzerland*
[19]*School of Physics and Astronomy, University of Birmingham, Birmingham, United Kingdom*
[20a]*Department of Physics, Bogazici University, Istanbul, Turkey*
[20b]*Department of Physics Engineering, Gaziantep University, Gaziantep, Turkey*
[20c]*Istanbul Bilgi University, Faculty of Engineering and Natural Sciences, Istanbul, Turkey*
[20d]*Bahcesehir University, Faculty of Engineering and Natural Sciences, Istanbul, Turkey*
[21]*Centro de Investigaciones, Universidad Antonio Narino, Bogota, Colombia*
[22a]*INFN Sezione di Bologna, Italy*
[22b]*Dipartimento di Fisica e Astronomia, Università di Bologna, Bologna, Italy*
[23]*Physikalisches Institut, University of Bonn, Bonn, Germany*
[24]*Department of Physics, Boston University, Boston, Massachusetts, USA*
[25]*Department of Physics, Brandeis University, Waltham, Massachusetts, USA*
[26a]*Universidade Federal do Rio De Janeiro COPPE/EE/IF, Rio de Janeiro, Brazil*
[26b]*Electrical Circuits Department, Federal University of Juiz de Fora (UFJF), Juiz de Fora, Brazil*
[26c]*Federal University of Sao Joao del Rei (UFSJ), Sao Joao del Rei, Brazil*
[26d]*Instituto de Fisica, Universidade de Sao Paulo, Sao Paulo, Brazil*
[27]*Physics Department, Brookhaven National Laboratory, Upton, New York, USA*
[28a]*Transilvania University of Brasov, Brasov, Romania*
[28b]*Horia Hulubei National Institute of Physics and Nuclear Engineering, Bucharest, Romania*
[28c]*Department of Physics, Alexandru Ioan Cuza University of Iasi, Iasi, Romania*
[28d]*National Institute for Research and Development of Isotopic and Molecular Technologies,
Physics Department, Cluj Napoca, Romania*
[28e]*University Politehnica Bucharest, Bucharest, Romania*
[28f]*West University in Timisoara, Timisoara, Romania*
[29]*Departamento de Física, Universidad de Buenos Aires, Buenos Aires, Argentina*
[30]*Cavendish Laboratory, University of Cambridge, Cambridge, United Kingdom*
[31]*Department of Physics, Carleton University, Ottawa, Ontario, Canada*
[32]*CERN, Geneva, Switzerland*
[33]*Enrico Fermi Institute, University of Chicago, Chicago, Illinois, USA*
[34a]*Departamento de Física, Pontificia Universidad Católica de Chile, Santiago, Chile*
[34b]*Departamento de Física, Universidad Técnica Federico Santa María, Valparaíso, Chile*
[35a]*Institute of High Energy Physics, Chinese Academy of Sciences, Beijing, China*
[35b]*Department of Physics, Nanjing University, Jiangsu, China*
[35c]*Physics Department, Tsinghua University, Beijing 100084, China*
[35d]*University of Chinese Academy of Science (UCAS), Beijing, China*
[36a]*Department of Modern Physics and State Key Laboratory of Particle Detection and Electronics,
University of Science and Technology of China, Anhui, China*
[36b]*School of Physics, Shandong University, Shandong, China*
[36c]*School of Physics and Astronomy, Key Laboratory for Particle Physics, Astrophysics and Cosmology,
Ministry of Education; Shanghai Key Laboratory for Particle Physics and Cosmology,
Tsung-Dao Lee Institute, Shanghai Jiao Tong University, China*
[36d]*Tsung-Dao Lee Institute, Shanghai, China*
[37]*Université Clermont Auvergne, CNRS/IN2P3, LPC, Clermont-Ferrand, France*
[38]*Nevis Laboratory, Columbia University, Irvington, New York, USA*

[39]Niels Bohr Institute, University of Copenhagen, Kobenhavn, Denmark

[40a]INFN Gruppo Collegato di Cosenza, Laboratori Nazionali di Frascati, Italy

[40b]Dipartimento di Fisica, Università della Calabria, Rende, Italy

[41a]AGH University of Science and Technology, Faculty of Physics and Applied Computer Science, Krakow, Poland

[41b]Marian Smoluchowski Institute of Physics, Jagiellonian University, Krakow, Poland

[42]Institute of Nuclear Physics Polish Academy of Sciences, Krakow, Poland

[43]Physics Department, Southern Methodist University, Dallas, Texas, USA

[44]Physics Department, University of Texas at Dallas, Richardson, Texas, USA

[45]DESY, Hamburg and Zeuthen, Germany

[46]Lehrstuhl für Experimentelle Physik IV, Technische Universität Dortmund, Dortmund, Germany

[47]Institut für Kern- und Teilchenphysik, Technische Universität Dresden, Dresden, Germany

[48]Department of Physics, Duke University, Durham, North Carolina, USA

[49]SUPA - School of Physics and Astronomy, University of Edinburgh, Edinburgh, United Kingdom

[50]INFN e Laboratori Nazionali di Frascati, Frascati, Italy

[51]Fakultät für Mathematik und Physik, Albert-Ludwigs-Universität, Freiburg, Germany

[52]Departement de Physique Nucleaire et Corpusculaire, Université de Genève, Geneva, Switzerland

[53a]INFN Sezione di Genova, Italy

[53b]Dipartimento di Fisica, Università di Genova, Genova, Italy

[54a]E. Andronikashvili Institute of Physics, Iv. Javakhishvili Tbilisi State University, Tbilisi, Georgia

[54b]High Energy Physics Institute, Tbilisi State University, Tbilisi, Georgia

[55]II Physikalisches Institut, Justus-Liebig-Universität Giessen, Giessen, Germany

[56]SUPA - School of Physics and Astronomy, University of Glasgow, Glasgow, United Kingdom

[57]II Physikalisches Institut, Georg-August-Universität, Göttingen, Germany

[58]Laboratoire de Physique Subatomique et de Cosmologie, Université Grenoble-Alpes, CNRS/IN2P3, Grenoble, France

[59]Laboratory for Particle Physics and Cosmology, Harvard University, Cambridge, Massachusetts, USA

[60a]Kirchhoff-Institut für Physik, Ruprecht-Karls-Universität Heidelberg, Heidelberg, Germany

[60b]Physikalisches Institut, Ruprecht-Karls-Universität Heidelberg, Heidelberg, Germany

[61]Faculty of Applied Information Science, Hiroshima Institute of Technology, Hiroshima, Japan

[62a]Department of Physics, The Chinese University of Hong Kong, Shatin, N.T., Hong Kong, China

[62b]Department of Physics, The University of Hong Kong, Hong Kong, China

[62c]Department of Physics and Institute for Advanced Study, The Hong Kong University of Science and Technology, Clear Water Bay, Kowloon, Hong Kong, China

[63]Department of Physics, National Tsing Hua University, Hsinchu, Taiwan

[64]Department of Physics, Indiana University, Bloomington, Indiana, USA

[65]Institut für Astro- und Teilchenphysik, Leopold-Franzens-Universität, Innsbruck, Austria

[66]University of Iowa, Iowa City, Iowa, USA

[67]Department of Physics and Astronomy, Iowa State University, Ames, Iowa, USA

[68]Joint Institute for Nuclear Research, JINR, Dubna, Dubna, Russia

[69]KEK, High Energy Accelerator Research Organization, Tsukuba, Japan

[70]Graduate School of Science, Kobe University, Kobe, Japan

[71]Faculty of Science, Kyoto University, Kyoto, Japan

[72]Kyoto University of Education, Kyoto, Japan

[73]Research Center for Advanced Particle Physics and Department of Physics, Kyushu University, Fukuoka, Japan

[74]Instituto de Física La Plata, Universidad Nacional de La Plata and CONICET, La Plata, Argentina

[75]Physics Department, Lancaster University, Lancaster, United Kingdom

[76a]INFN Sezione di Lecce, Italy

[76b]Dipartimento di Matematica e Fisica, Università del Salento, Lecce, Italy

[77]Oliver Lodge Laboratory, University of Liverpool, Liverpool, United Kingdom

[78]Department of Experimental Particle Physics, Jožef Stefan Institute and Department of Physics, University of Ljubljana, Ljubljana, Slovenia

[79]School of Physics and Astronomy, Queen Mary University of London, London, United Kingdom

[80]Department of Physics, Royal Holloway University of London, Surrey, United Kingdom

[81]Department of Physics and Astronomy, University College London, London, United Kingdom

[82]Louisiana Tech University, Ruston, Louisiana, USA

[83]Laboratoire de Physique Nucléaire et de Hautes Energies, UPMC and Université Paris-Diderot and CNRS/IN2P3, Paris, France

[84]Fysiska institutionen, Lunds universitet, Lund, Sweden

[85]*Departamento de Fisica Teorica C-15, Universidad Autonoma de Madrid, Madrid, Spain*
[86]*Institut für Physik, Universität Mainz, Mainz, Germany*
[87]*School of Physics and Astronomy, University of Manchester, Manchester, United Kingdom*
[88]*CPPM, Aix-Marseille Université and CNRS/IN2P3, Marseille, France*
[89]*Department of Physics, University of Massachusetts, Amherst, Massachusetts, USA*
[90]*Department of Physics, McGill University, Montreal, Quebec, Canada*
[91]*School of Physics, University of Melbourne, Victoria, Australia*
[92]*Department of Physics, The University of Michigan, Ann Arbor, Michigan, USA*
[93]*Department of Physics and Astronomy, Michigan State University, East Lansing, Michigan, USA*
[94a]*INFN Sezione di Milano, Italy*
[94b]*Dipartimento di Fisica, Università di Milano, Milano, Italy*
[95]*B.I. Stepanov Institute of Physics, National Academy of Sciences of Belarus, Minsk, Republic of Belarus*
[96]*Research Institute for Nuclear Problems of Byelorussian State University, Minsk, Republic of Belarus*
[97]*Group of Particle Physics, University of Montreal, Montreal, Quebec, Canada*
[98]*P.N. Lebedev Physical Institute of the Russian Academy of Sciences, Moscow, Russia*
[99]*Institute for Theoretical and Experimental Physics (ITEP), Moscow, Russia*
[100]*National Research Nuclear University MEPhI, Moscow, Russia*
[101]*D.V. Skobeltsyn Institute of Nuclear Physics, M.V. Lomonosov Moscow State University,*
Moscow, Russia
[102]*Fakultät für Physik, Ludwig-Maximilians-Universität München, München, Germany*
[103]*Max-Planck-Institut für Physik (Werner-Heisenberg-Institut), München, Germany*
[104]*Nagasaki Institute of Applied Science, Nagasaki, Japan*
[105]*Graduate School of Science and Kobayashi-Maskawa Institute, Nagoya University, Nagoya, Japan*
[106a]*INFN Sezione di Napoli, Italy*
[106b]*Dipartimento di Fisica, Università di Napoli, Napoli, Italy*
[107]*Department of Physics and Astronomy, University of New Mexico, Albuquerque, New Mexico, USA*
[108]*Institute for Mathematics, Astrophysics and Particle Physics, Radboud University Nijmegen/Nikhef,*
Nijmegen, Netherlands
[109]*Nikhef National Institute for Subatomic Physics and University of Amsterdam, Amsterdam, Netherlands*
[110]*Department of Physics, Northern Illinois University, DeKalb, Illinois, USA*
[111]*Budker Institute of Nuclear Physics, SB RAS, Novosibirsk, Russia*
[112]*Department of Physics, New York University, New York, New York, USA*
[113]*Ohio State University, Columbus, Ohio, USA*
[114]*Faculty of Science, Okayama University, Okayama, Japan*
[115]*Homer L. Dodge Department of Physics and Astronomy, University of Oklahoma,*
Norman, Oklahoma, USA
[116]*Department of Physics, Oklahoma State University, Stillwater, Oklahoma, USA*
[117]*Palacký University, RCPTM, Olomouc, Czech Republic*
[118]*Center for High Energy Physics, University of Oregon, Eugene, Oregon, USA*
[119]*LAL, Univ. Paris-Sud, CNRS/IN2P3, Université Paris-Saclay, Orsay, France*
[120]*Graduate School of Science, Osaka University, Osaka, Japan*
[121]*Department of Physics, University of Oslo, Oslo, Norway*
[122]*Department of Physics, Oxford University, Oxford, United Kingdom*
[123a]*INFN Sezione di Pavia, Italy*
[123b]*Dipartimento di Fisica, Università di Pavia, Pavia, Italy*
[124]*Department of Physics, University of Pennsylvania, Philadelphia, Pennsylvania, USA*
[125]*National Research Centre "Kurchatov Institute" B.P.Konstantinov Petersburg Nuclear Physics Institute,*
St. Petersburg, Russia
[126a]*INFN Sezione di Pisa, Italy*
[126b]*Dipartimento di Fisica E. Fermi, Università di Pisa, Pisa, Italy*
[127]*Department of Physics and Astronomy, University of Pittsburgh, Pittsburgh, Pennsylvania, USA*
[128a]*Laboratório de Instrumentação e Física Experimental de Partículas - LIP, Lisboa, Portugal*
[128b]*Faculdade de Ciências, Universidade de Lisboa, Lisboa, Portugal*
[128c]*Department of Physics, University of Coimbra, Coimbra, Portugal*
[128d]*Centro de Física Nuclear da Universidade de Lisboa, Lisboa, Portugal*
[128e]*Departamento de Fisica, Universidade do Minho, Braga, Portugal*
[128f]*Departamento de Fisica Teorica y del Cosmos, Universidad de Granada, Granada, Spain*
[128g]*Dep Fisica and CEFITEC of Faculdade de Ciencias e Tecnologia, Universidade Nova de Lisboa,*
Caparica, Portugal
[129]*Institute of Physics, Academy of Sciences of the Czech Republic, Praha, Czech Republic*

[130]Czech Technical University in Prague, Praha, Czech Republic

[131]Charles University, Faculty of Mathematics and Physics, Prague, Czech Republic

[132]State Research Center Institute for High Energy Physics (Protvino), NRC KI, Russia

[133]Particle Physics Department, Rutherford Appleton Laboratory, Didcot, United Kingdom

[134a]INFN Sezione di Roma, Italy

[134b]Dipartimento di Fisica, Sapienza Università di Roma, Roma, Italy

[135a]INFN Sezione di Roma Tor Vergata, Italy

[135b]Dipartimento di Fisica, Università di Roma Tor Vergata, Roma, Italy

[136a]INFN Sezione di Roma Tre, Italy

[136b]Dipartimento di Matematica e Fisica, Università Roma Tre, Roma, Italy

[137a]Faculté des Sciences Ain Chock, Réseau Universitaire de Physique des Hautes Energies - Université Hassan II, Casablanca, Morocco

[137b]Centre National de l'Energie des Sciences Techniques Nucleaires, Rabat, Morocco

[137c]Faculté des Sciences Semlalia, Université Cadi Ayyad, LPHEA-Marrakech, Morocco

[137d]Faculté des Sciences, Université Mohamed Premier and LPTPM, Oujda, Morocco

[137e]Faculté des sciences, Université Mohammed V, Rabat, Morocco

[138]DSM/IRFU (Institut de Recherches sur les Lois Fondamentales de l'Univers), CEA Saclay (Commissariat à l'Energie Atomique et aux Energies Alternatives), Gif-sur-Yvette, France

[139]Santa Cruz Institute for Particle Physics, University of California Santa Cruz, Santa Cruz, California, USA

[140]Department of Physics, University of Washington, Seattle, Washington, USA

[141]Department of Physics and Astronomy, University of Sheffield, Sheffield, United Kingdom

[142]Department of Physics, Shinshu University, Nagano, Japan

[143]Department Physik, Universität Siegen, Siegen, Germany

[144]Department of Physics, Simon Fraser University, Burnaby, British Columbia, Canada

[145]SLAC National Accelerator Laboratory, Stanford, California, USA

[146a]Faculty of Mathematics, Physics & Informatics, Comenius University, Bratislava, Slovak Republic

[146b]Department of Subnuclear Physics, Institute of Experimental Physics of the Slovak Academy of Sciences, Kosice, Slovak Republic

[147a]Department of Physics, University of Cape Town, Cape Town, South Africa

[147b]Department of Physics, University of Johannesburg, Johannesburg, South Africa

[147c]School of Physics, University of the Witwatersrand, Johannesburg, South Africa

[148a]Department of Physics, Stockholm University, Sweden

[148b]The Oskar Klein Centre, Stockholm, Sweden

[149]Physics Department, Royal Institute of Technology, Stockholm, Sweden

[150]Departments of Physics & Astronomy and Chemistry, Stony Brook University, Stony Brook, New York, USA

[151]Department of Physics and Astronomy, University of Sussex, Brighton, United Kingdom

[152]School of Physics, University of Sydney, Sydney, Australia

[153]Institute of Physics, Academia Sinica, Taipei, Taiwan

[154]Department of Physics, Technion: Israel Institute of Technology, Haifa, Israel

[155]Raymond and Beverly Sackler School of Physics and Astronomy, Tel Aviv University, Tel Aviv, Israel

[156]Department of Physics, Aristotle University of Thessaloniki, Thessaloniki, Greece

[157]International Center for Elementary Particle Physics and Department of Physics, The University of Tokyo, Tokyo, Japan

[158]Graduate School of Science and Technology, Tokyo Metropolitan University, Tokyo, Japan

[159]Department of Physics, Tokyo Institute of Technology, Tokyo, Japan

[160]Tomsk State University, Tomsk, Russia

[161]Department of Physics, University of Toronto, Toronto, Ontario, Canada

[162a]INFN-TIFPA, Italy

[162b]University of Trento, Trento, Italy

[163a]TRIUMF, Vancouver, British Columbia, Canada

[163b]Department of Physics and Astronomy, York University, Toronto, Ontario, Canada

[164]Faculty of Pure and Applied Sciences, and Center for Integrated Research in Fundamental Science and Engineering, University of Tsukuba, Tsukuba, Japan

[165]Department of Physics and Astronomy, Tufts University, Medford, Massachusetts, USA

[166]Department of Physics and Astronomy, University of California Irvine, Irvine, California, USA

[167a]INFN Gruppo Collegato di Udine, Sezione di Trieste, Udine, Italy

[167b]ICTP, Trieste, Italy

[167c]Dipartimento di Chimica, Fisica e Ambiente, Università di Udine, Udine, Italy

^{168}*Department of Physics and Astronomy, University of Uppsala, Uppsala, Sweden*
^{169}*Department of Physics, University of Illinois, Urbana, Illinois, USA*
^{170}*Instituto de Fisica Corpuscular (IFIC), Centro Mixto Universidad de Valencia - CSIC, Spain*
^{171}*Department of Physics, University of British Columbia, Vancouver, British Columbia, Canada*
^{172}*Department of Physics and Astronomy, University of Victoria, Victoria, British Columbia, Canada*
^{173}*Department of Physics, University of Warwick, Coventry, United Kingdom*
^{174}*Waseda University, Tokyo, Japan*
^{175}*Department of Particle Physics, The Weizmann Institute of Science, Rehovot, Israel*
^{176}*Department of Physics, University of Wisconsin, Madison, Wisconsin, USA*
^{177}*Fakultät für Physik und Astronomie, Julius-Maximilians-Universität, Würzburg, Germany*
^{178}*Fakultät für Mathematik und Naturwissenschaften, Fachgruppe Physik, Bergische Universität Wuppertal, Wuppertal, Germany*
^{179}*Department of Physics, Yale University, New Haven, Connecticut, USA*
^{180}*Yerevan Physics Institute, Yerevan, Armenia*
^{181}*Centre de Calcul de l'Institut National de Physique Nucléaire et de Physique des Particules (IN2P3), Villeurbanne, France*
^{182}*Academia Sinica Grid Computing, Institute of Physics, Academia Sinica, Taipei, Taiwan*

[a]Deceased.
[b]Also at Department of Physics, King's College London, London, United Kingdom.
[c]Also at Institute of Physics, Azerbaijan Academy of Sciences, Baku, Azerbaijan.
[d]Also at Novosibirsk State University, Novosibirsk, Russia.
[e]Also at TRIUMF, Vancouver, BC, Canada.
[f]Also at Department of Physics & Astronomy, University of Louisville, Louisville, KY, USA.
[g]Also at Physics Department, An-Najah National University, Nablus, Palestine.
[h]Also at Department of Physics, California State University, Fresno, CA, USA.
[i]Also at Department of Physics, University of Fribourg, Fribourg, Switzerland.
[j]Also at II Physikalisches Institut, Georg-August-Universität, Göttingen, Germany.
[k]Also at Departament de Fisica de la, Universitat Autonoma de Barcelona, Barcelona, Spain.
[l]Also at Departamento de Fisica e Astronomia, Faculdade de Ciencias, Universidade do Porto, Portugal.
[m]Also at Tomsk State University, Tomsk, and Moscow Institute of Physics and Technology, State University, Dolgoprudny, Russia.
[n]Also at The Collaborative Innovation Center of Quantum Matter (CICQM), Beijing, China.
[o]Also at Universita di Napoli Parthenope, Napoli, Italy.
[p]Also at Institute of Particle Physics (IPP), Canada.
[q]Also at Horia Hulubei National Institute of Physics and Nuclear Engineering, Bucharest, Romania.
[r]Also at CPPM, Aix-Marseille Université and CNRS/IN2P3, Marseille, France.
[s]Also at Department of Physics, St. Petersburg State Polytechnical University, St. Petersburg, Russia.
[t]Also at Borough of Manhattan Community College, City University of New York, New York City, USA.
[u]Also at Department of Financial and Management Engineering, University of the Aegean, Chios, Greece.
[v]Also at Centre for High Performance Computing, CSIR Campus, Rosebank, Cape Town, South Africa.
[w]Also at Louisiana Tech University, Ruston, LA, USA.
[x]Also at Institucio Catalana de Recerca i Estudis Avancats, ICREA, Barcelona, Spain.
[y]Also at Department of Physics, The University of Michigan, Ann Arbor, MI, USA.
[z]Also at LAL, Univ. Paris-Sud, CNRS/IN2P3, Université Paris-Saclay, Orsay, France.
[aa]Also at Graduate School of Science, Osaka University, Osaka, Japan.
[bb]Also at Fakultät für Mathematik und Physik, Albert-Ludwigs-Universität, Freiburg, Germany.
[cc]Also at Institute for Mathematics, Astrophysics and Particle Physics, Radboud University Nijmegen/Nikhef, Nijmegen, Netherlands.
[dd]Also at Institute of Theoretical Physics, Ilia State University, Tbilisi, Georgia.
[ee]Also at CERN, Geneva, Switzerland.
[ff]Also at Georgian Technical University (GTU), Tbilisi, Georgia.
[gg]Also at Ochadai Academic Production, Ochanomizu University, Tokyo, Japan.
[hh]Also at Manhattan College, New York, NY, USA.
[ii]Also at Hellenic Open University, Patras, Greece.
[jj]Also at The City College of New York, New York, NY, USA.
[kk]Also at Departamento de Fisica Teorica y del Cosmos, Universidad de Granada, Granada, Spain.
[ll]Also at Department of Physics, California State University, Sacramento, CA, USA.
[mm]Also at Moscow Institute of Physics and Technology, State University, Dolgoprudny, Russia.
[nn]Also at Departement de Physique Nucleaire et Corpusculaire, Université de Genève, Geneva, Switzerland.
[oo]Also at Department of Physics, The University of Texas at Austin, Austin, TX, USA.

[pp]Also at Institut de Física d'Altes Energies (IFAE), The Barcelona Institute of Science and Technology, Barcelona, Spain.

[qq]Also at School of Physics, Sun Yat-sen University, Guangzhou, China.

[rr]Also at Institute for Nuclear Research and Nuclear Energy (INRNE) of the Bulgarian Academy of Sciences, Sofia, Bulgaria.

[ss]Also at Faculty of Physics, M.V.Lomonosov Moscow State University, Moscow, Russia.

[tt]Also at National Research Nuclear University MEPhI, Moscow, Russia.

[uu]Also at Department of Physics, Stanford University, Stanford, CA, USA.

[vv]Also at Institute for Particle and Nuclear Physics, Wigner Research Centre for Physics, Budapest, Hungary.

[ww]Also at Giresun University, Faculty of Engineering, Turkey.

[xx]Also at Institute of Physics, Academia Sinica, Taipei, Taiwan.

[yy]Also at University of Malaya, Department of Physics, Kuala Lumpur, Malaysia.